THESIS REPORT

Prepared for:
MSc Graduation FNT HvU/PTO
Engineering Product Design - Faculteit Natuur en Techniek
Hogeschool van Utrecht

PRELIMINARY ALTERNATIVE DESIGN OF ARIANE 5 MAIN ENGINE FRAME (EPC-BME) WITH ADDITIONAL SKIRT

(Cone - Skirt Concept)

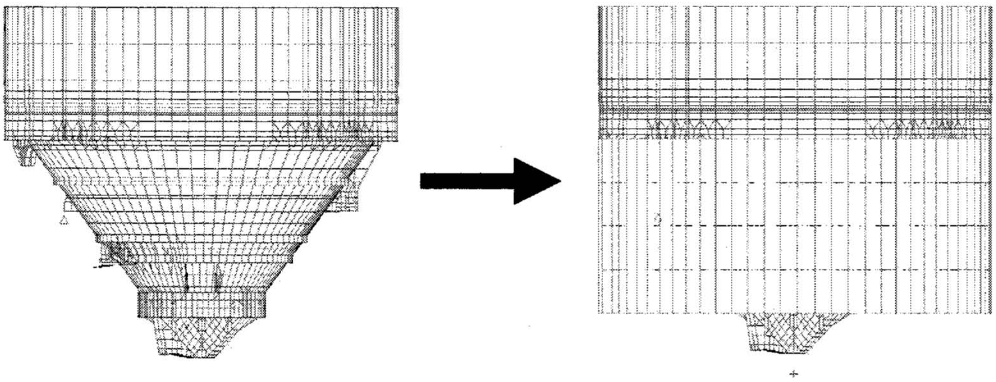

by :
Indra Hastoadi Nugroho

Hogeschool
van Utrecht

Faculteit Natuur en Techniek
Postbus 182
3500 AD Utrecht
The Netherlands

Dutch Space

P.O. Box 32070
2302 DB Leiden
The Netherlands

Dutch Space
P.O. Box 32070
2303 DB LEIDEN
The Netherlands

SOURCE AUTHORITY	CLASS : 1	CATEGORY : 1
Dutch Space	1 = Unrestricted 2 = A10 Programme 3 = Restricted 4 = Confidential	1 = Configured for approval 2 = Non-configured for approval 3 = Non-configuredfor acceptance 4 = Other
	CONTRACT	
LEIDEN	Contract no.	Source authority

Program number + issue + revision	Program	Contractual document	Contract work Unit No.	Work Package No.
AR2010-DS-SER-021 Issue: 1	ARIANE 2010	No		

TITLE :

PRELIMINARY ALTERNATIVE DESIGN OF ARIANE 5 MAIN ENGINE FRAME (EPC-BME) WITH ADDITIONAL SKIRT (Cone-Skirt Concept)

AUTHOR(S) :		Indra Hastoadi Nugroho	Signature(s) :
Issue date : 01-06-2005	Internal document number: AR2010-DS-SER-021	Number of pages : (incl. appendices) 138 pages	Number of appendices : 5 (38pages)

ABSTRACT :
This report specifies the detailed finite element modeling of the EPC-BME Box structure. The finite element analysis result is compared with the result of the old, rather coarse model. The comparison result is used as the basis of the skirt design. A trade-off is made in order to generate the skirt design concept. Optimization is done in order to obtain the minimum mass of the skirt. The impact of the skirt to the EPC-BME is also investigated.

Host	Hardware	Medium	Software
	Nature : n/a Manufacturer : n/a	Nature and type :n/a Identification : n/a	Name : n/a Version : n/a

	NAME	DEPARTMENT	SIGNATURE	DATE
Author	I.H. Nugroho	HvU		
Checked	F.Maitimo	SMS DS		03/06/05
Agreed	D. Spanjer	SMS DS		3-6-'05
Approved:	H. Meijer	SMS DS		3-jun-2005
Authorized:	H. Cruijssen	SMS DS		03/06/05

Language code : ENG

PROGRAMME ARIANE 2010	DISTRIBUTION LIST		Page D1/1

INTERNAL

NAMES (OPTIONAL)	ACRONYM	COPIES	PURPOSE		
			APPROV.	ACCEPT	INFOR.
H. Cruijssen	SMS	1	x		
D. Spanjer	SMS	1		X	
F. Maitimo		1		X	
F. Annink	SMS	1			X
M. Brooker	SMS	1			X
J. Koorevar	SMS	1			X
M. Lemmen	SMS	1			X
	SMS				

EXTERNAL

NAMES (OPTIONAL)	ACRONYM	COPIES	PURPOSE		
			APPROV.	ACCEPT	INFOR.
J. Oomens	Hogeschool van Utrecht Engineering Product Design	3	x		
I.H. Nugroho	Author	2			x

Revision Record

Issue	Date	Total pages	Authorization	Pages affected	Brief description of change
Draft 1	January '05	45	H. Cruijssen	All	First issue
Draft 2	March '05	92	H. Cruijssen	All	Comments H. Cruijssen included
Draft 3	May '05	103	H. Cruijssen	All	Comments H. Cruijssen included
Concept 1	May '05	123	H.Cruijssen	All	Comments HAR. Adams, F.Maitimo, H. Cruijssen included
Issue 1	June '05	132	H. Crujssen	85-95	Comments H. Cruijssen included

Table of contents

Preface

This report is the result of a graduation project performed at Structural and Mechanical Systems (SMS) department of Dutch Space B.V. in Leiden, the Netherlands.

I express my deepest appreciation to Henk Cruijssen for his advice throughout this project. Without his guidance, this project could not have been accomplished.

I am grateful to Floor Maitimo and Dirk Spanjer as my co-supervisor, who always helpful with the finite element modelling and structural analysis. Their sharing of knowledge is a positive input for me to improve myseff as an engineer and as a person.

Thanks are also expressed to Hakon Eijsermans and Rogier van der Leede as my room mates at Dutch Space, with whom I got a great moment and support as well.

Furthermore, I want to thank the entire SMS department for the help and good cooperation during my time at Dutch Space.

Finally, I dedicate this report to my family in Indonesia.

June 2005

Indra Hastoadi Nugroho

Summary

This report contains the preliminary study for the concept design of EPC-BME ARIANE 2010. The EPC-BME (BME) is primary load carrying structure, also called lower engine frame, of ARIANE launcher. The project EPC-BME ARIANE 2010 is part of ARIANE 2010 launcher program. The ARIANE 2010 project main goal is to reduce the recurring cost drastically in order to become competitive in the future aerospace business. In addition, the launcher's performance will need to be increased to accomrnodate higher payload for future needs.

From preliminary study (Internal technica1notes; Ref. 12) a preferred concept which is the 'load carrying' skirt concept has been selected. This new cylindrical skirt concept has been chosen primary to reduce costs of the current complicated high cost structure. On the contrary, the concept is vulnerable to buckling. The design has now been made of a cone / box concept. It has been envisaged that all equipment is installed inside the cone and therefore requires a considerable integration effort. In this study, the new design concept to be studied is the so called: Cone-Skirt concept. The major primary load carrying structures are to be kept and maintained in this concept.

Within the design process, there are 2 considerable problems, i.e.:

- Buffeting problem
- Out-of-date finite element model

In this study a new detailed finite element model of the BME Box structure is made using MSC PATRAN and analyzed using MSC NASTRAN. The result is verified with respect to the old model (version A5-v6A) and hand calculation.

This study also elaborates the additional skirt design concept in order to overcome the buffeting problem. After the design concepts being generated, trade-off matrices are used to single out the preferred concept. The dimension of the skirt is optimized in order to minimize the mass of the skirt. This will influence the total mass of the BME.

The last part of this study is the analysis of the impact of the skirt to the existing BME on stiffness parameters. This analysis is done using the finite element model.

List of Abbreviations

AS	Aerospatiale (EADS)
BAF	Final Assembly Building (Batiment d'Assembled Final)
BEVO/BEVH	Boitier Electro Vanne Oxygene / Hydrogene
BIL	Launcher Integration Building (Batiment d'Integration Lanceur)
BME	Bati Moteur Equipe (Lower engine frame)
CC	Centre Cardan (Vulcain Engine Rotation Point)
CNES	Centre National D'Etudes Spatiales Agence Francaise De L'Espace
CSG	Guiana Space Centre
DAAR	Dispositif d'Accrochage ARrière (Lower Booster Bar Plane)
DS	Dutch Space (Fokker Space)
EADS	European Aeronautic Defense and Space
EAP	Etage d'Acceleration a Poudre (Solid Propellant Booster)
ECO/ECH	Equipement de Chasse Oxygene / Hydrogene
EPC	Etage Principal Cryotechnique (Core Cryogenic Main Stage)
EPSO/EPSH	Equipement de Pressurisation Sol Oxygene / Hydrogene
ERVO/ERVH	Equipement de Remplissage Vidange Oxygene / Hydrogene
ESA	European Space Agency
FMECA	Failure Modes Effects and Criticality Analysis
FS	Fokker Space Leiden (Dutch Space)
FSP	Fokker Special Products Hoogeveen
GAM	Groupe d'Activation Moteur
GH	Groupe Hydraulique
H2	Hydrogen
HeHP	High Pressure Helium Sphere
I/F	Interfaces
LBS	Liaison Bord/Sol (Ground Linkage)
LDE	Ligne de Dégazage Hélium
LH2	Liquid Hydrogen
LOx	Liquid Oxygen
LPO/LPH	Ligne de Pressurisation Oxygene / Hydrogene (also named EPSO/EPSH on Box)
LRE	Ligne de Remplissage Hélium
MS	Margin of Safety
0 2	Oxygen
PAF	Plaques-8-Flexibles
PCP/PCE	Prise Culot Pneumatique / Electrique
PGD	Platine de Gonflage Détente
RIE	Reservoir Isolé Equipé (Cryogenic tank)
SCD	Single Cable Duct
SCF	Stress Concentration Factor
SCR	Système de Contrôle Roulis
SSHeL	Sous-Systeme Helium Liquide
tbc	to be confirmed
TBD	To Be Defined
tbd	to be determined
tbs	to be specified
TPCO/TPCH	Tuyauterie de Purge Circulation Oxygène / Hydrogene
VEB	Vehicle Equipment Bay

Reference Documents

Internal Technical Notes :

1.	A5-NT-1232000-A-022-FOKK	Material data of ARIANE 5 EPC-BM structure
2.	A5-NT-1232000-B-039-FOKK	Specification thermal environment EPCIBME
3.	A5-NT-1232000-A-067-FOKK	Mass properties report
4.	A5-NT-1232000-B-142-FOKK	Description of Finite Element model
5.	A5-NT-1232000-B-295-FOKK	Mass Status
6.	A5-NT-1232000-B-00x-FOKK	ARIANE 5 EPC-BME 2010 Cost Reduction Programme
7.	A5-DF-1232000-B-001-FOKK	Functional File
8.	A5-ST-1232000-B-001-FOKK	Technical Specification BME for A5 Evolution
9.	A5-DJ-1232000-B-001-FOKK	ARIANE 5 EPC-BME-E Justification File
10.	A5-EF-1232000-C-001-ASET-EADS-Tome 1	Etage Principal Cryotechnique Exigences De Face Du Bati-Moteur Equipe
11.	A5-EF-1232000-C-001-ASET-EADS-Tome 2&3	Etage Principal Cryotechnique Exigences De Face Du Bati-Moteur Equipe
12.	AR2010-DS-SER-001	ARIANE 2010 CONCEPT DESIGN OF EPC-BME Primary Load Carrying Structure
13.	AR2010-DS-SER-003	ARIANE 2010 CONCEPT DESIGN OF EPC-BME Box Preliminary Design

External References :

1 MSC.Patran 2001, User's Guide and Reference Manuals Volume 1

2 MSC.Patran 2001 , Example Problems

3 NAS101-Basic : MSC.Patran/NASTRAN ; Linear Static and Normal Mode Analysis, Volume 1 ; 2001

4 MSC NASTRAN Version 70 "Quick Reference Guide" ; Kilroy, Kevin

5 Design Sensitivity and Optimization in MSC.NASTRAN, Seminar Notes, 1995

6 The Engineering Sciences Data Unit (ESDU) ; Structures series volume 9 ; data nurnber 84006

7 "Roark's Formulas for Stress & Strain" ; Young, W.C. ; Mc Graw-Hill, 6th edition, 1989

8 "Theory of Elastic Stability'.; Timoshenko, S.P. and Gere J.M ; McGraw-Hill, 2nd edition, 1961

9 "An introduction to the Elastic Stability of Structures" ; Simitses, G.J.; Prentice-Hall, 1976

10 "Total Design ; Integrated Methods for Successful Product Engineering" ; Pugh, Stuart ; Addison Wesley 1990

11 "Mechanical Design Process " ; Ullman, David G. ; Mc Graw Hill , 3rd ed, 2002

12 "Mechanics of Materials" ; Gere, J.M. and Timoshenko, S.P. ; Chapman & Hall; 3rd edition; 1991

13 "Fundamentals of Aerodynamics" ; Anderson, J.D.; McGraw-Hill; 1991

14 "Structural Shape Optimization Considering Both Performance and Manufacturing Cost" ; Nadir,W. and Kim, IY ; AIAA ; 2004

f. Introduction

1.1 Company Profile

Dutch Space, formerly known as Fokker Space, is a Dutch company that develops and produces high quality products for space industry, e.g. solar arrays and the engine frame of the ARIANE 5 launcher. As a specialist in advanced robotics technology, Dutch Space is also the prime contractor of the ERA (European Robot Arm), which will be placed at the ISS (International Space Station). A track record stretching back to the early days of the space industry has secured the company's enviable expertise, which has led to close involvement in the ARIANE launcher development and production program. The expertises of Dutch Space are summed below.

- System engineering
- Control engineering
- Mechanical engineering
- Software engineering
- Test and integration

The company mission is to develop, produce and deliver excellent high quality space products translating in value for their customers in a competitive market position. The product range consists of:

- Solar Arrays (ARA III and Flat pack)
- Launching structures (ARIANE 4 and ARIANE 5) and future launchers (VEGA)
- Advanced control systems (ERA)
- Test and validation software systems (Eurosim)
- Earth Observation payload (Sciammachy)

To manage the company into the rnain core business, the company has an organization structure, depicted into the organigram as shown below:

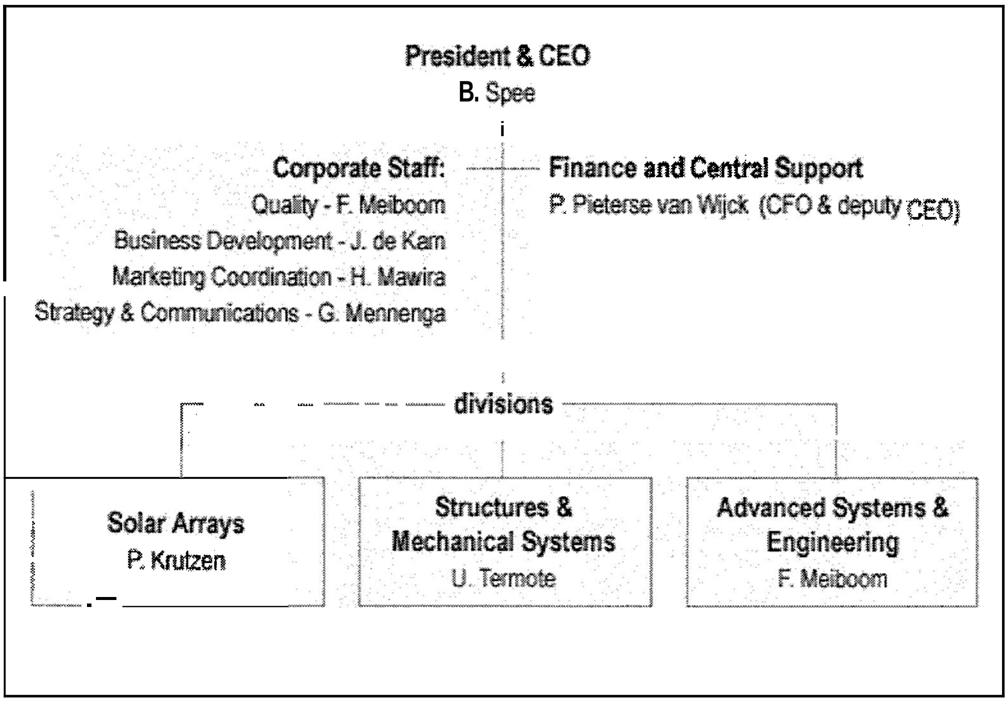

Figure 1-1 Organigram of Dutch Space

Dutch Space consists of three main divisions; Solar arrays, Structures and Mechanical Systems and Advanced Systems and Engineering. This thesis project is written for the division Structures and Mechanical Systems.

1.2 Product Description: The ARIANE 5 Launcher

In the 70s, the Americans and Soviets divided up the launcher market. Little by little, the market rnatured and gradually shifted from a performance-based perspective to the notion of service. This led to the emergence of commercial space transport. In 1973, Europe, concerned with its independence in launcher market field, started the ARIANE program. The first test flight was launched successfully in December 1979.

The name ARIANE, the launchers name, originates from the Greek mythology. In Greek mythology, when Theseus came to Crete to fight the Minotaur, Ariane gave him a ball of thread that helped him find his way out of the labyrinth after slaying the beast.

Very quickly, technical success brought commercial success. Within 12 years ARIANE 1 to 4 had launched over half of the commercial satellites in space. The more powerful ARIANE 5, first launch in 4 June 1996, has now taken over, with the objective of confirming European dominance in the civil launch rnarket, in spite of stiff cornpetition from the United States, Russia, China and Japan. The objective of the ARIANE launchers is to affirm Europe's independency and status in space transport, creating employment and to promote collaboration between industries and between countries.
Some key figures of the ARIANE 5 in dual launch configuration are listed below in table 3.

Table b.1: ARIANE 5 information table

	Total propellant mass	***Launch mass***	***Thrust form boosters @lift off***	***Thrust Vulcain engine @ lift off***	***Dimensions***	***Geostationary transfer orbit lift capacity***
Dimension	650 ton	746 ton	6709 kN	880 kN	Height 46m	5.7 ton ('96) 10 ton ('04) 12.5 ton ('08)

The ARIANE 5 launcher is designed to meet the challenges of the new millennium. The launcher is capable to launch larger satellites in dual launch configuration into GTO. Furthermore, the ARIANE 5 can be used to bring the ATV (mass total max. 20.231kg) into low orbits, approximately 500km. These ATVs are used for instance for sewicing the ISS.
The ARIANE 5 is well known for its high reliability. This is the reason why it is used to launch communication-satellites, earth observation and scientific research satellites into geostationary orbits and Sun synchronous orbits.

The ARIANE 5 launcher is developed and produced under supervision of the ESA, CNES, ARIANEspace and the European industry. Dutch Space has many years of experience in the space industry and in structural analysis. This is partly the reason why Dutch Space is contracted to develop and produce different parts of the ARIANE *5* launcher. The most important part that is developed by Dutch Space (and produced under supervision of Dutch Space) is the BME, or the so-called engine frame.

The ARIANE 5 launcher consists of 6 main parts:

- The Fairing
- The SPELTRA
- The EPS
- The VEB
- The EPC
- The EAP

These 6 main parts is described on the next sub-chapters.

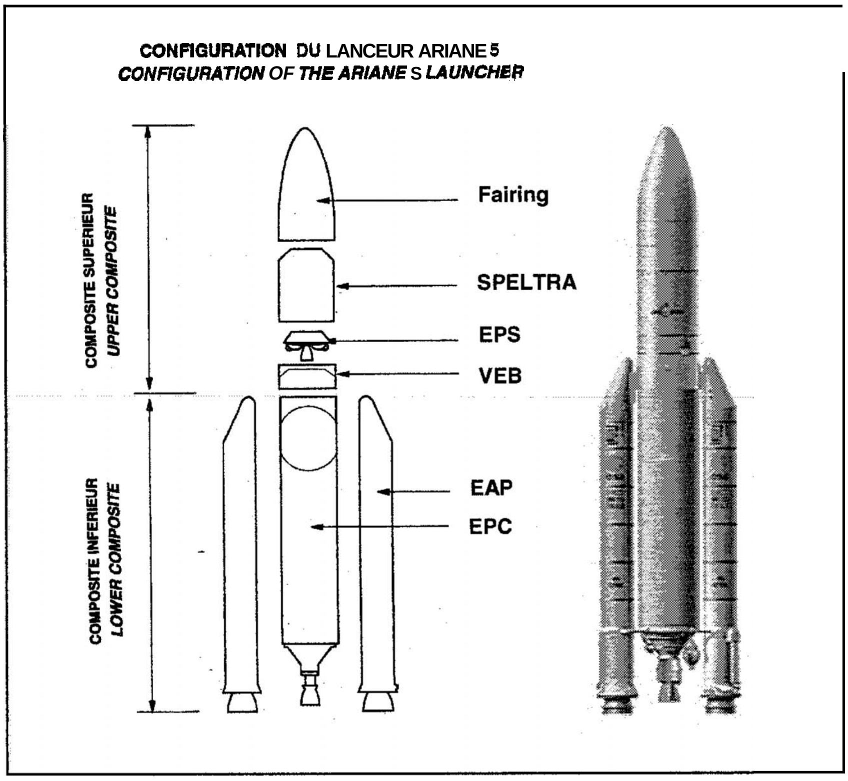

Figure 1-2 Configuration of the ARIANE 5 Launcher

1.2.1 The Fairing

The Fairing (figure 1-3) is the upper Cone structure which protects the payload as the launcher passes through the denser layers of the atmosphere.

Figure 1-3 Fairing

1.2.2 SPELTRA

The SPELTRA (figure 1-4) is a structure which supports the upper and houses the lower payloads. The ARIANE multiple launch external bearing structure known by its French abbreviation as the SPELTRA is used for multiple launches. It enables multiple payloads to be placed in orbit independent of one another.

Fiaure 1-4 SPELTRA

1.2.3 EPS

The EPS {figure 1-5) is the first upper stage developed for ARIANE 5. It propels the launcher's payload to its final orbit and provides an accurate orbital injection.

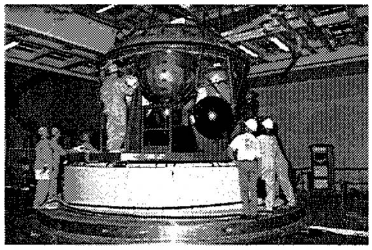

Figure 1-5 EPS

1.2.4 VEB

The VEB (vehicle equipment bay, figure 1-6) provides the flight guidance and other functions.

This is the electronic brain of ARIANE 5, holding in its computer, memory and alf the instructions needed for the flight of the launcher. ARIANE 5 is guided not from the ground but by its own two gyro lase inertial platforms and its two onboard computers.

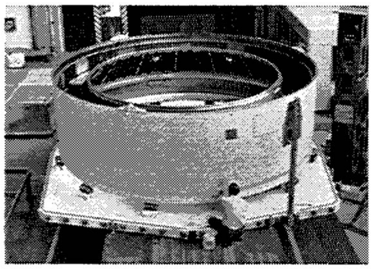

Figure 1-6 VEB

1.2.5 EPC

ARIANE 5's cryogenic **H155** main stage is referred to as the EPC (figure 1-7) from its title in French, Etage Principal Cryotechnique. The EPC is essentially composed of an aluminium tank with two compartrnents: one for liquid oxygen and one for liquid hydrogen.

At the base of the EPC is the Vulcain engine which transfers thrust to the launcher through the BME (Bâti Moteur Equipé) structure. The BME structure also transfers the thrust frorn the two solid boosters into the launcher.

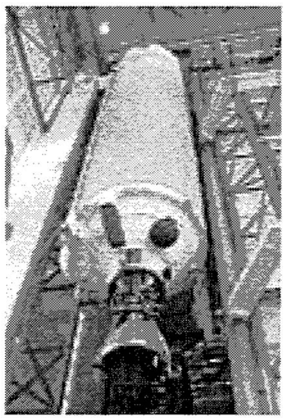

Figure 7-7 EPC

1.2.6 EAP

The EAP (solid propellant booster stage, figure 1-8), covers the launcher's initial propulsion phase and delivering 90% of the liftoff thrust during the first 120 seconds.

Each booster has a forward assembly, with an inclined cone transferring thrust to the core body of the launcher via a forward attachment device with separation systems, and an aft skirt supporting the launcher on the table. The boosters incorporate nozzle actuator units, a set of rear attachment struts and separation systerns.

In some flights, a parachute recovery system is installed in the inclined cone. Dutch Space is responsible for this subsystem.

Figure 1-8 EAP

1.3 Product Description: The EPC-BME

The BME (Bâti Moteur Equipé) is the lower part of the EPC structure. The EPC is a structure that has as main function the storage of the propellant. The main functions of the BME are listed below.

- Transfer the main engine thrust loads into the launcher
- Transfer the loads (from the two EAPs) into the lower attachrnent points, the DAAR-lugs
- Housing the equipment and lines, including feeding connectors
- Withstand connection loads implented by the LBS floor and its line attachment
- Withstand the handling and transportation loads of EPC
- To enable the foad transfer of the servo-actuators for the steering control of the Vulcain nozzle.

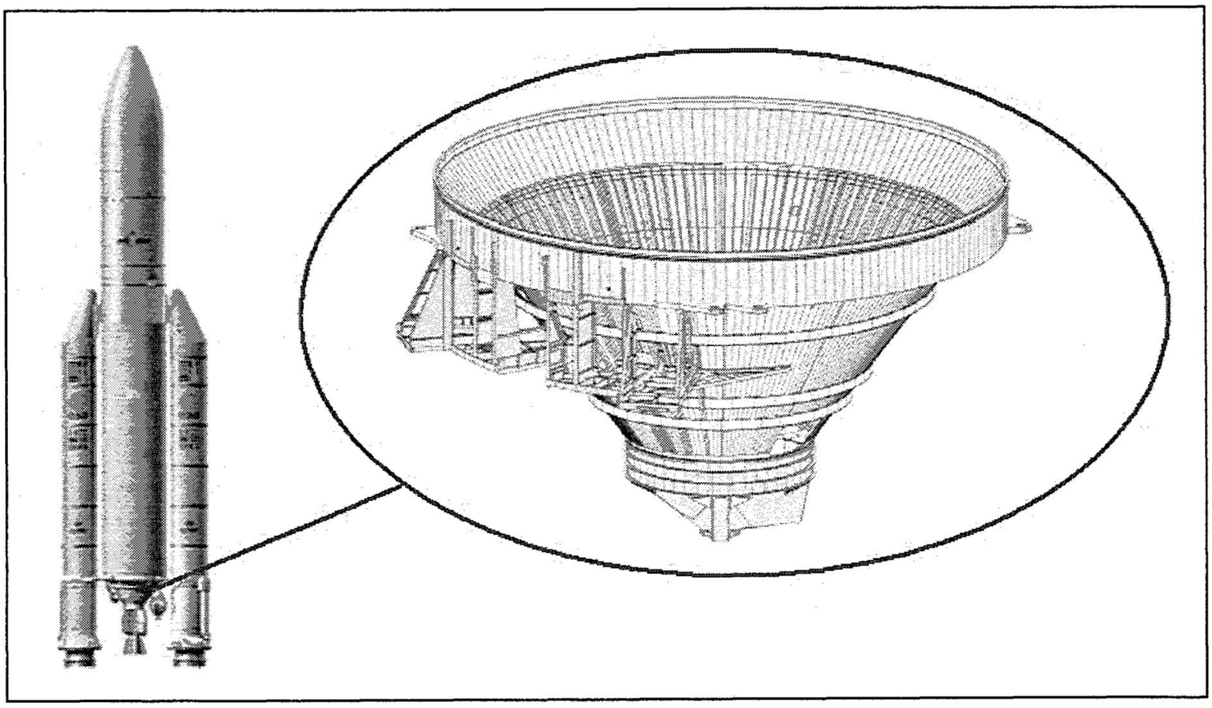

Figure 1-9 Location of the EPC-BME within the ARIANE 5 Launcher

The BME consists of four various mechanical substructures that will be described in section 1.3.1 to 1.3.4. These four substructures are:

- Cross
- Cone
- LBS
- Box

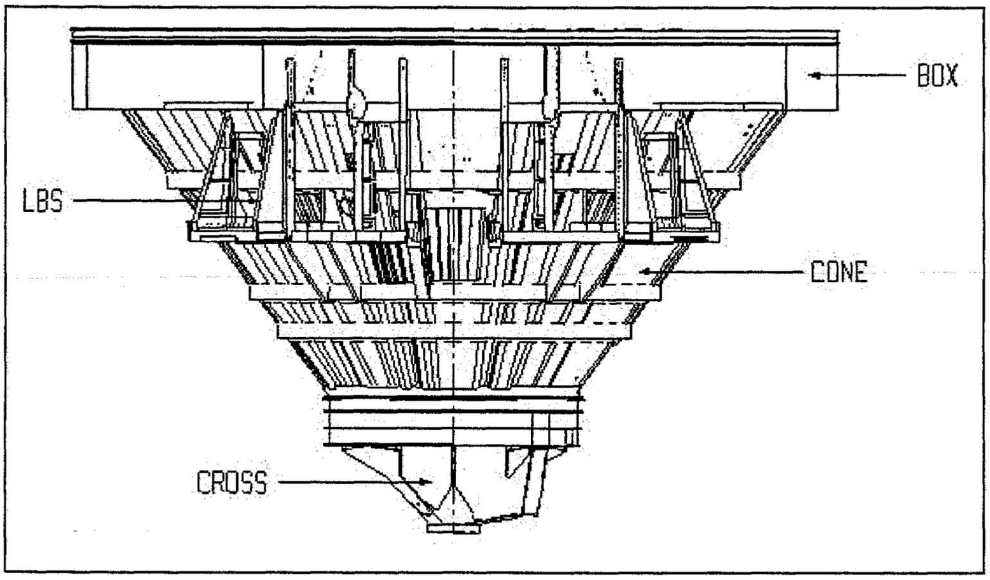

Figure 1-10 The 4 Substructures of the BME

These four substructures are protected by a thermal protection system. Besides thermal gradient due to the environment, the thermal protection system has also to protect the structure to the thermal loads produced by the exhaust gasses of the engine and the cold liquid in the tank. The reason to protect a structure from extreme temperatures is that if the temperature would exceed 300^{0}C, meaning that Aluminum loses its strength properties: the thermal gradient will introduce additional internal stresses in a mechanical structure. The Norcoat layer, a part of the thermal protection system, which is the thermal protection layer, will sacrifice itself during the launch; it will burn up completely during launch.

The BME is one of the most complex structural system of the ARIANE 5, due to the combination of extremely high mechanical and thermal loads, plus the many load introducing interfaces. The complete BME-structure has over 400 interfaces.
Each of these four mechanical structures has several supports and brackets for connection of equipment. This equipment is for instance electrical boxes and feeding lines.

During the lift-off of the ARIANE 5 launcher, the Vulcain engine produces huge noises. This noise can reach up to 150dB. The noise is a form of acoustic dynamic load, and the BME should be resistant to this load.

Figure 1-11 shows the five interface planes of the BME. These interface planes are intended to use it for calculation of mass distribution, inertia values and interface systems. The planes of reference can be defined as follow:

- P1: The interface of the flanged connection between the BME and EPC.
- P2: The interface of the point of attachment of the Vulcain engine to the BME.
- P3: The interface of the LBS disconnection lines between launcher and launcher platform.
- P4: The interface of connection of the lower cross cylinder with the cone structure.
- P5: The interface of connection of the lower cross cylinder with the upper cross.
- {0 0 0} The centre cardan shows the centre of gravity of the Vulcain engine and the primary point for the thrust load introduction.

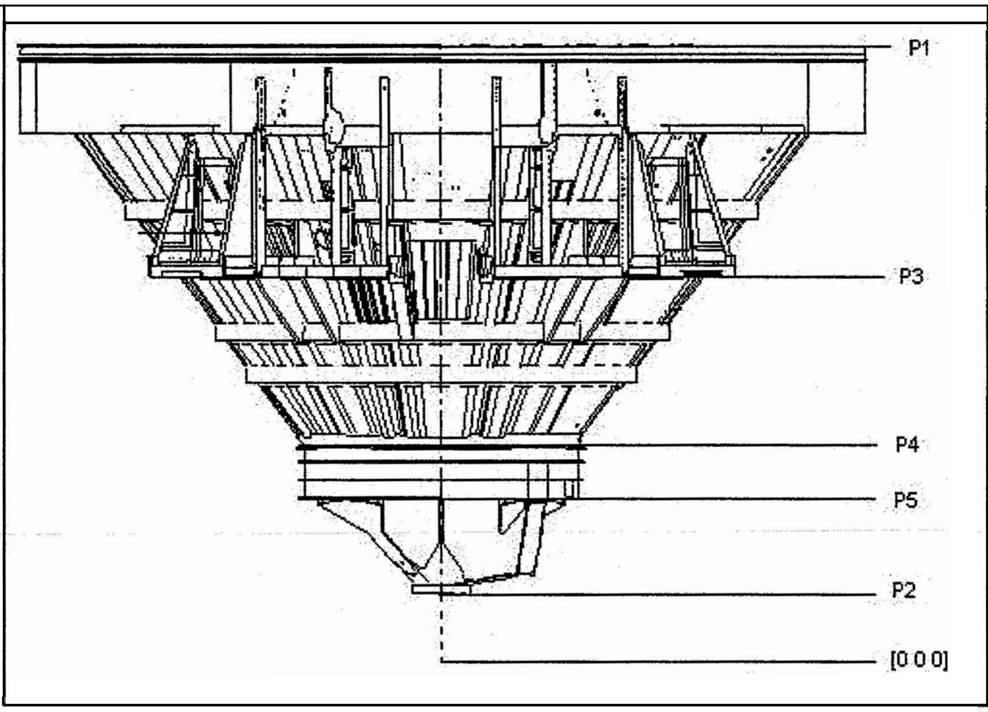

Figure 1-11 The interface planes of the BME

The main point distances are depicted in table 1-2 below:

Table 1-2 The main point distances of the BME

BME part	*Diameter*	*Height*	*Distance*
	mm	mm	mm
Cross			
lower cylinder(from P4-P5)	1795.5	340.500	
lower cross(from P5-P2)	1795.5	610.000	
Cone			
(from connection with box-P4)	5455.0	2042.55	
Box			
from P1-connection with cone	5455.0	526.950	
P1-P2			3520
P1 – Centre Cardan			3660
P2 - Centre Cardan			140

1.3.1 The Cross Structure

The cross structure has to fulfill following tasks:

- Provide the load path by which the forces from the Vulcain engine are transferred into the conical shell structure.
- Provide attachment points and lugs for the Vulcain engine and for the actuators.

The engine thrust load of 200kN in axial direction F_{AX}, and in radial direction F_{RAD}, is the primary load that is acting on the BME. This results in transverse forces, shear forces and bending moments on the rectangular cross section of the cross beam. Due to steering movements during the launch initiated by the Vulcain steering actuators, the cross will also be subjected to torsion. A top view (left) and a side view (right) is given in figure 1-12.

The cross structure is not connected to the LBS. The cross only interfaces with the cone structure.

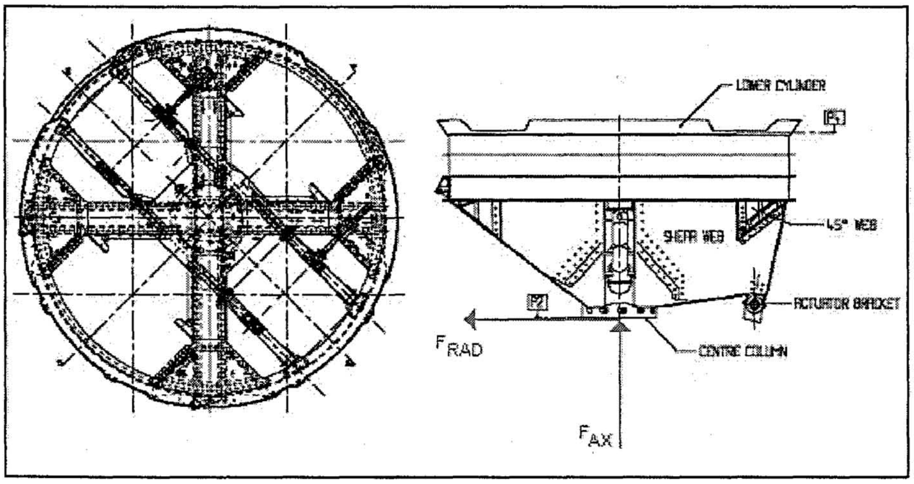

Figure 1-12 The Cross Structure

1.3.2 The Cone Structure

The function of the cone is:

- To transfer the load from the cross structure into the box structure.
- To provide attachment points for the cross, the box and the LBS.
- To provide connection points for equiprnent.

The cone is cornposed by twelve cylindrical panels, which are stiffened axially by twelve integrally machined stringers on the inner side of each panel. To give the cone stiffness in lateral direction and to withstand the shear load, three rings have been attached on the cone. At two of these ring frames, the girders of the LBS are mounted on.

The cone has many line-attachments, equipment supports and brackets. Furthermore, local perturbations, by means of two access hatches and some other holes are presented. Figure 1-13 shows a top view of the cone (left) and a cone section with stiffeners (right).

The LBS-girders and the LBS-lateral stiffeners connect the LBS to the cone. These structures are connected with fasteners.

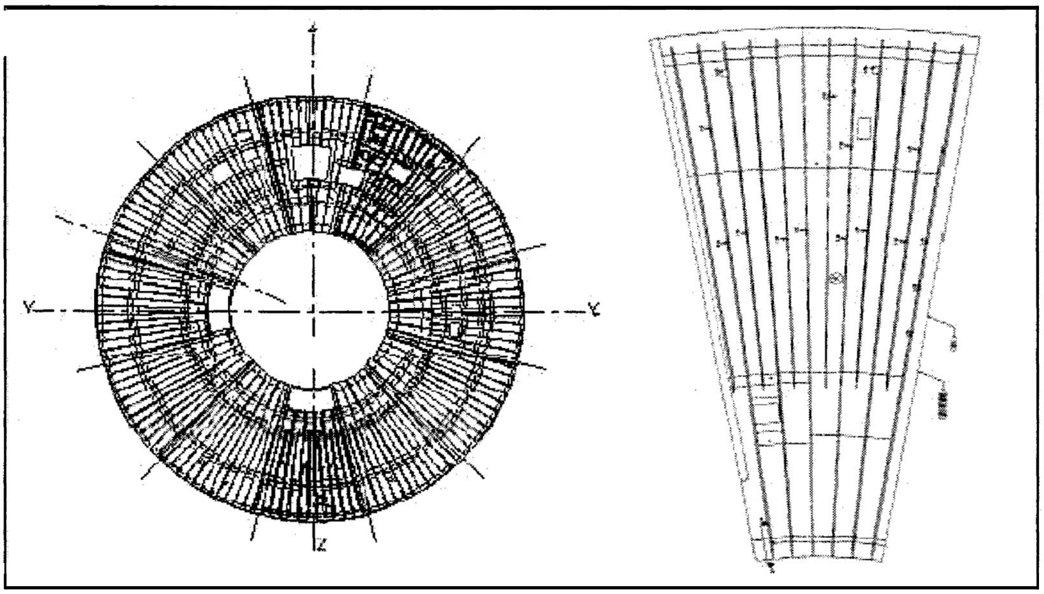

Figure 1-13 The Cone structure

1.3.3 The LBS Structure

During heating up of the Vulcain engine, the engine consumes rocket fuel. At the moment of take-off, the tank is not filled to the maximum because of this heating up. This condition results in an ineffective launcher. This is the reason why the ARIANE 5 is supplied with fuel until take-off. To accomplish this, the LH, and LO_x fuel lines lead from the launch platform to the tank. The function of the LBS is to provide a connection for the both fuel lines between the launch platform and the tank.

The LBS is intended to withstand the disconnection load (e.g. by physical rupture) once the launcher starts its lift-off. This structure will also support several pressurisation lines and perform the connection with the ground platform. The most important part of the LBS is the LBS floor panels. The LBS floors are comprised in two sides: A hydrogen side and an oxygen cide. For the H-side must be sealed in order to avoid contamination with O-side. Otherwise it will explode. The present LBS is depicted in figure 7.14.

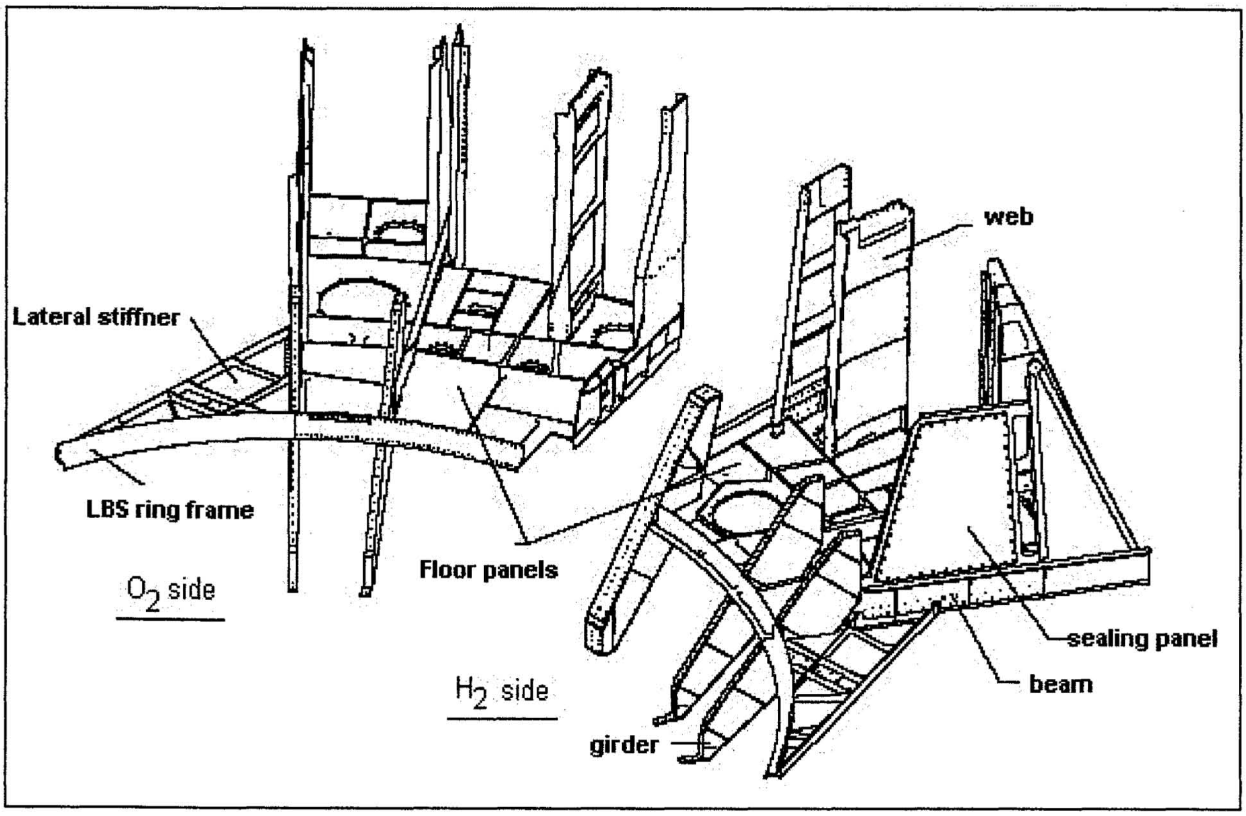

Figure 1-14 The most important parts of the LBS

1.3.4 The Box Structure

The Box structure of the present EPC-BME is depicted in figure 1-15. The box is located at the top of the BME structure and it has interfaces amongst other things with the cylindrical skirt, the EAP's and the RIE tank. The Box Ras multiple functions which can be subdivided into primary functions and secondary functions:

1. Primary functions
   - To ensure the lower mechanical connection between the boosters and the cryogenic main stage (RIE tank)

- To transfer the engine thrust load to the upper structure
- To transfer the loads at the lower attachments of the EAP's (Solid Boosters) into the EPC
- To ensure an even flux distribution

2. Secondary functions
- To ensure the higher mechanical connection between the HeHP sphere and the BME structure
- To ensure the higher mechanical connection between the **GAM** and the **BME** structure
- To ensure a mechanical connection between the SCR and the **BME**

To meet the functions mentioned above, the box shape is designed in such a way that it can withstand the transverse loads from the EAPs and transfers the axial load from the Vulcain engine to the EPC. The top ring interface is the single connection of the **BME** structure with the RIE tank.

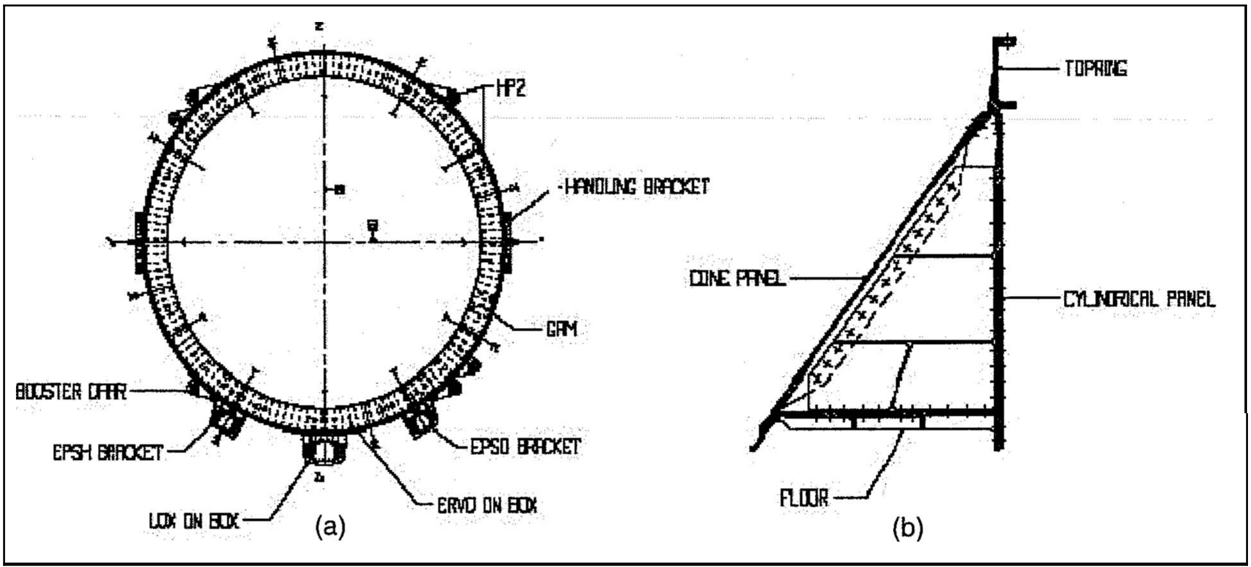

Figure 1-15 The Box structure. (a) Top view. (b) Cross section.

The top interface ring is the single connection of the **BME** structure with the RIE tank. This ring is connected by 360 equal distributed bolts (size M8). The present Box is made up of the following sub parts:

1. Floor segments incl. DAAR lugs
2. Cylindrical Panels
3. Conical Panels
4. Internal web plates
5. Top interface ring
6. LOX support
7. EPSO/H brackets
8. He **HP2** support
9. ERVO support
10. GH support
11. Fairings
12. SCR support
13. Handling brackets (not flight structure)

Sub parts 1-5 are described on the chapter 3, while the others are described on Appendix C.

2. Project Aspects

2.1 Problem Description

The existing BME was successfully launched on various ARIANE 5 launchers (AR501-AR520). Its function is to support and pass on the major Vulcain engine thrust load. From preliminary study which has done in Dutch Space (Internal technical notes; Ref. 5), one preferred concept which is the 'load carrying' skirt concept has been selected. This new cylindrical skirt concept has been chosen primary to reduce costs of the current complicated high cost structure. On the contrary, the concept is vulnerable to buckling. The design has now been made of a cone / box concept. It has been envisaged that alt equipment is installed inside the cone and therefore requires a considerable integration effort.

Within the design process, there are 2 considerable problems, i.e.:

- Buffeting problem
- Out-of-date finite element model

These problems are described on the next sub-chapters.

2.1.1 Buffeting Problem

Buffeting loads occur during the first part of the flight (180 seconds into flight). The buffeting loads are caused by aerodynamic currents, being instable at subsonic speeds.

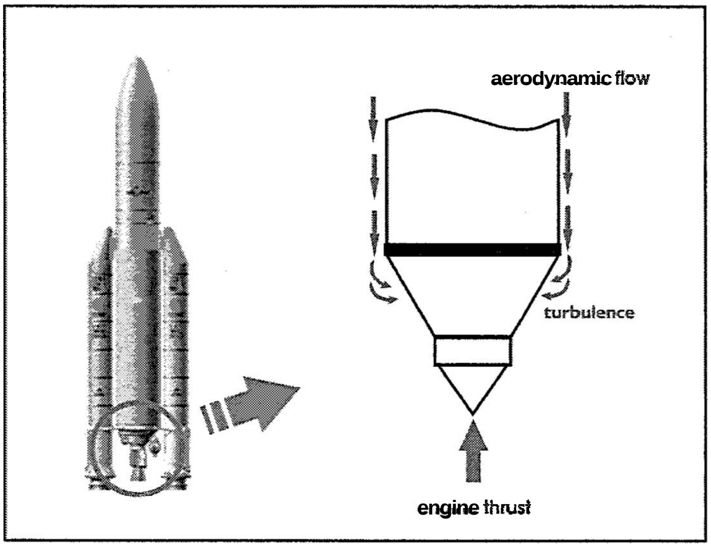

Figure 2-1 Buffeting problem

During the first part of the flight, which occurs in atmospheric environment, there is an aerodynamic flow along the surface of the ARIANE 5. At the position of the BME, the smoothly flowing, laminar airflow is disrupted, due to the shape of the BME. This phenomenon is called turbulence. Hence, the flow is called turbulent flow.

The variable pressure cause unpleasant vibration on the lower structure, mainly on the Vulcane engine.

Still it is thought that the introduction of an aerodynamic skirt could solve this problem. For that reason, this project is focused to design the skirt and analyze the impact of the skirt to the existing BME.

2.1.2 Out-of-Date Finite Element Model (FEM)

The design process of the skirt needs a structural analysis to be carried out.

For the ARIANE-5 project the current structural analyses of the Bati Moteur Equipe (BME) are carried out with a finite element model (FEM) which was created in the late eighties. The way in which the model was created was rather coarse with respect to today standards. This had to do with the limited computer resources and power by the time the model was created.

As the design changed, the model was updated, resulting in higher model versions and in 1994 the model was correlated with a structural test. The result of this update was model version 04. Nowadays four different model versions are used. This is caused by the fact that the current design comprises two versions: the **P2.1** series and the **P2.2** series (the latter one is also referred to as the PA-version). Furthermore the more powerful Vulcan II engine is introduced. All possible design options are reflected in the different finite element models.

It is thought that it is not very useful to stick to updates of the current (outdated) model. It is better to create a complete new model with a sufficient fineness and consequently accuracy, and reflecting the latest design changes. Nevertheless creating such a FEM remains very laborious and time-consuming. Therefore the following approach is adopted. The BME-model is split up in four main parts. Each main part is modeled by somebody else. In order to keep the model generation costs as low as possible, students will perform the task, of course supervised by DS-analysts and people.

However the individual FEMs need to be coupled afterwards. In order to be able to do so, appointments and requirements are needed to smooth the coupling process. Especially at the interfaces between the four main parts a clear definition of the number and location of the nodes is required; otherwise coupling becomes far more difficult. These requirements and appointments are described in Appendix B.

The following table gives the division in main parts and the responsible student.

Table 2-1 The division of the BME structure and responsible student to build the finite element model

Division of the BME in four main parts and responsible person		
BME-main part	**Student**	**From Insitute**
BM€-Box	I.H. Nugroho	HvU
BME-Cone	Guo Yunyan	HvU
BME-Cross	Timon Duurkoop	HTS-Eindhoven
BME-LBS	Tim Garritsen	TU-Delft

Thus, one of this project's goal is to build a detailed finite element model of the BME-Box structure and compare the result with the result of the old model. A comparison with hand calculation is also needed in order to verify the result.

2.2 Study Goal

There are two main issues of the project's goal, i.e.:

1. The detailed finite element model of the BME Box structure which fulfill the requirements and appointments to be the basis of the structural analysis.
2. The design concept of additional skirt with the optimum dimension in order to minimize the mass increase.

Then the wanted results will be:

1. A detailed finite element model of the BME Box structure shall be generated to be the basis of the structural analysis
2. The hand calculation of the BME Box structure shall be done in order to verify the result of the finite element analysis
3. Have maximum 3 design concepts of the skirt to be attached to the existing BME structure
4. The optimization of the skirt dimension in order to minimize the mass increase
5. The impact of the skirt addition to the stiffness of the existing BME should be analyzed.

2.3 Problem Approach

In order to achieve the study goal as defined above, the envisaged investigation was formulated into the following phases:

1. Familiarization about the ARIANE project in general and in detail
   The purpose is to investigate and understand the problem. This step is done with survey of existing documentation concerning ARIANE project.

2. Review of the technical drawing
   This step is done in order to understand the geometry of the structure. Discussion with the experts is also done to obtained comprehension of the drawing and the structure as well.

3. Generate requirements for the detailed finite element model of the Box structure
   The requirements for the detailed FEM of the Box structure is generated based on the interface control document (Appendix B) and the load case of the Box structure.

4. Generate design requirements for the skirt
   The design requirements will be the result of the study literature and discussion with the experts. The design requirements are the starting point of the design process.

5. Generate simple hand calculation of the existing Box structure
   A simple hand calculation is needed in order to verify the result of the finite element analysis. The hand calculation is made by simplifying the Box structure as a ring with uniform cross section.

6. Build the detailed finite element model of the existing Box structure
   The detailed FEM is made based on the technical drawing and as detail as possible. The model will be built using MSC-PATRAN software as pre- and post processor and MSC-NASTRAN software as finite element analysis package.

7. Verify the result of finite element analysis with the hand calculation
   As mentioned above, the result of the finite element analysis should be verified with the hand calculation. The comparison between the old model, the detailed model, and the hand calculation will be the basis of the structural analysis of the skirt.

8. Generate the design concepts for the skirt
   In order to understand the Cone-Skirt concept, review of the previous studies should be done. The design concepts for the skirt will be generated by considering 4 main aspects of the skirt, i.e.:
   - The shape of the skirt
   - The shape of the stiffener
   - The concept for the bottom part
   - The level of attachment of the bottom part

   This step determines "Top 3 design concepts

9. Select the preferred concept using the trade-off matrix
The Top 3" design concepts will be analyzed by the trade-off matrix, regarding the skirt design requirernents

10. Optimize the skirt dimension
The purpose of the skirt optimization is to minimize the mass. It will minimize the increase of the BME total mass. Consequently, minimize the cost.

1 Analyze the impact of the skirt to the existing BME
Even though the skirt is not a load carrying part, the addition of it will give impact to the loading condition of the existing BME. The impact to be analyzed is the impact of the skirt to the stiffness of the BME.

The flowchart of the project is depicted below.

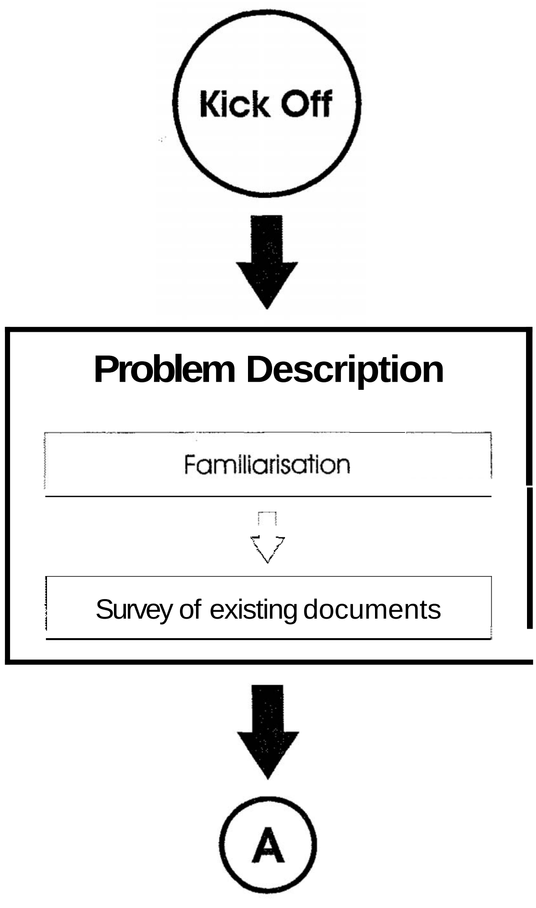

Dutch Space
P.O. Box 32070
2303 DB LEIDEN
The Netherlands

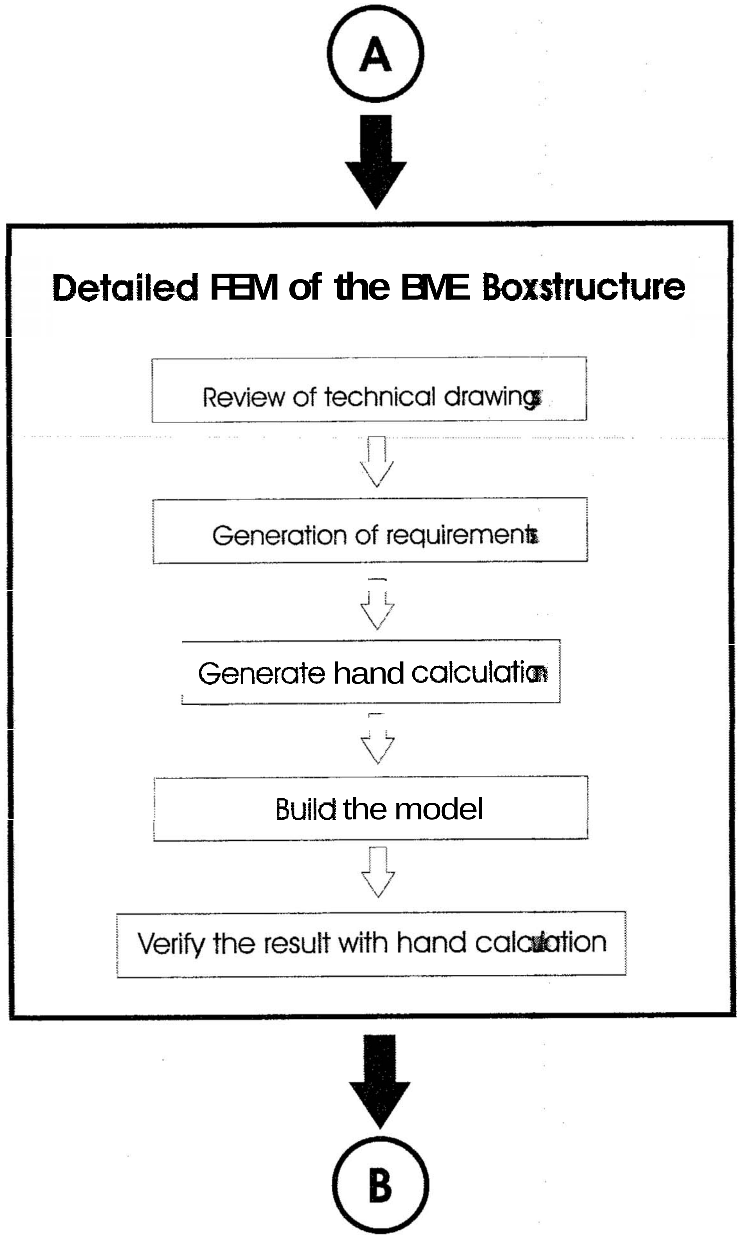

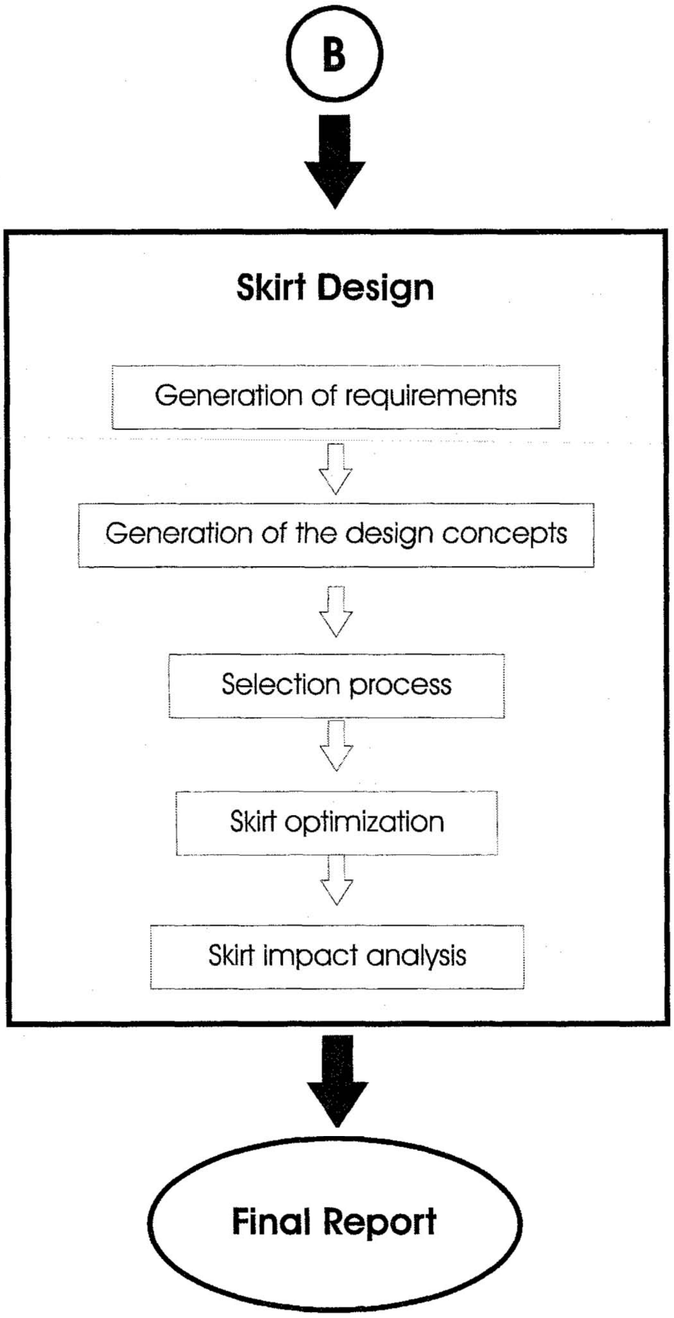
B
Skirt Design
Generation of requirements
Generation of the design concepts
Selection process
Skirt optimization
Skirt impact analysis
Final Report

3. Finite Element Model (FEM) Description of ARIANE 5 EPC-BME Box

As mentioned on section 2.1.2, it is needed to generate a detailed finite element model of the BME. It is also mentioned that in order to time- and cost saving, the BME structure is split to 4 main parts and each will be modeled by one student.

This section describes the finite element model of the ARIANE 5 EPC-BME Box which will be crosschecked with the original model and the hand calculation.

3.1 Requirements for the FEM

The main objective of the detailed finite element modelling is to verify the applicable strength and stiffness requirements of the ARIANE 5 EPC-BME. Therefore, all analysis needed should be possible to be perforrned with this model. Those analyses are:

- Static analysis
  In order to calculate the strength and stiffness of a structure, the first analysis to be done is static analysis. One of the outcomes of the analysis is displacement. Dividing the applied load with displacement, the stiffness of the structure can be obtained.
  In this study, the static analysis will be done considering the engine load in axial and lateral direction and the DAAR loads.

- Buckling analysis
  Buckling anafysis is one of the important structural analyses. Since the critical buckling load is rnuch lower than the yield strength of the material.
  The loading condition of the BME and the geometry of the BME itself make the BME vulnerable to buckling. Therefore, the buckling analysis should be done.

- Mass calculation
  A mass calculation with NASTRAN can be used to determine the centre gravity of the Box structure.

3.2 Unit System of Measures

Table 3-1 Used units

Quantity		Unit	
Mass	M	Kilogram	Kg
Force	F	Newton	N
Length	L	Meter	M
Time	t	Second	S
Frequency	f	Hertz	Hz
Angle	a	Radial	Rad
Angular velocity	ω		rad/sec

The drawings are dimensioned in mm.
Dimensions in the Finite Element Model are in m.

3.3 Drawing Tree

Figure 3-1 shows a diagram of technical drawing of the BME-Box structure. Only drawings with shaded block will be modelled in this study. The equipment brackets are not modelled in this study.

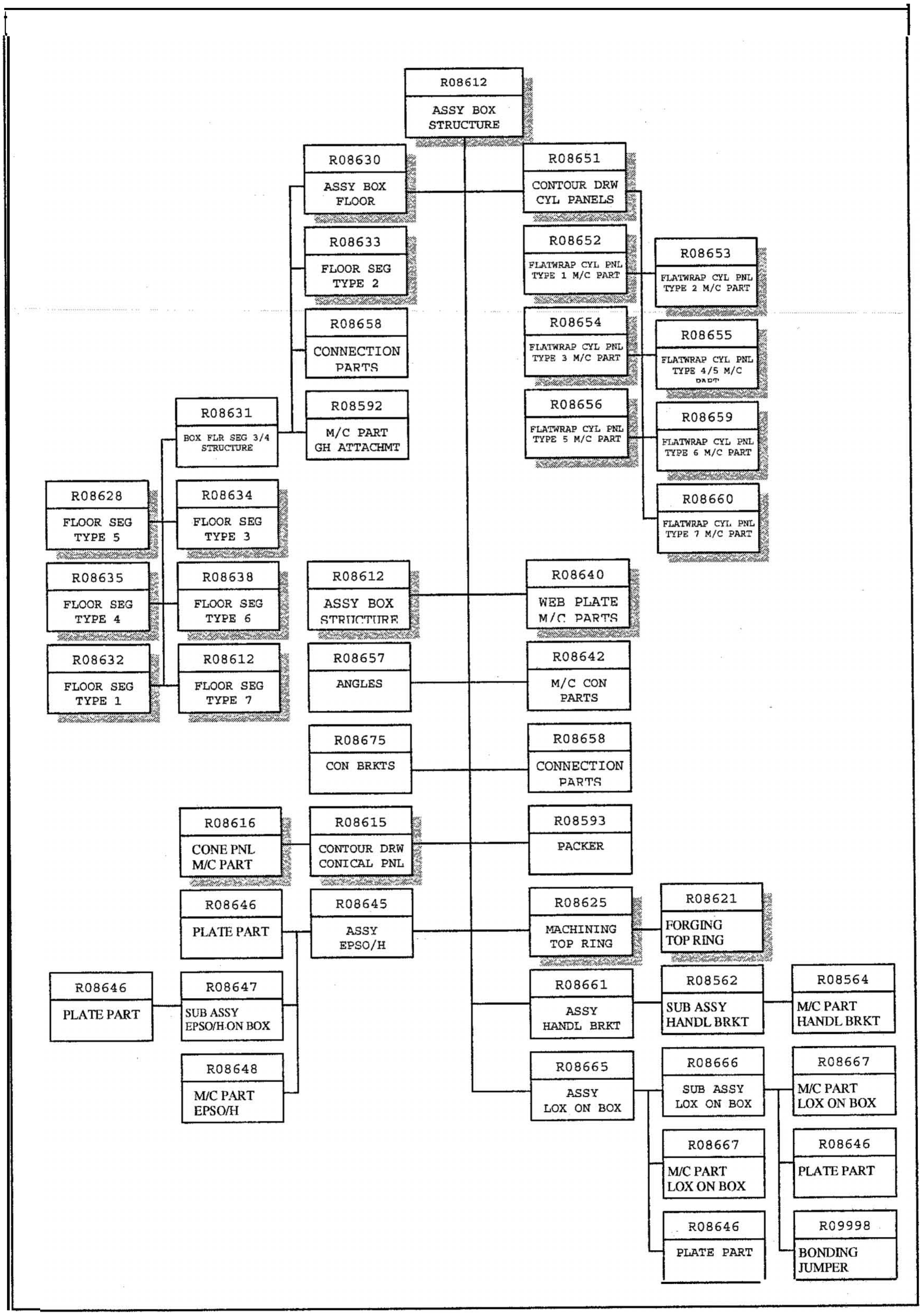

Figure 3-1 Drawing Tree of the ARIANE 5 EPC-BME Structure

3.4 General Description

This model only represents 5 main parts of the ARIANE 5 EPC-BME Box, i.e.:

- Box floor with DAAR lugs
- Conical panels
- Cylindrical panels
- Web plates
- Top interface ring.

The figure 3-2 shows the 5 main parts.

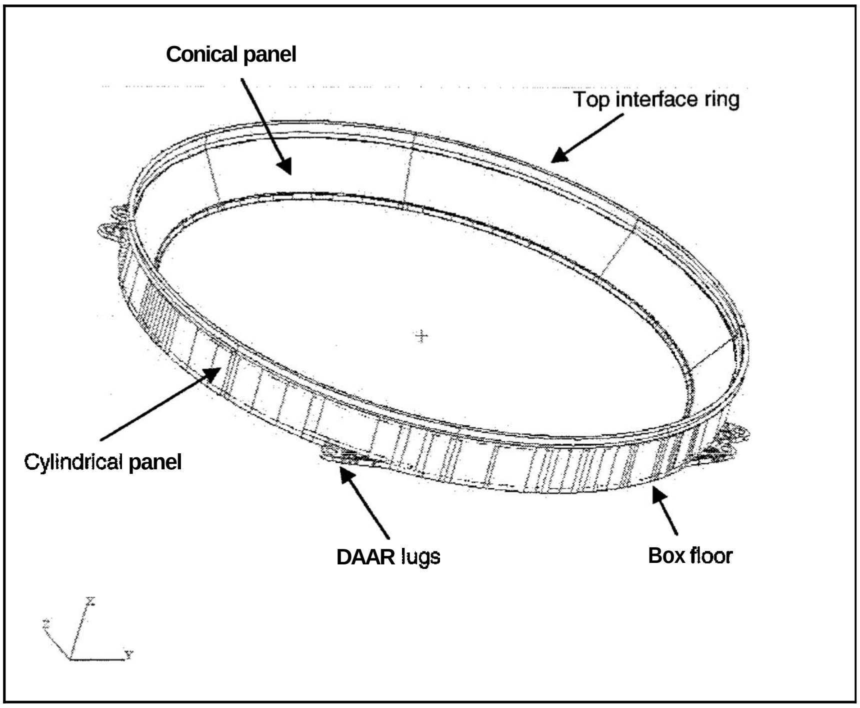

Figure 3-2 The ARIANE 5 EPC BME Box Structure

The connections within those parts are modelled with equivalence nodes. Equivalence nodes means more than one node is connected and consequently has exactly the same displacements.

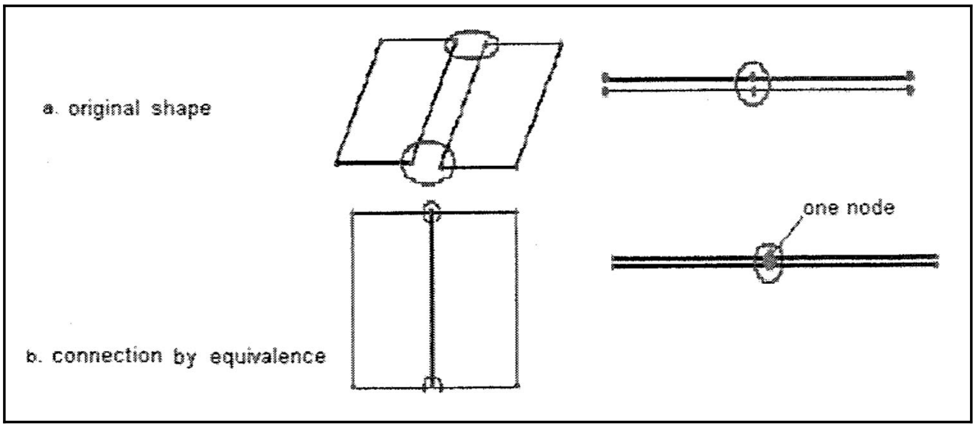

Figure 3-3 Connection by equivalence nodes

The majority of elernents in the Box model consist of CQUAD4 shell elements, to represent its plate shape. The description of the element type is described on Appendix D.

The radii in the corners of the plates have not been modelled, which can give unrealistic stress level at these locations.

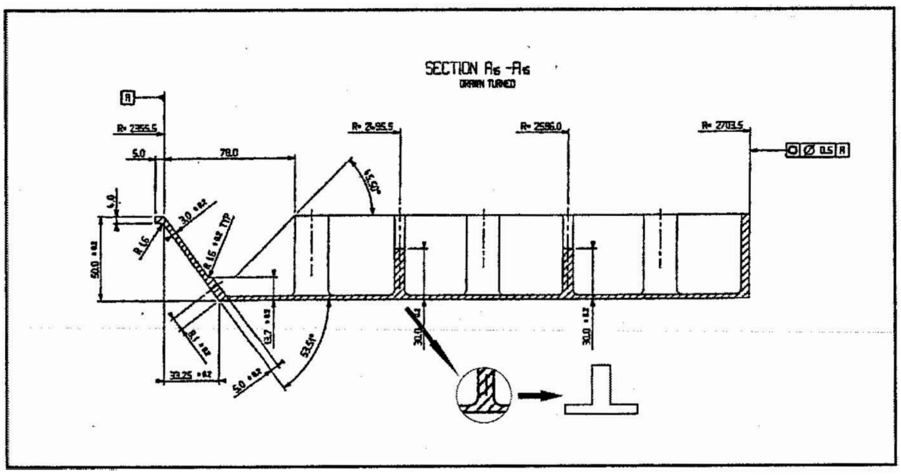

Figure 3-4 Simplification of the radii in the corners

On the box floor, the plate thickness which is lower than ***6*** mm has no offset (internal ref. 1). Plates having thickness higher than 6 mm will be modelled with CHEXA elements (solid). Figure 3-5 shows the simplification of the box floor thickness.

CHEXA efements also applied on the DAAR lugs and the top interface ring. It gives more detailed geometry, as required by the purpose of this model.

The stiffeners in the conical panels are modelled with CQUAD4 elements in order to obtain the detail geometry.

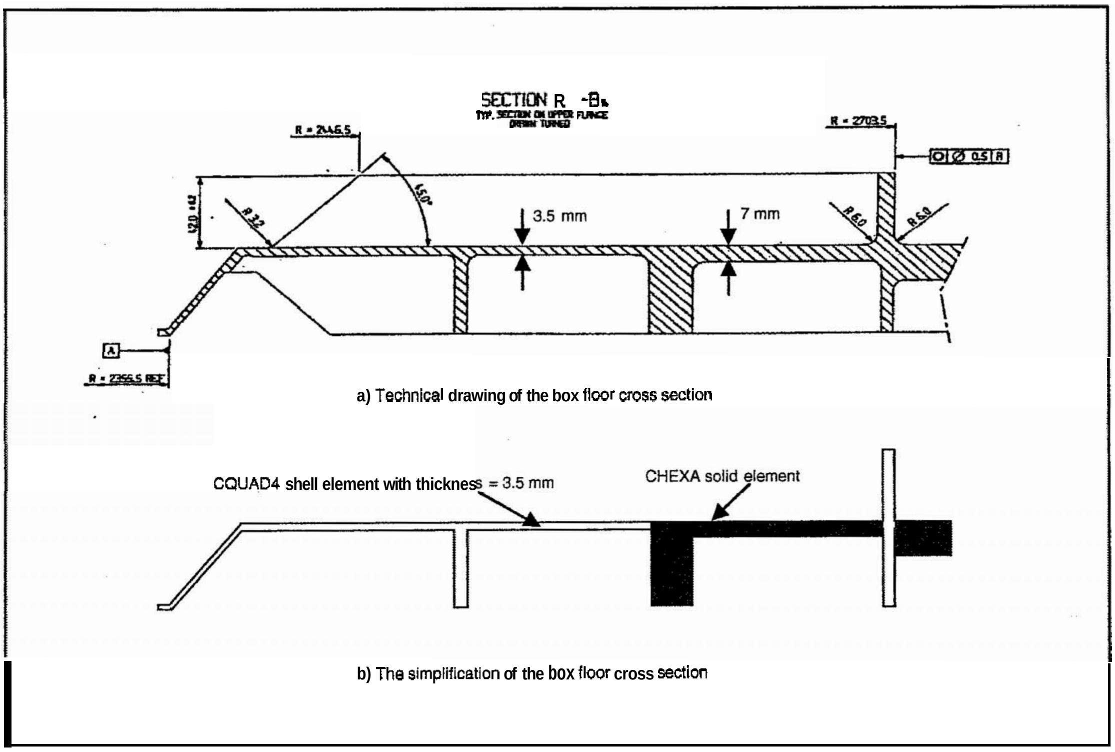

a) Technical drawing of the box floor cross section

b) The simplification of the box floor cross section

Figure 3-5 Simplification of the Box floor thickness

The figure 3-6 shows the flowchart of the modeling process.

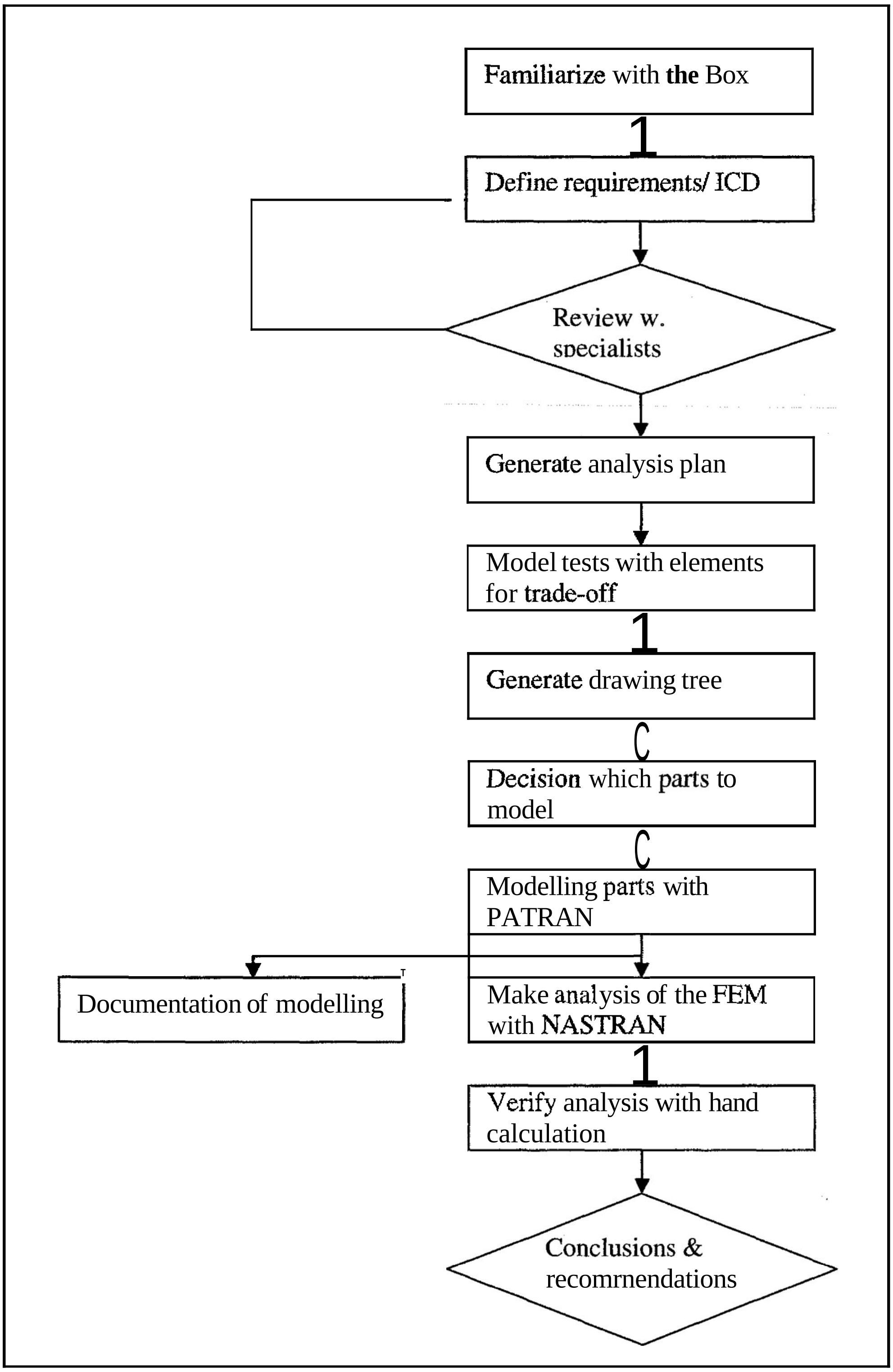

Figure 3-6 The flowchart of the modeling process

3.4.1 Model summary

The following table presents the total number of Grid points and Elements in the model of the ARIANE 5 EPC-BME Box (no adjacent structures applied). The numbering is based on the BME Interface Control Document.

Table 3-2 Model summary

Type of card	Total number
GRID	**434793**
CQUAD4	**358118**
CTRIA3	**2034**
CHEXA	**106229**
CPENTA	**3367**

Table 3-3 Nodes and elements numbering

part	Node nr.	Element nr.
Box floor	1000000 - 1187677	1000000 - 1170632
Conical panel	1200000 - 1277780	1200000 - 1276320
Stringer	1300000 - 1322764	1300000 - 1318246
Cylindrical panel	1400000 - 1478345	1400000 - 1479344
Internal web	1500000 - 1587675	1500000 - 1597653
Top I/F ring	1600000 - 1641762	1600000 - 1640320

3.4.2 Coordinate frames

The origin coordinate system (coord. 0) of the BME-Box model is defined at the base of the box floor. This coordinate system is shown in figure **3-7.**

There are also 10 local coordinate systems which are defined in order to build the geometry of the box structure. These coordinate systems are defined based on the local coordinate system in the technical drawing of 8 box floor segments. Figure **3-8** shows the local coordinate systems.

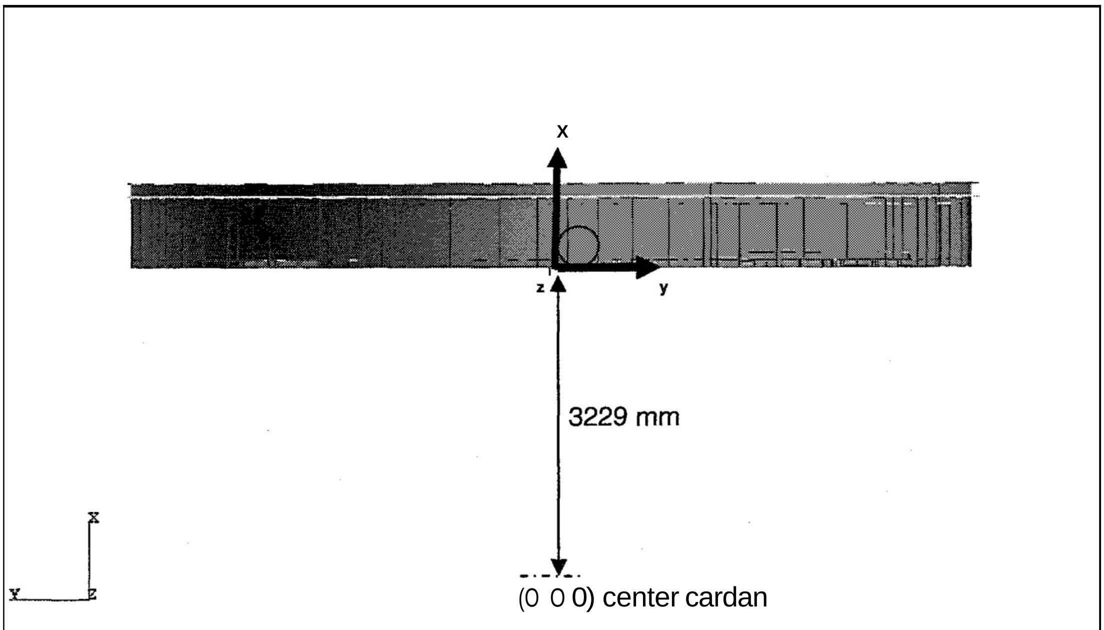

Figure 3-7 Basic coordinate system (Coord).) of the Box FEM

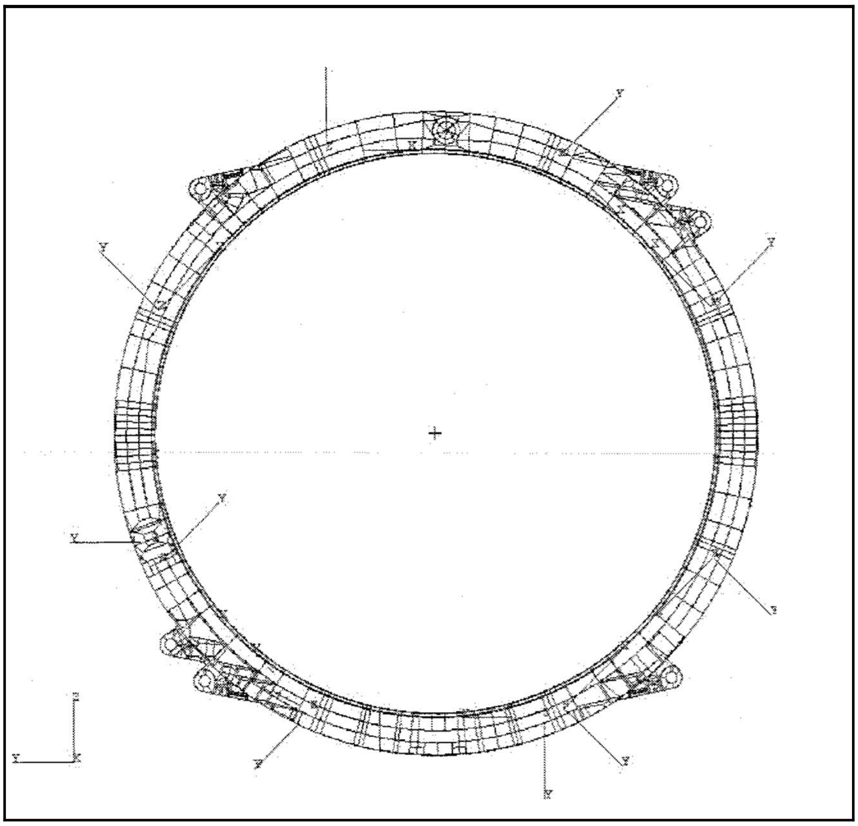

Figure 3-8 Local coordinate systems

3.4.3 Analysis code compatibility

The model is designed for the MSC NASTRAN analysis code (version 2004)

3.4.4 Pre/post processor compatibility

Pre- and post-processing are performed with MSC. PATRAN (version 2004), by importing the NASTRAN .BDF bulk data file(s) and .OP2 file for generating graphics. Before post processing, the .F06 file should be checked for "FATAL ERROR" and "WARNING" messages.

3.5 Finite Element Modeling

This section presents the detailed description of the geometry and modelling of the Box parts:

- Top I/F ring
- Box floor
- Box webs
- Conical panels
- Cylindrical panels

3.5.1 Top I/F ring

3.5.1.1 Top I/F ring description

For the existing BME, the top interface ring which is part of the Box assembly is the mechanica1 interface between the BME and the RIE tank. The connection is performed by 360 equidistant M8 bolts. For this purpose the ring has 360 holes of diameter 9mm. The bolts are placed at a pitch diameter of 5435 mm.

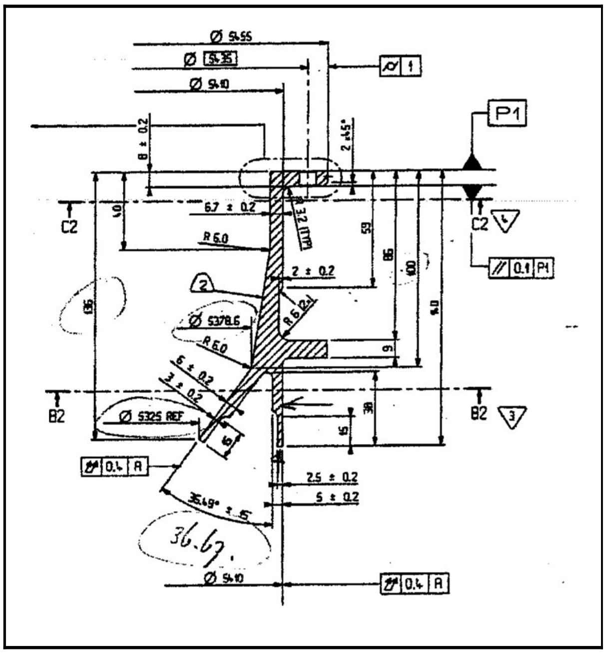

Figure 3-9 Top //F ring dimension

The top I/F ring also connects the conical box panels and the cylindrical box panels.

3.5.1.2 Top I/F ring model

The top I/F ring is modelled based on the technical drawing R08625 – 003. The assembly is described on the technical drawing R08612 – 807.

The top I/F ring is modelled by solid elements as depicted in the Figure 3-10. Radii in the corners are not considered, which is the worst case for stress calculations. In this model, the holes for bolts are not modelled. The material of the top I/F ring is Al7075-T7351 die forging (heat treated, precipitation hardened).

Table 3-4 Top I/F ring material data

Part of the structure	*Top I/F ring*
Material	Al 7075 T7351 (TH 5.31 615)
E(c) [N/m^2]	73×10^9
E(t) [N/m^2]	71×10^9
P [N/m^2]	27×10^9
Φ [kg/m^3]	2800
Poisson's ratio	0.33

The top I/F ring is meshed in circumferential direction. Each segment is 1° wide.

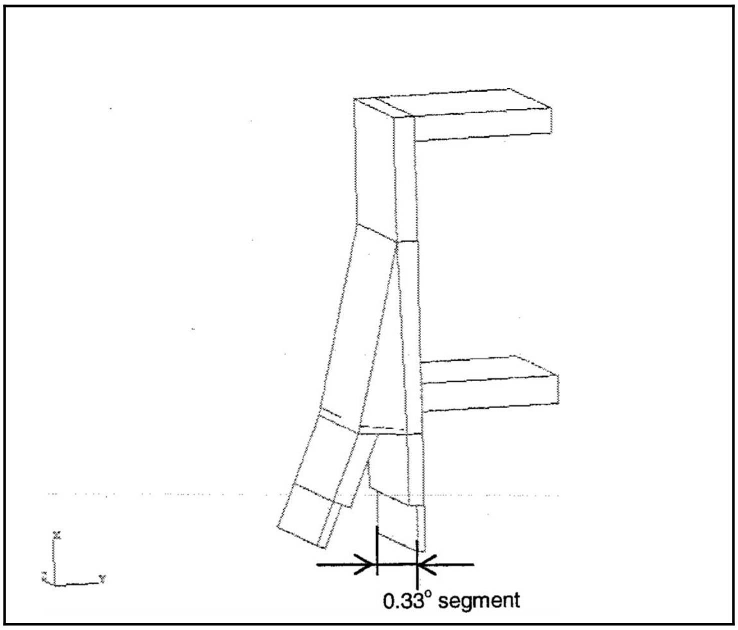

Figure 3-10 Top I/F ring segment showing solid eiements

NASTRAN input **for** the element **properties:**

```
$ Elements and Element Properties for region : solid-mat3165
PSOLID   4        3165    0
MAT1     3165     7.1+10          .33      2800.
```

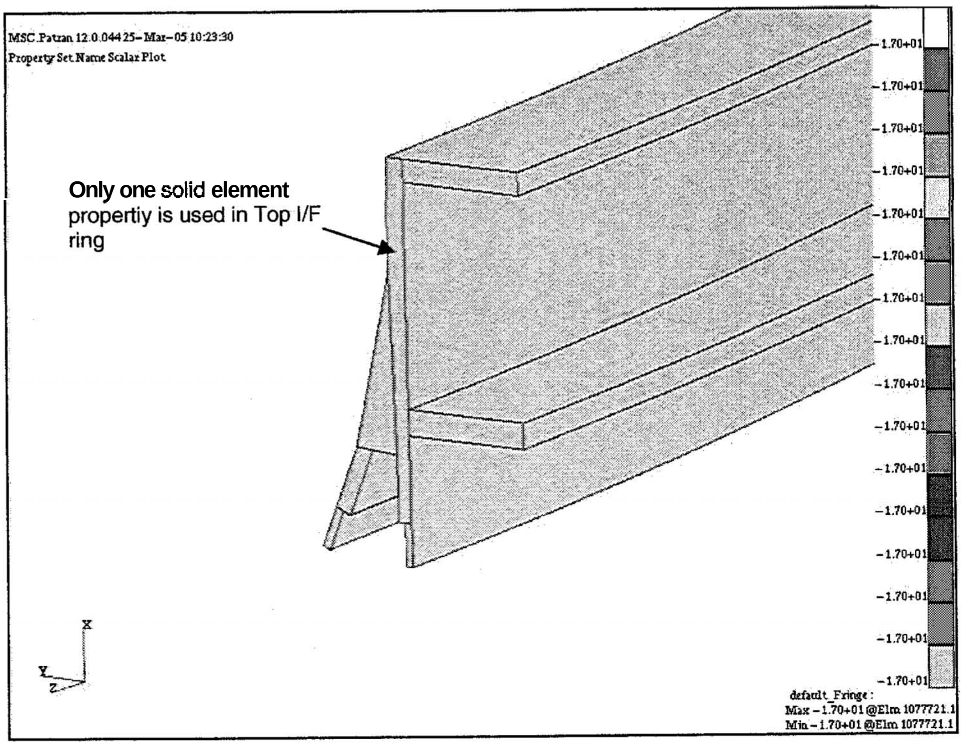

Figure 3-11 Elements in the top I/F ring model

3.5.1.3 Top I/F ring interfaces with other Box parts

The top I/F ring is connected to the conical panels and the cylindrical panels. These connections are modelled by means of equivalence nodes. Figure 3-12 shows the technical drawing of the connections (taken from **R08612 –** 087). Then Figure 3-13 shows the connections in the model.

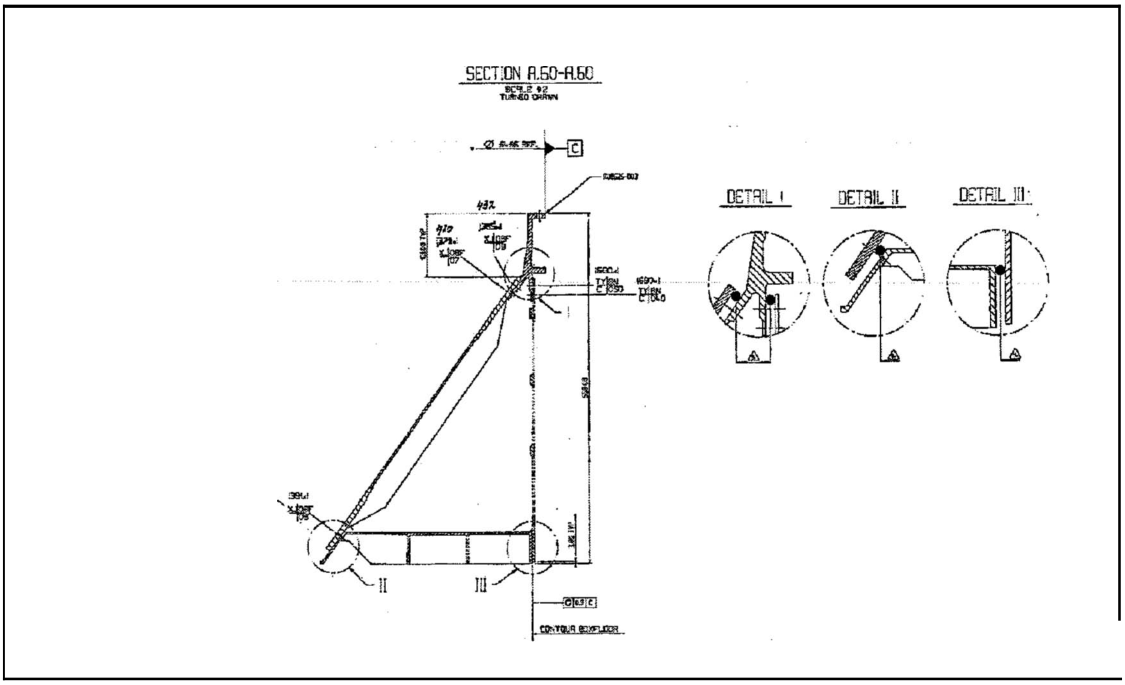

Figure 3-12 Connections between the box parts

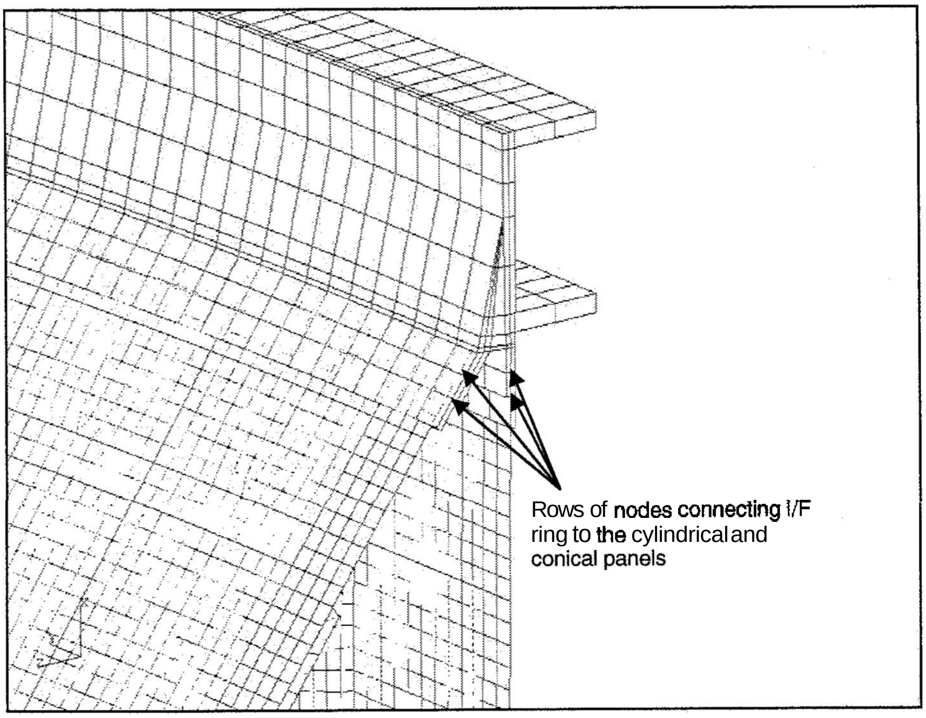

Figure 3-13 Connections of the Top I/F ring to the conical panels and the cylindrical panels

3.5.2 Box floor

3.5.2.1 Box floor description

The box floor has three functions, which are:

- To ensure the mechanical connection to the cone structure
- To ensure the mechanical connection to EAP booster (by means of the DAAR lugs)
- To ensure the mechanical connection to the thermal dome (through the cylindrical panels and the top I/F ring)

The box floor consists of **8** segments, which are described on the drawing:

- **R08631 - 457**
- **R08631 - 451**
- **R08633 - 007**
- **R08631 - 447**
- **R08631 - 455**
- **R08631 - 453**
- **R08631 - 459**
- **R08631 - 449**

The assembly is described on the drawing **R08612 - 087**

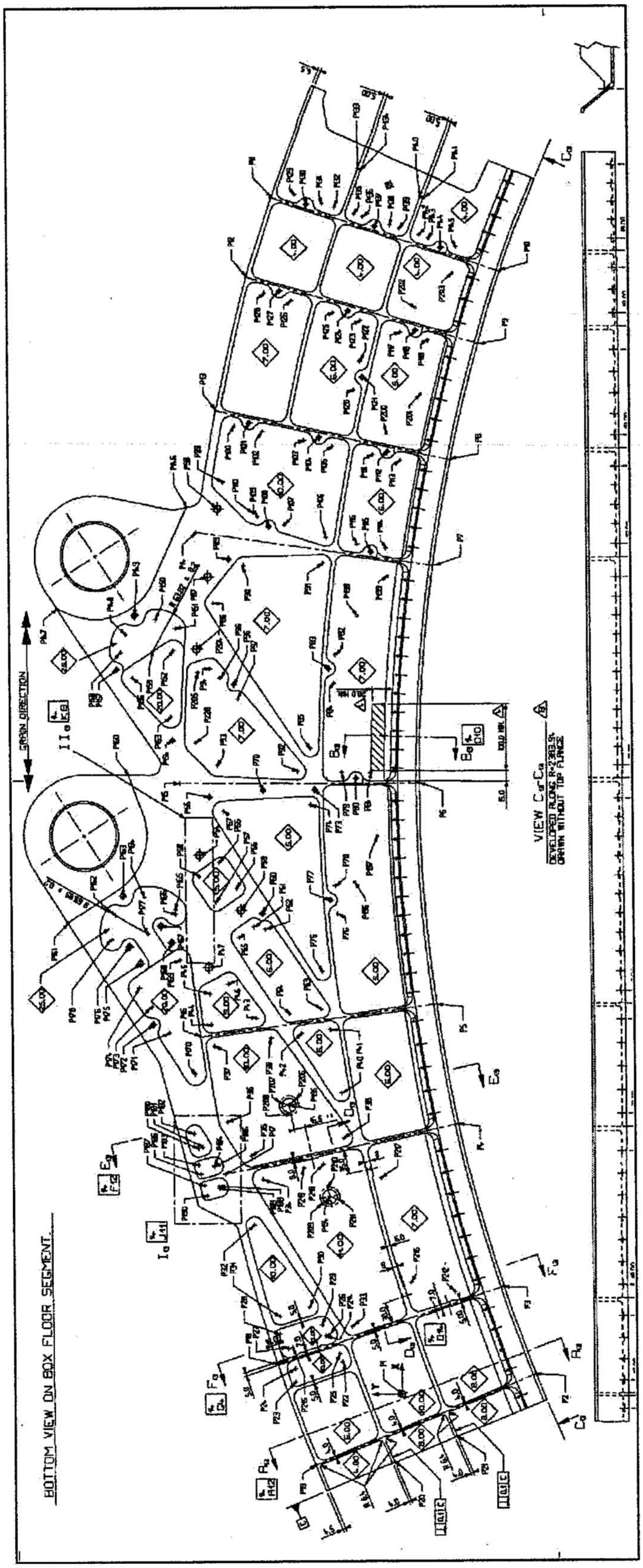

Figure 3-14 Bottom view of a Box floor segment with DAAR lugs

3.5.2.2 Box floor model

In order to build a detail FE model, the box floor is modelled mainly with CQUAD4 (shell) and CHEXA (solid) elements. Using iso-mesh method, consequently there are CTRIA3 and CPENTA elements within the box floor. The description of the element type is depicted on Appendix D.

The plate elements representing the top surface of the box floor have been given an offset of 3mm. Because the plane in which the box floor nodes are defined is located 3 mm below the top surface of the actual box floor, all box floor plates having a thickness higher than 6 mm are modelled by solid elements.

Radii in the corners are not considered.

The radial box floor stiffeners are modelled with plate elements, even if have thickness bigger than 6 mm.

Table 3-5 Box floor material data

Part of the structure	*Boxfloor*
Material	Al 7075 T7351 (TH 5.316/5)
E(c) [N/m^2]	73 x 10^9
E(t) [N/m^2]	71 x 10^9
ρ [N/m^2]	27 x 10^9
Φ [kg/m^3]	2800
Poisson's ratio	0.33

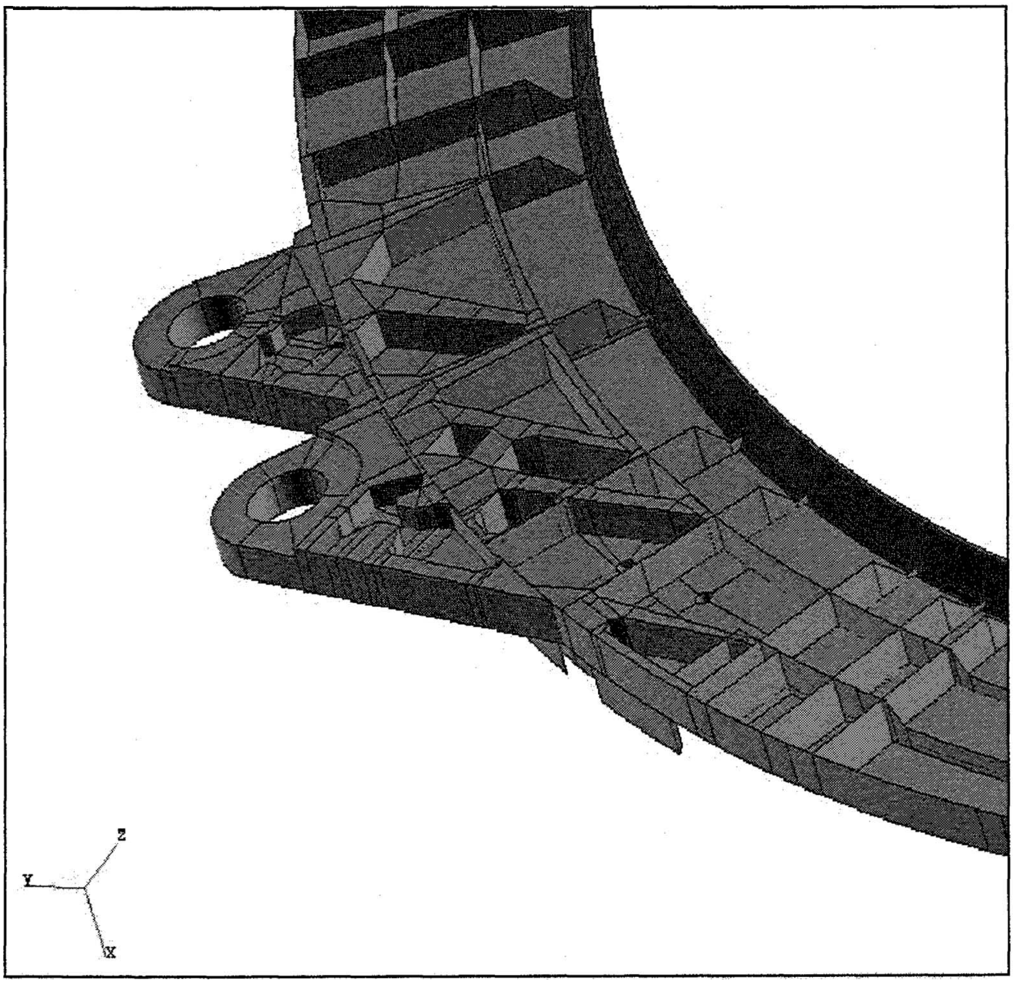

Figure 3-15 Schematization of box floor segment t with DAAR lugs

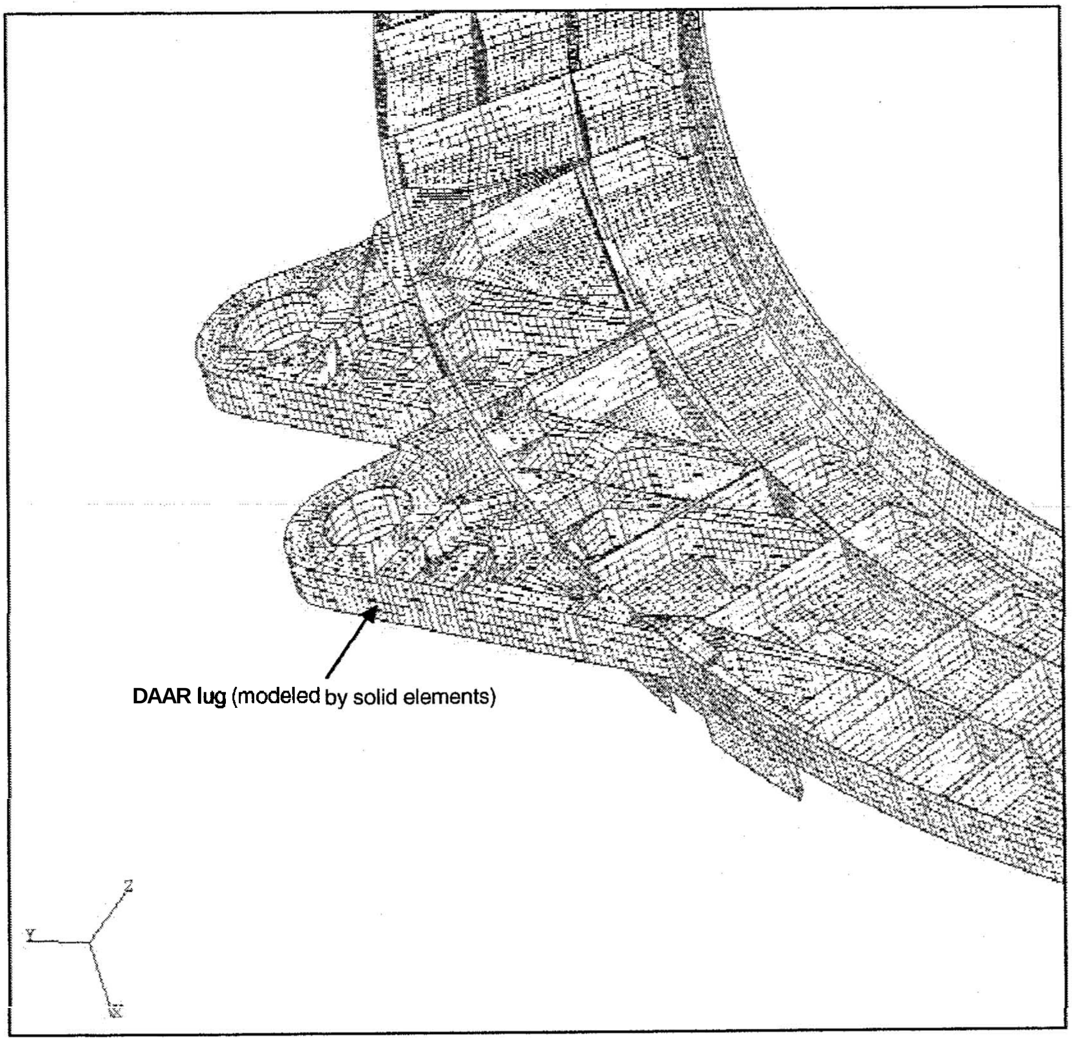

Figure 3-16 Model of box fioor segment with DAAR lugs

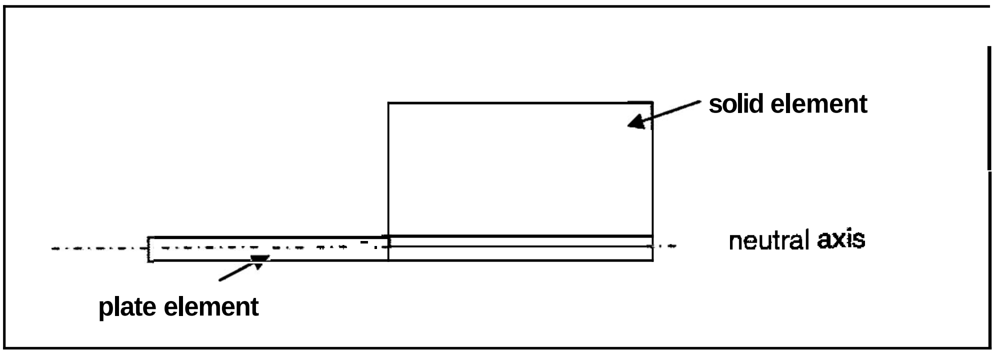

Figure 3-17 Plate and solid elements connection

NASTRAN input for the element properties :

```
$ Direct Text Input for Bulk Data
PSHELL    1       3165    .002    3165            3165
PSHELL    5       3165    .0025   3165            3165
PSHELL    4       3165    .003    3165            3165
PSHELL    7       3165    .004    3165            3165
PSHELL    9       3165    ,0045   3165            3165
PSHELL    10      3165    .005    3165            3165
PSHELL    6       3165    .0316   3165            3165
PSHELL    2       3165    .0262   3165            3165
PSHELL    11      3165    .0182   3165            3165
PSHELL    12      3165    .0222   3165            3165
PSHELL    13      3165    .0195   3165            3165
PSHELL    14      3165    .006    3165            3165
PSHELL    15      3165    .008    3165            3165
PSHELL    16      3165    .0065   3165            3165
PSHELL    17      3165    .0125   3165            3165
PSHELL    18      3165    .0035   3165            3165
PCOLID    19      3165    0
$ Referenced Material Records
$ Material Record : 5.3165Aluminum7075
MAT1      3165    7.1+10          .33     2800.
```

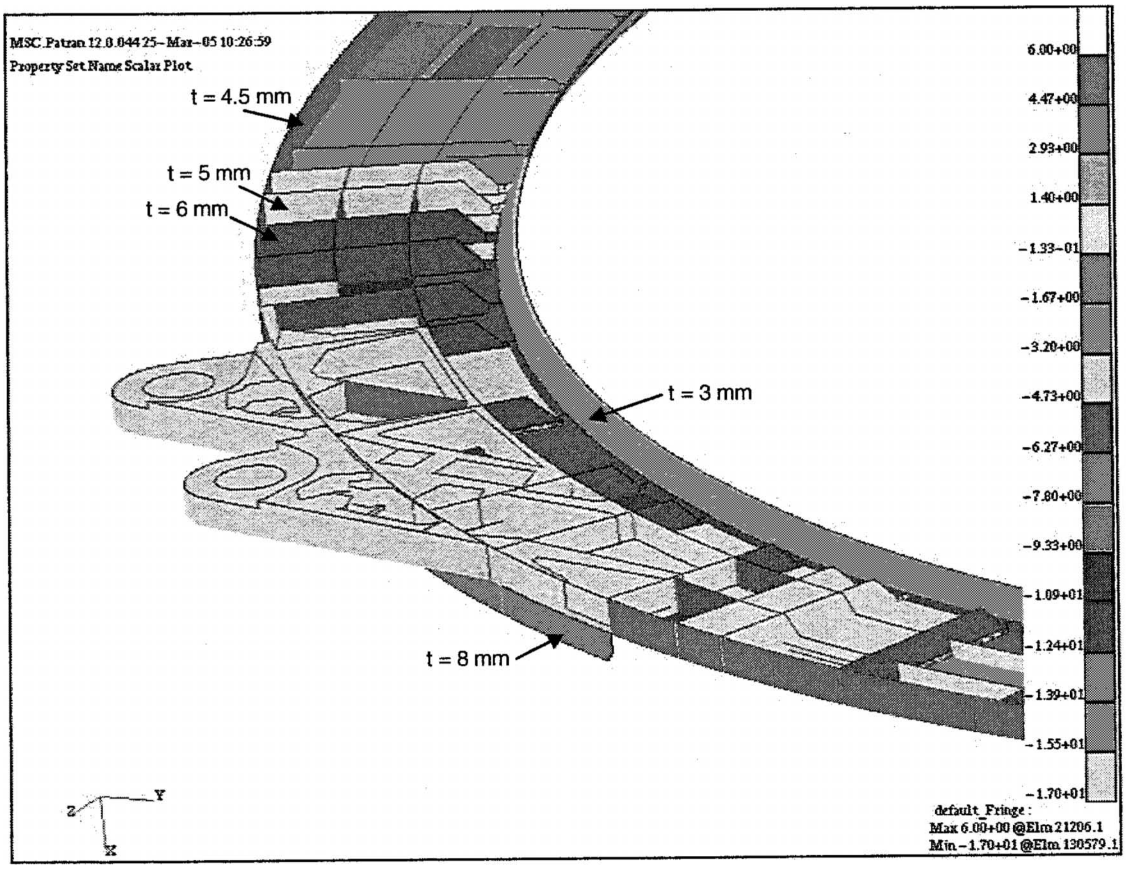

Figure 3-18 Element thickness in the box floor model

3.5.2.3 Box floor interfaces with other Box parts

To transfer the axial load frorn the Vulcan engine and the radial load from DAAR lugs to the top I/F ring, the box floor is connected to the conical and the cylindrical panels. The connection is represented by equivalence nodes. The technical drawing of the connection depicted on the Figure 3-12

Figure 3-19 shows two rows of nodes which connect the box floor with the conical panels, while the Figure 3-20 shows the connection between the box floor and the cylindrical panels.

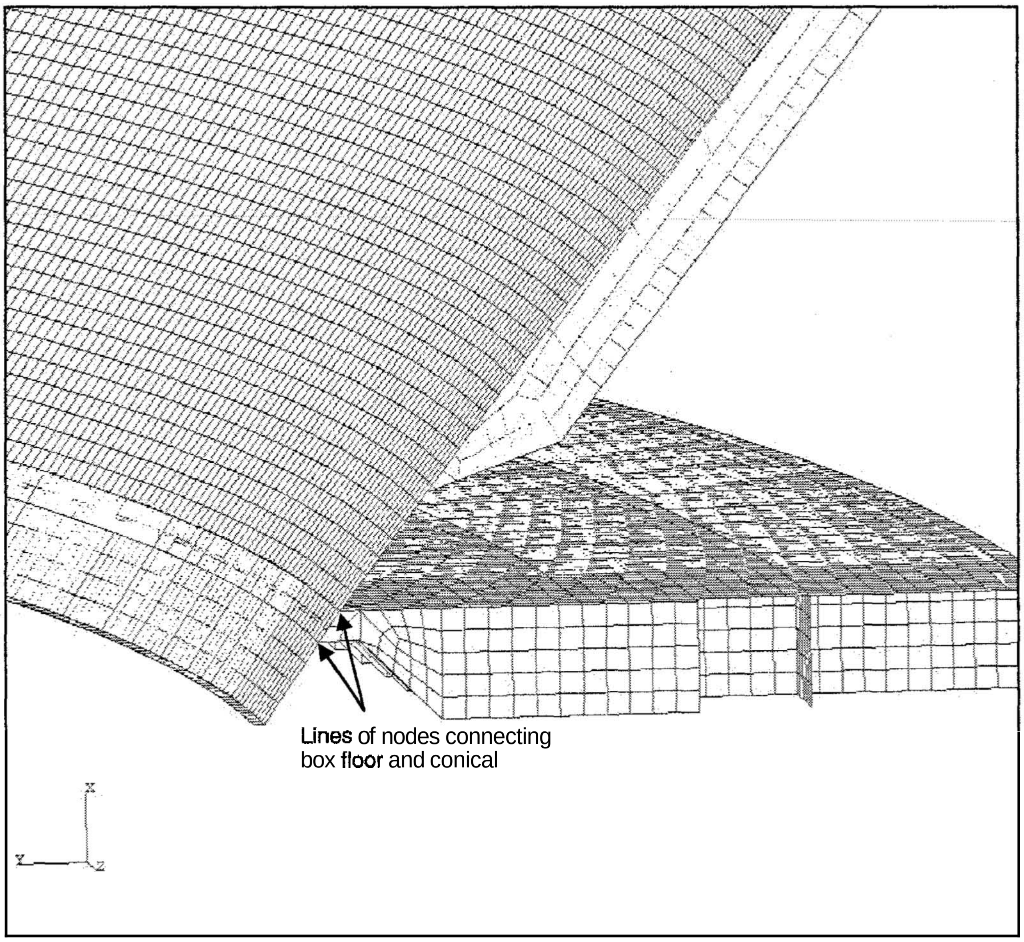

Figure 3-19 shows the equivalence nodes which connect the box floor with cylindrical panels.

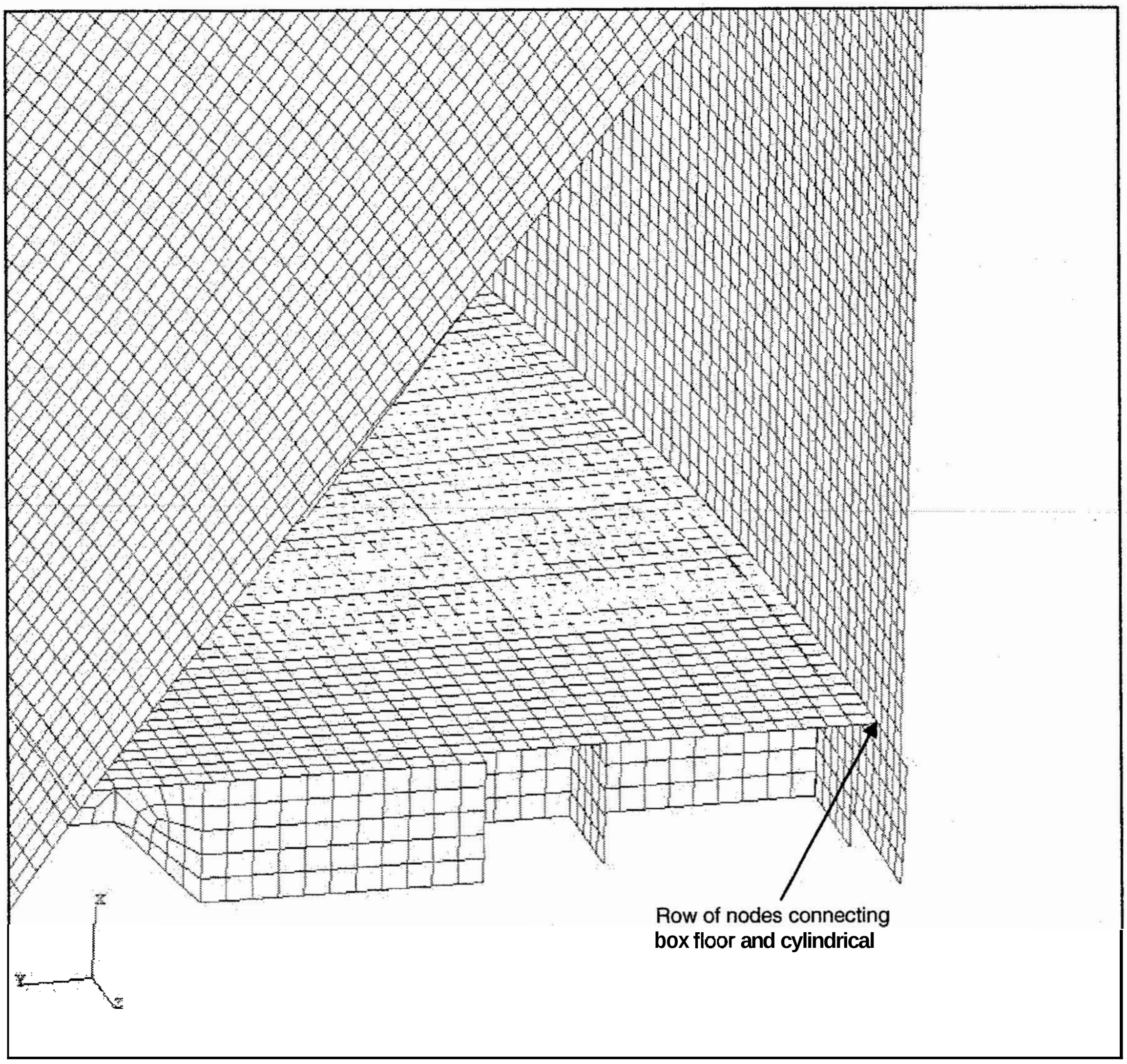

Figure 3-20 Nodes connecting box floor and cylindrical panels

3.5.3 Box web

3.5.3.1 Box web description

The function of the web is to provide radial stiffness of the box structure. There are 34 box webs within the box structure. Reference is made to drawings R08640 and R08612 - 087.

Figure 3-21 taken from drawing R08640-079 shows one of the webs.

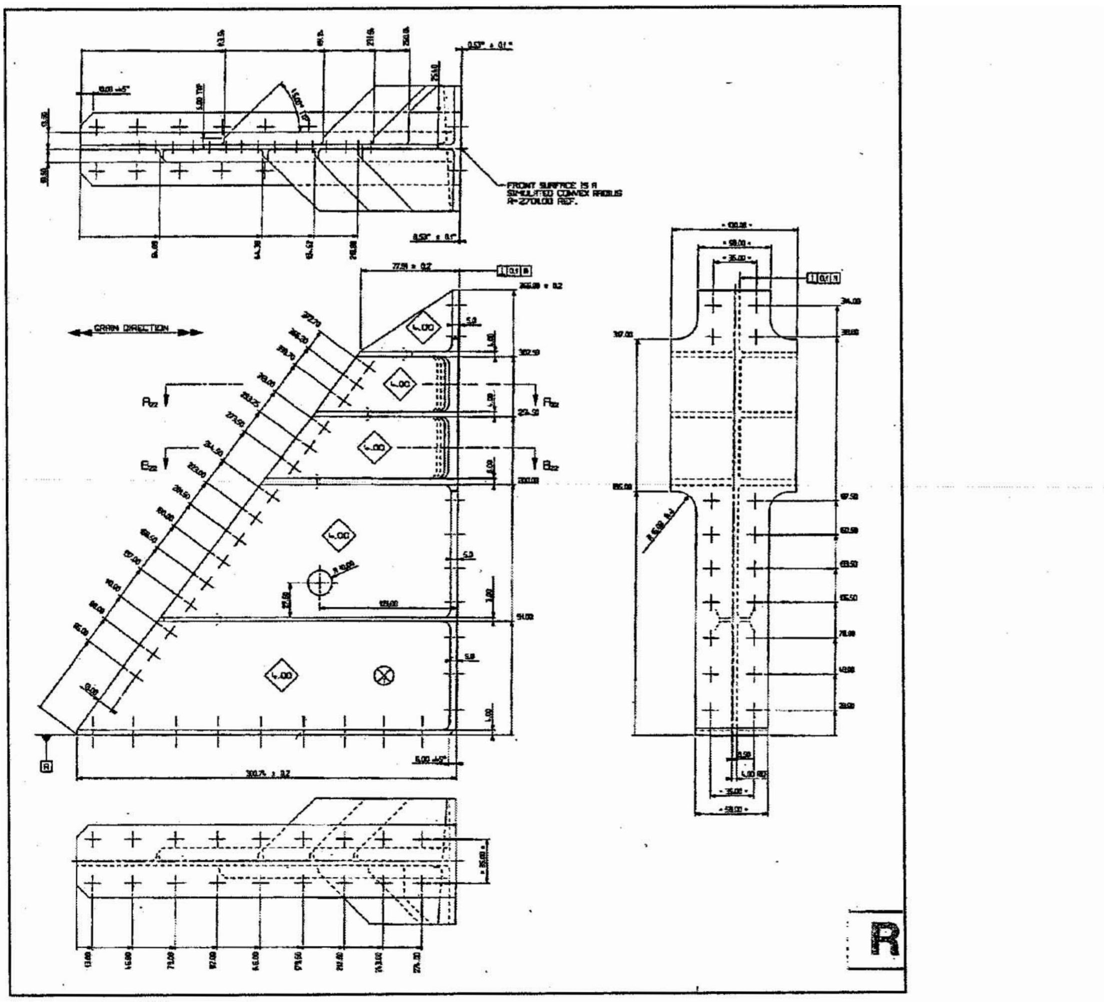

Figure 3-21 Example of box web (technical drawing R08640-079)

3.5.3.2 Box web model

The box webs are modelled by CQUAD4 elements, with paver mesh. This mesh type is described on Appendix D. The radii in the corners are not considered.

Figure 3-22 shows the schematiration of the box webs. The Figure 3-23 shows the box web model.

Table 3-6 Box web material data

Part of the structure	Box web
Material	Al 7075 T7351 (TH 5.316/5)
E(c) [N/m²]	73×10^9
E(t) [N/m²]	71×10^9
ρ [N/m²]	27×10^9
Φ [kg/m³]	2800
Poisson's ratio	0.33

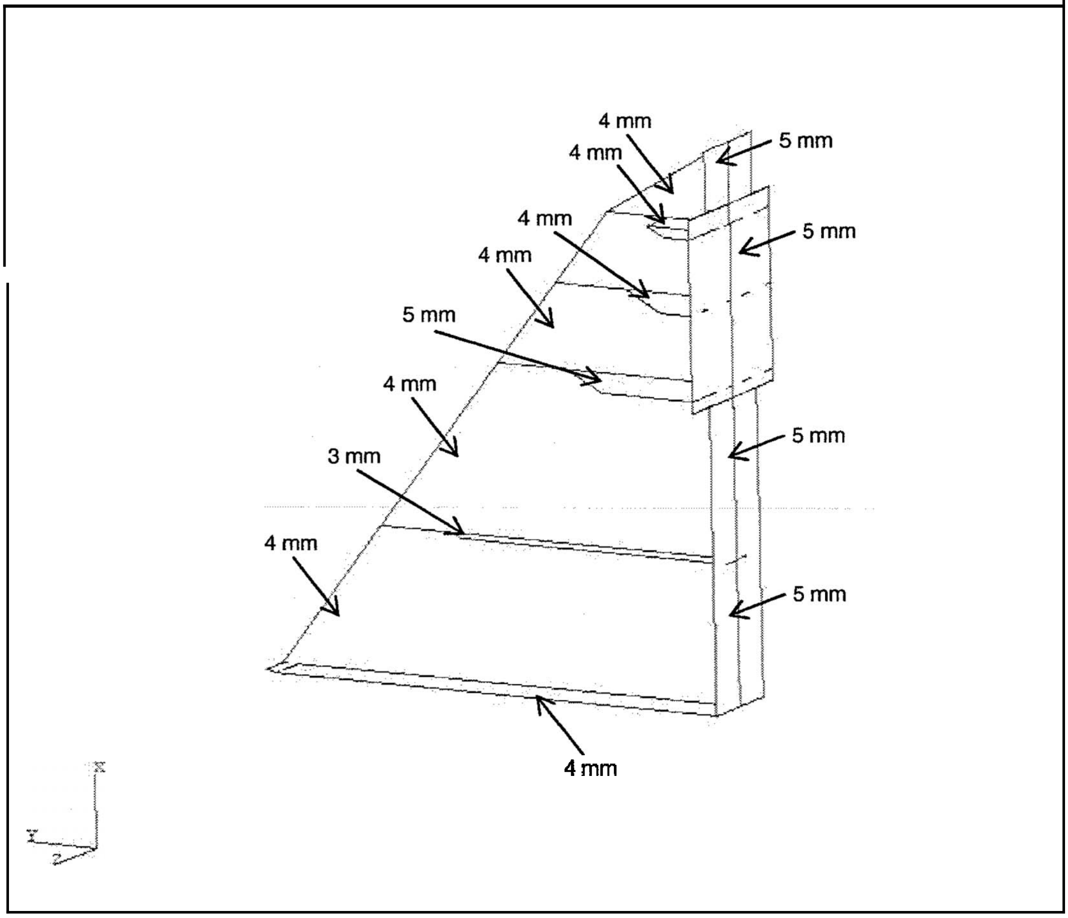

Figure 3-22 Schematization of box web

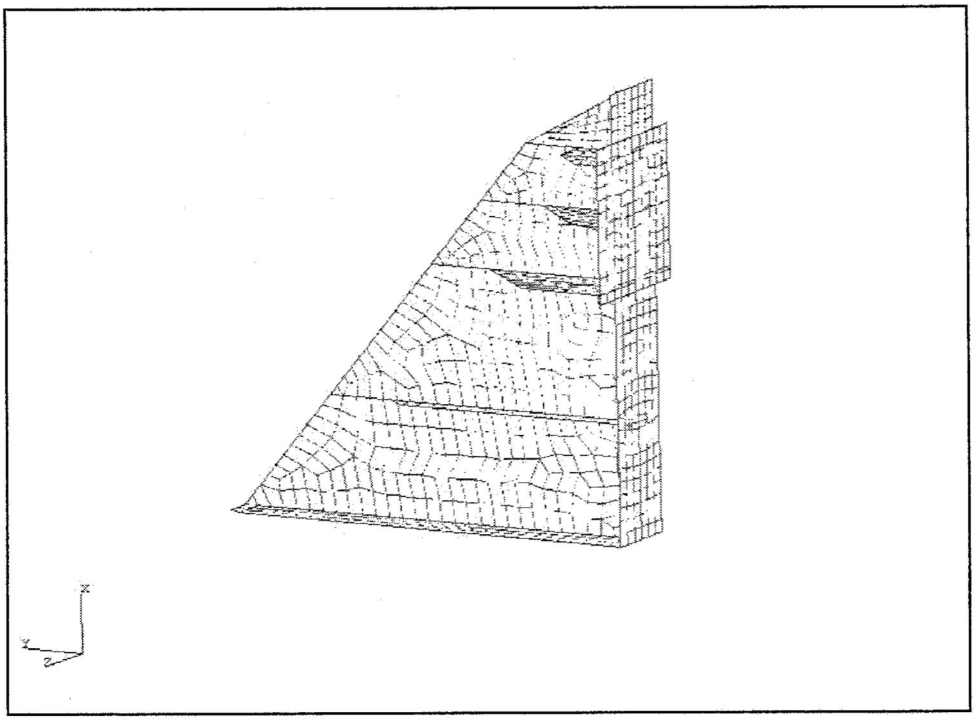

Figure 3-23 Model of box web (technical drawing R08640-079)

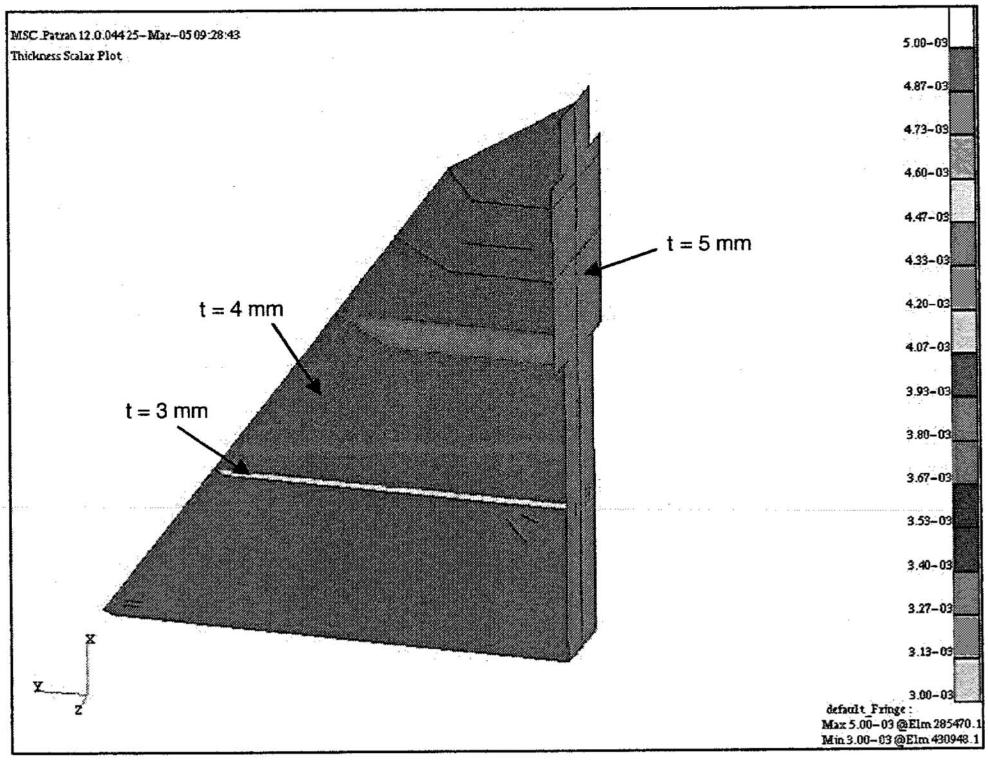

Figure 3-24 Element thickness in box web model (tech. drawing R08640-079)

NASTRAN input for element properties for all box webs:

```
$ Direct Text Input for Bulk Data
PSHELL   1        3165     .002     3165             3165
PSHELL   5        3165     .0025    3165             3165
PSHELL   4        3165     .003     3165             3165
PSHELL   7        3165     .004     3165             3165
PSHELL   9        3165     .0045    3165             3165
PSHELL   10       3165     .005     3165             3165
PSHELL   11       3165     .008     3165             3165
PSHELL   13       3165     .007     3165             3165
$ Referenced Material Records
$ Material Record : 5.3165Aluminum7075
MAT1     3165     7.1+10           .33      2800.
```

3.5.3.3 Box web interfaces with other Box parts

The box webs are connected to the box floor, the cylindrical panels and the stringer on the conical panels. These connections are modelled by rneans of equivalence nodes.

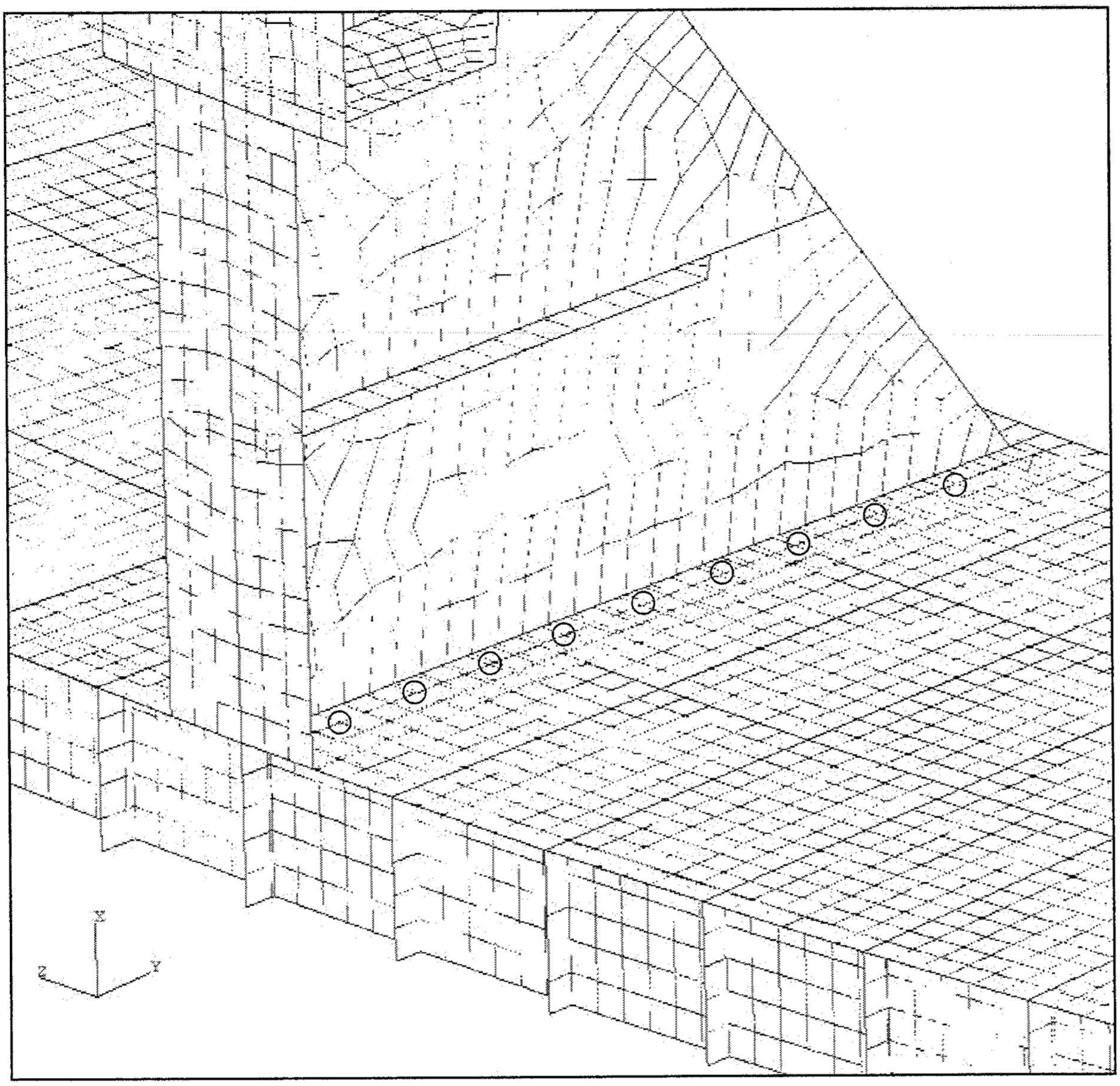

Figure 3-25 Nodes connecting box web and box floor

Figure 3-25 shows connection between the box web and the box floor. The red circle shows the connected nodes. This connection represents the rivet connection between the box web and the box floor. This type of connection is typical for all box webs. The number of the equivalence nodes for each web is difference. It is described on the technical drawing.

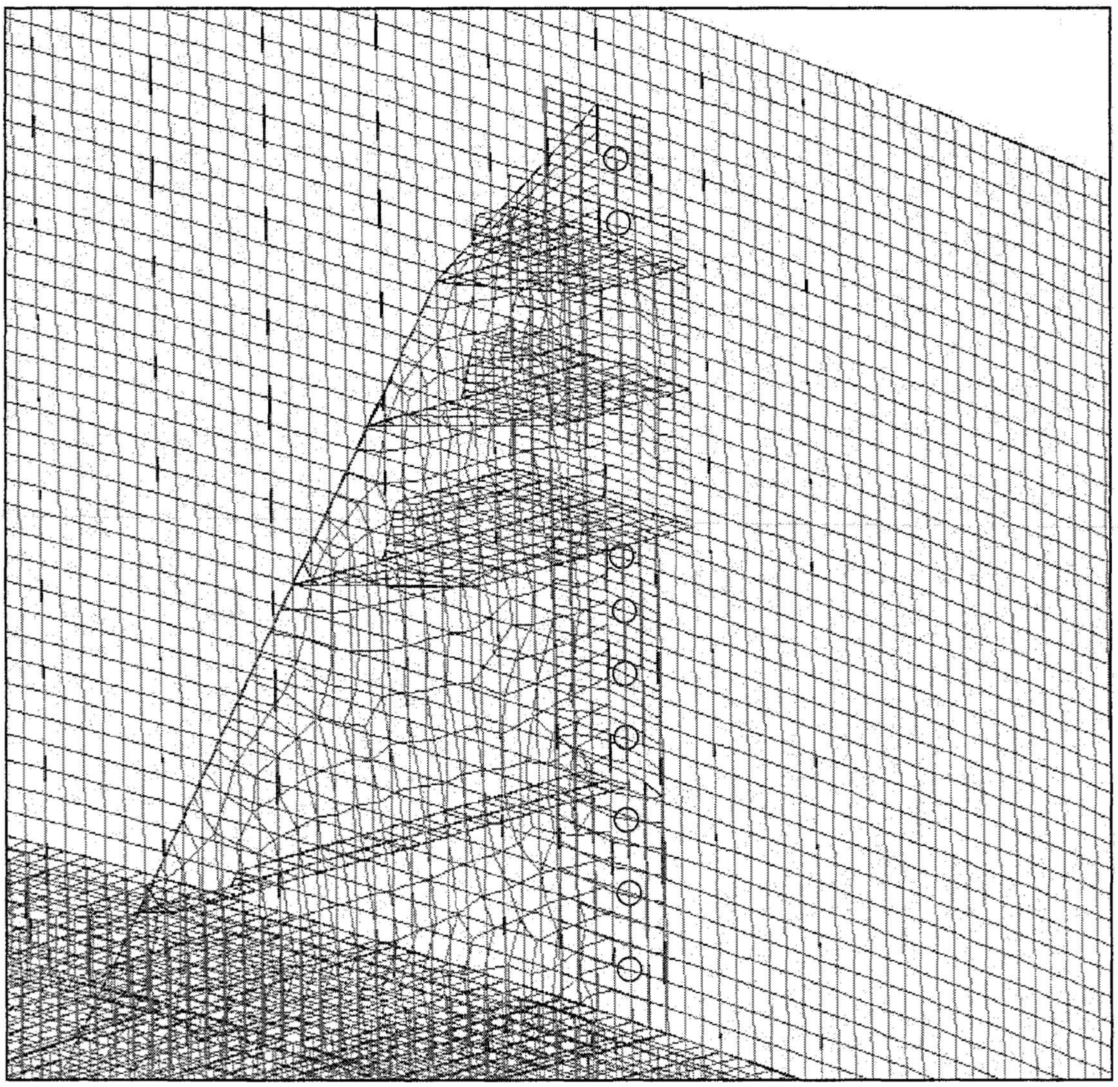

Figure 3-26 Nodes connecting box web and cylindrical panel

Figure 3-26 shows connection between the box web and the cylindrical panel. The red circle shows the connected nodes. This type of connection is typical for all box webs.

3.5.4 Cylindrical panels

3.5.4.1 Cylindrical panels description

The function of the cylindrical panels is to transfer the load from the box floor to the top I/F ring, mainly the radial load from the DAAR lugs.

The technical drawings which describe the cylindrical panels are:

- R08652 – 009
- R08655 – 013
- R08660 – 009
- R08656 – 011
- R08655 – 015
- R08654 – 011
- R08653 – 009
- R08659 – 005

The assembly is made based on the technical drawing **R08612 - *087***

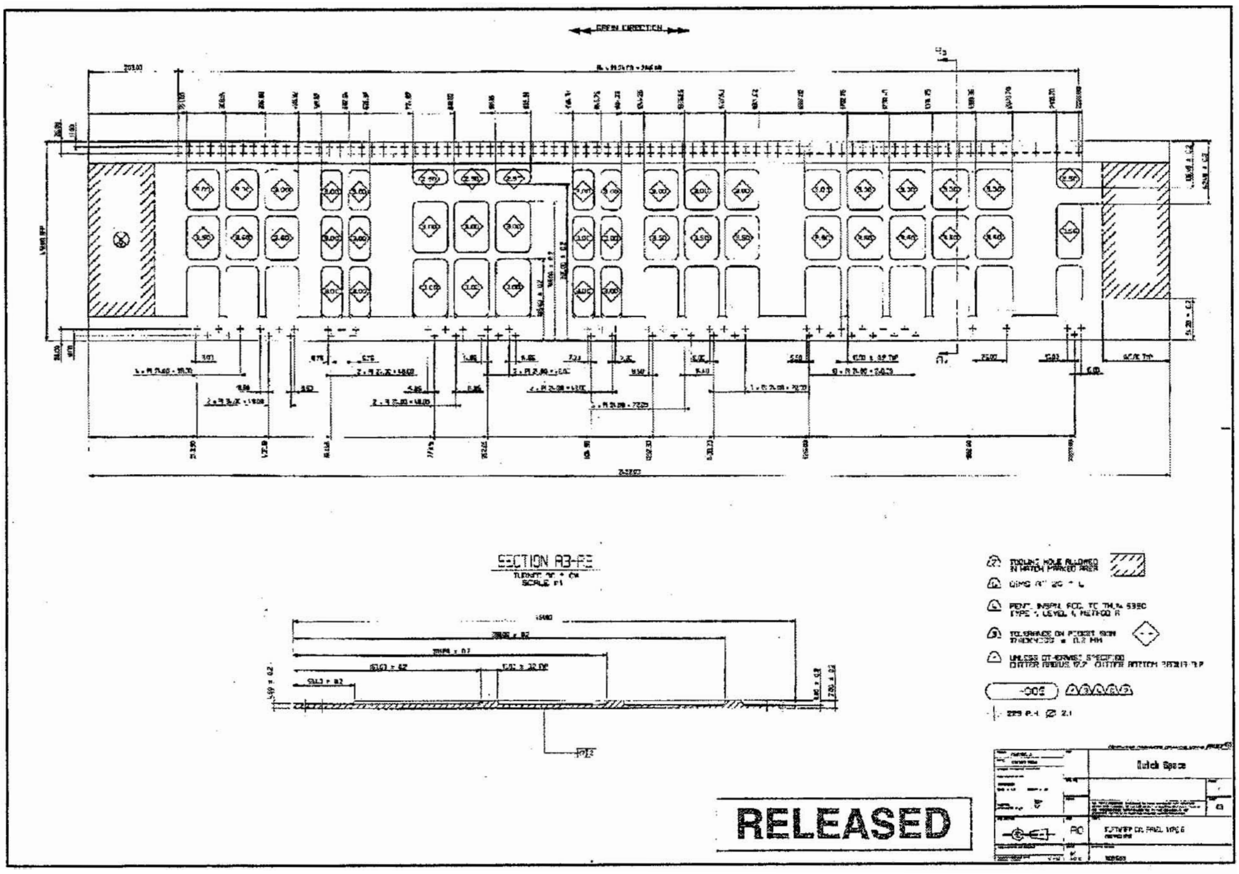

Figure 3-27 A pari of cylindrical panel (taken from R08659 – 005)

3.5.4.2 Cylindrical panels model

The cylindrical panels are modelled by CQUAD4 elements.

Table 3-7 Cylindrical panels material data

Part of the structure	***Cylindrical panels***
Material	Al 7075 T7351 (TH 5.61 315)
E(c) [N/m^2]	73×10^9
E(t) [N/m^2]	71×10^9
ρ [N/m^2]	27×10^9
Φ [kg/m^3]	2800
Poisson's ratio	0.33

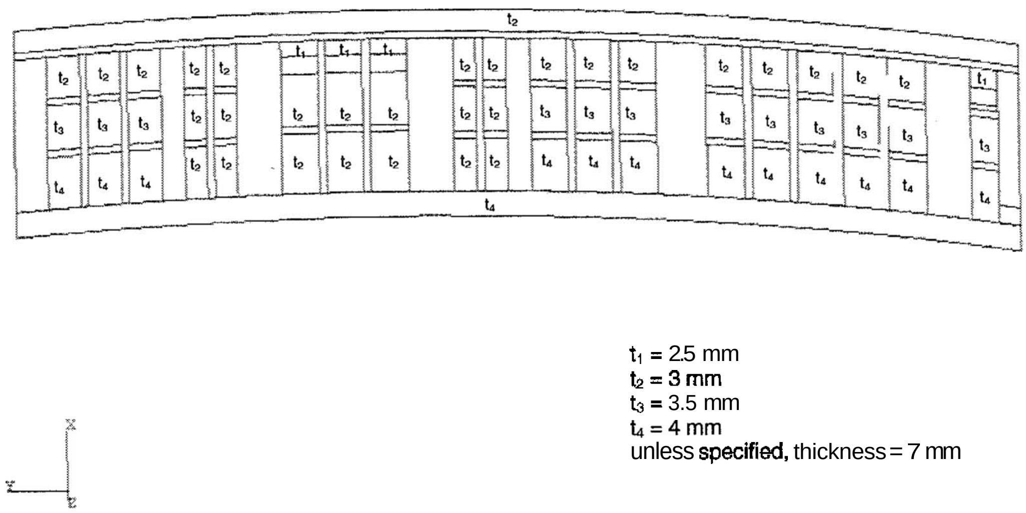

t_1 = 2.5 mm
t_2 = 3 mm
t_3 = 3.5 mm
t_4 = 4 mm
unless specified, thickness = 7 mm

Figure 3-28 Schematization of cylindrical panel

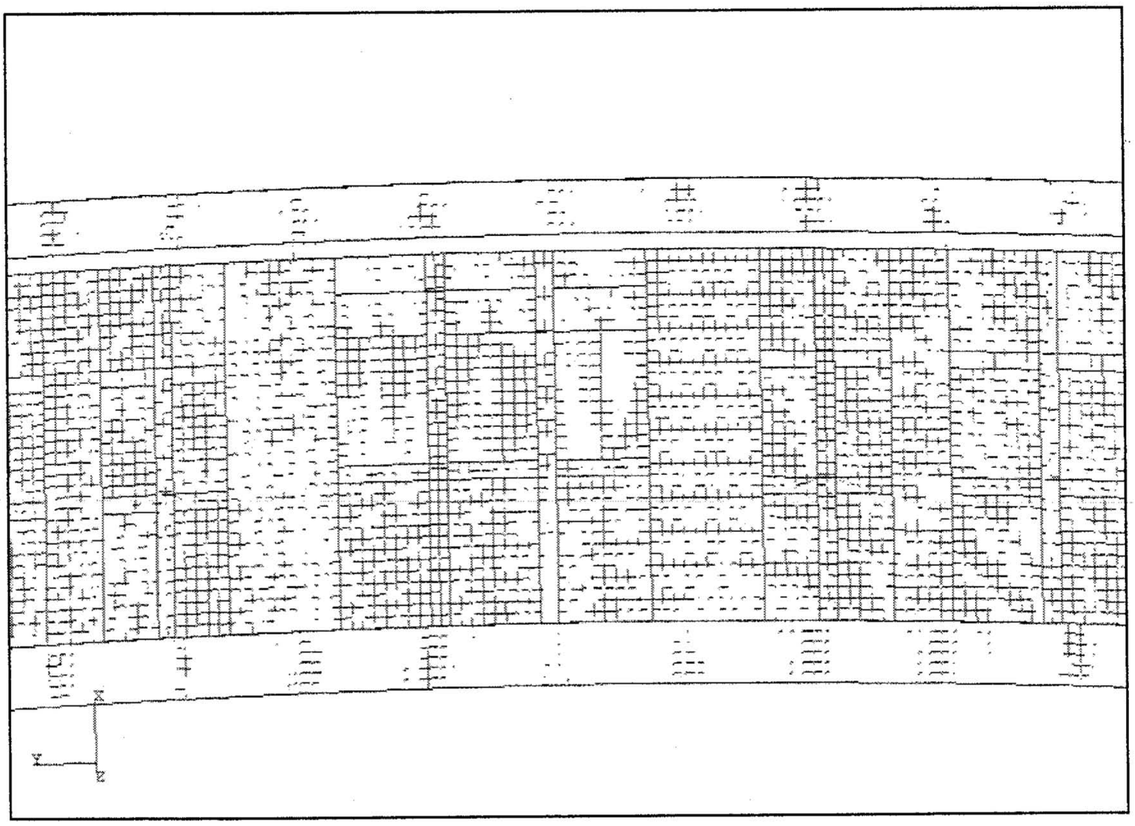

Figure 3-29 Model of cylindrical panel

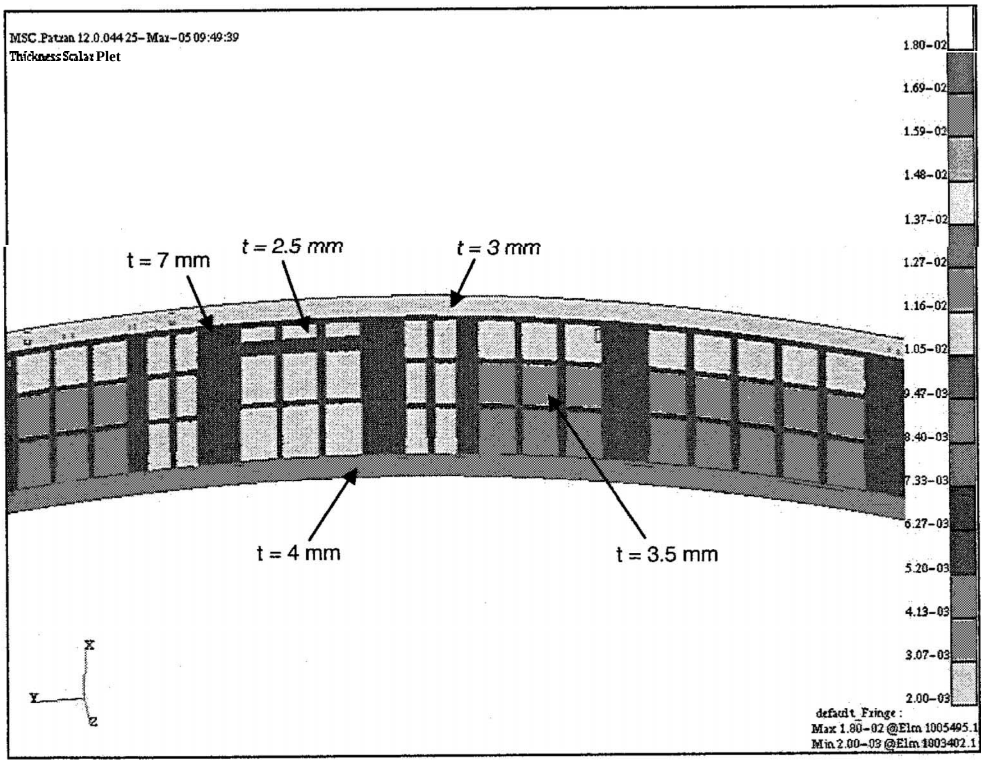

Figure 3-30 Element thickness in the cylindrical panel model

NASTRAN input for **elements properties:**

```
$ Direct Text Input for Bulk Data
PSHELL   I       3165    .002    3165            3165
PSHELL   5       3165    .0025   3165            3165
PSHELL   4       3165    .003    3165            3165
PSHELL   7       3165    .004    3165            3165
PSHELL   9       3165    .0045   3165            3165
PSHELL   10      3165    .005    3165            3165
PSHELL   11      3165    .006    3165            3165
PSHELL   12      3165    ,0035   3165            3165
PSHELL   8       3165    .018    3165            3165
PSHELL   14      3165    .0055   3165            3165
$ Referenced Material Records
$ Material Record : 5.3165Aluminum7075
MAT1     3165    7.1+10          .33     2800
```

3.5.4.3 Cylindrical panels interfaces with other Box parts

The interfaces are described in section 3.5.1.3, 3.5.2.3 and 3.5.3.3

3.5.5 Conical panels

3.5.5.1 Conical panels description

The function of the cylindrical panels is to transfer the load from the box floor to the top I/F ring, mainly the axial load from the Vulcain engine.

There are 144 stiffeners which are equally distributed along 12 conical panels. A typical conical panel is shown in Figure 3-31. All twelve panels are identical.

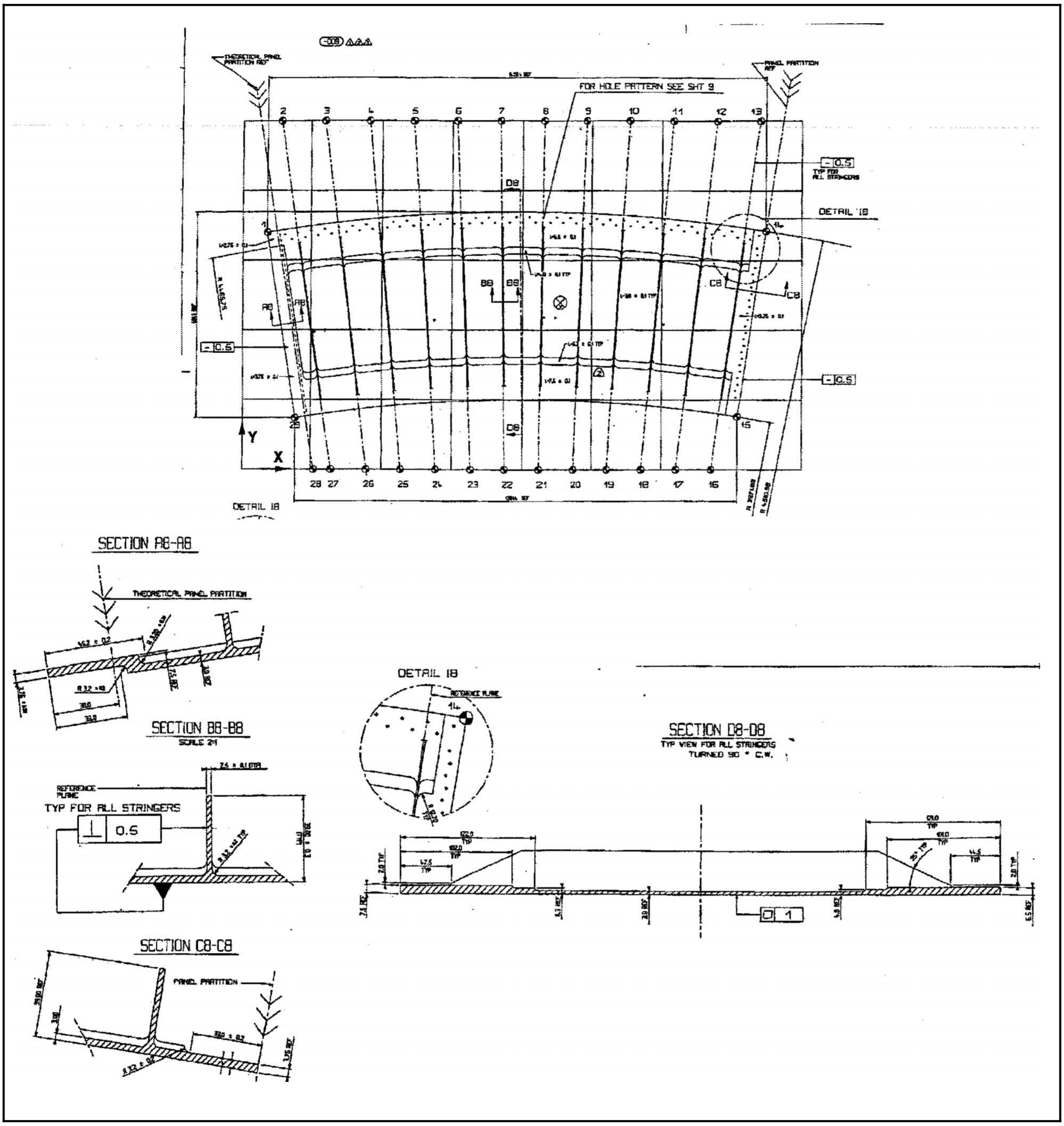

Figure 3-31 Typical conical panel

The typical conical panel is described on the technical drawing R08616 – 009 and R08615 – 403. The assembly is described on the technical drawing R08612 - 087

3.5.5.2 Conical panel model

The conical panels are modelled by CQUAD4 elements.The stiffeners are modelled by CQUAD4 elements, pave meshed.

Table 3-8 Conical panels material data

Part of the structure	***Conical panels***
Material	Al 7075 T7351 (TH 5.31 615)
E(c) [N/m²]	73 x 10^9
E(t) [N/m²]	71 x 10^9
P [N/m²]	27 x 10^9
Φ [kg/m³]	2800
Poisson's ratio	0.33

Figure 3-32 and **4-33** shows the schematization of the conical panels, while Figure **3-34** shows the model of conical panel.

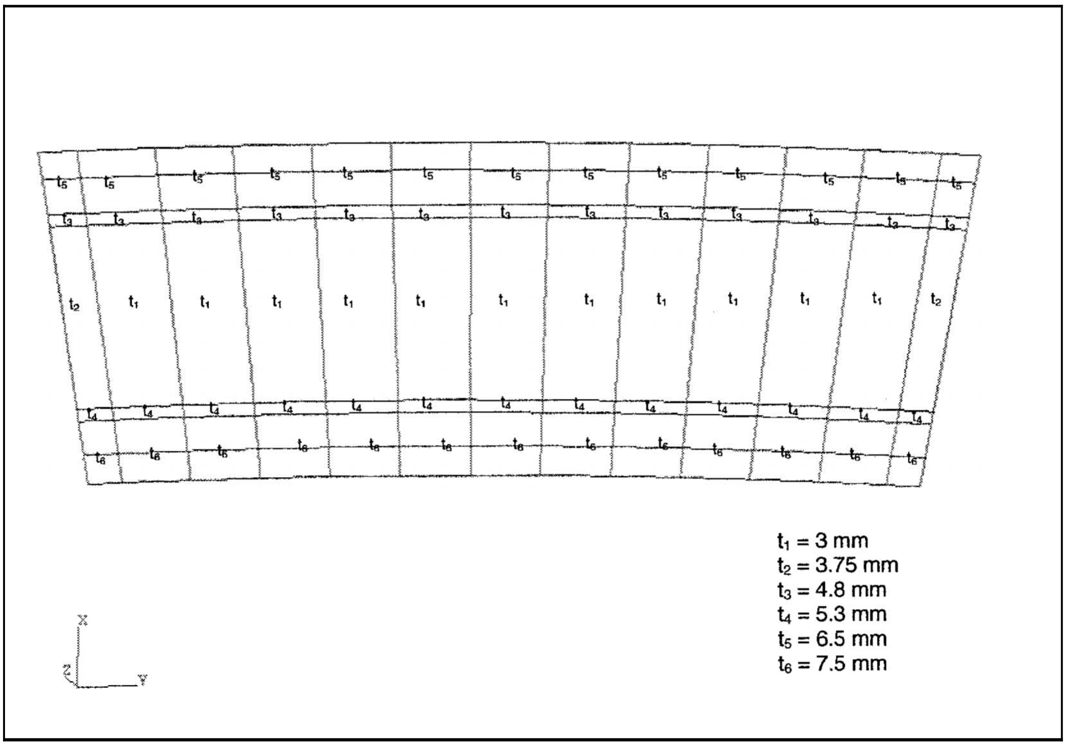

Figure 3-32 Schematization of the conical panels

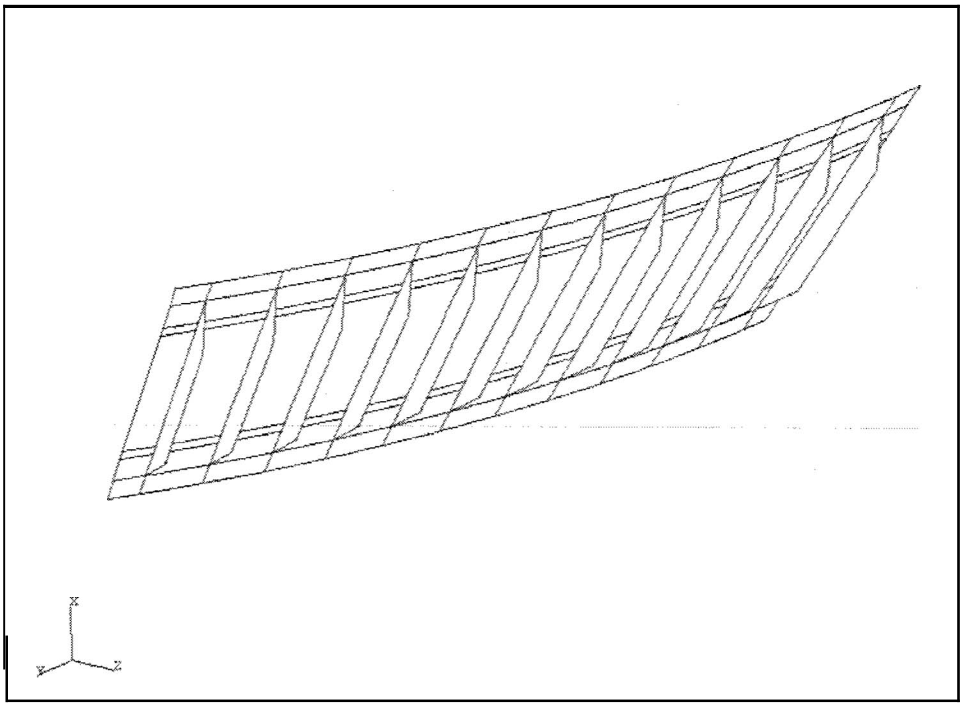

Figure 3-33 Conical panel with stiffeners

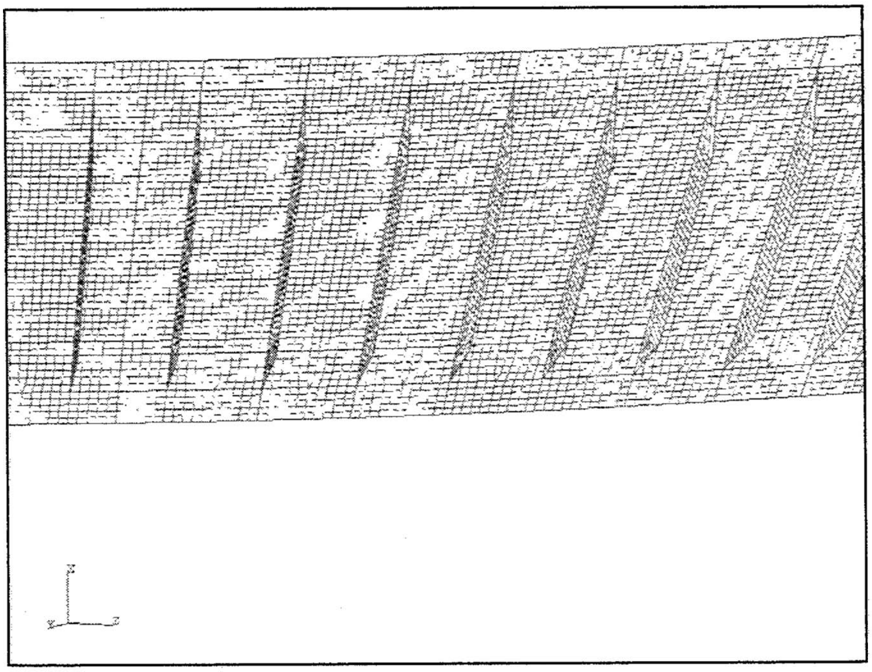

Figure 3-34 Conical panels model

NASTRAN input for elements properties:

```
$ Direct Text Input for Bulk Data
PSHELL   6       3165    .00275  3165            3165
PSHELL   1       3165    .003    3165            3165
PSHELL   4       3165    .0065   3165            3165
PSHELL   7       3165    .0075   3165            3165
PSHELL   3       3165    .0053   3165            3165
PSHELL   9       3165    .0048   3165            3165
$ Referenced Material Records
$ Material Record : 5.3165Aluminum7075
MAT1     3165    7.1+10          .33     2800.
```

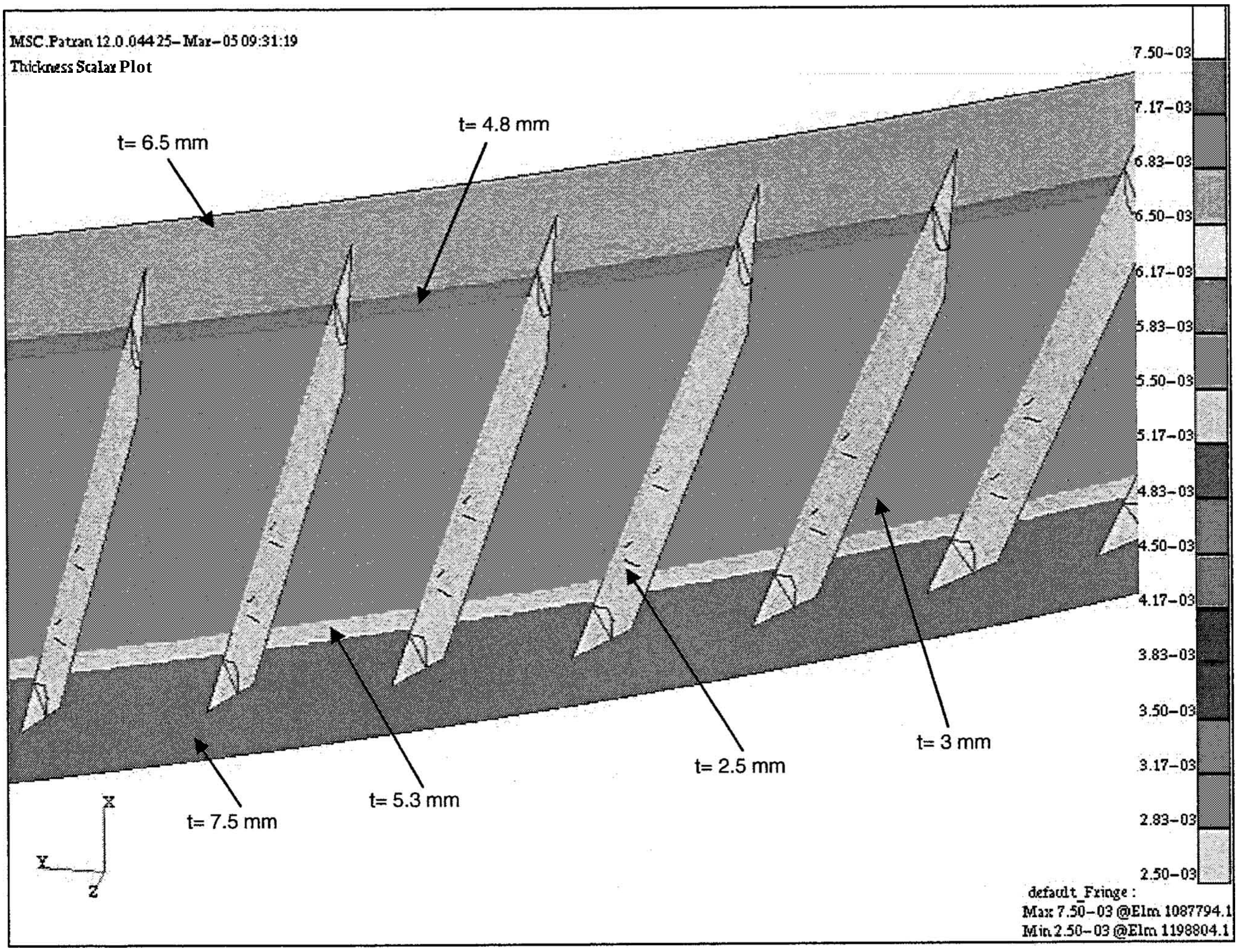

*Figure 3-35 **Element** thickness in the conical **panels model***

3.5.5.3 Conical panels interfaces with other Box parts

The interfaces are described in section 3.5.1.3 and 3.5.2.3

3.6 Load and Boundary Conditions

3.6.1 Load Case

3.6.1.1 Loading condition of the existing BME

All the coupled loads which work on the existing BME are shown below.

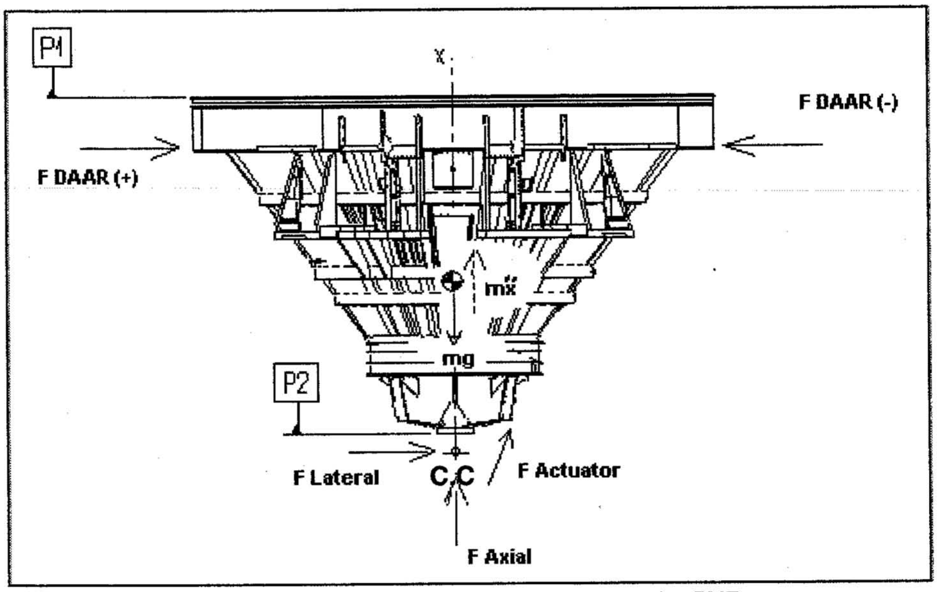

Figure 3-36 The loading condition on the existing BME

The figure 3-36 shows that only DAAR loads are applied on the Box structure. Thus, the load case for the detailed FEM of the BME Box structure is only regarding the DAAR loads.

Meanwhile, the assernbly of the Cross, the Cone and the Box forms the mechanical interface between the Vulcain engine and the RIE. The cross provides the load path by which the loads at the centre-cardan are transferred into the conical shell structure. This is the primary load for the BME.

The axiat load (F) is resulting in an equal-distributed axial load along the cone (figure 3-37a). The lateral load from the engine (F,) results in a sinusoidal distributed axial load along the cone (figure 3-37b).
The resulting flux of both loads is shown in figure 3-38.

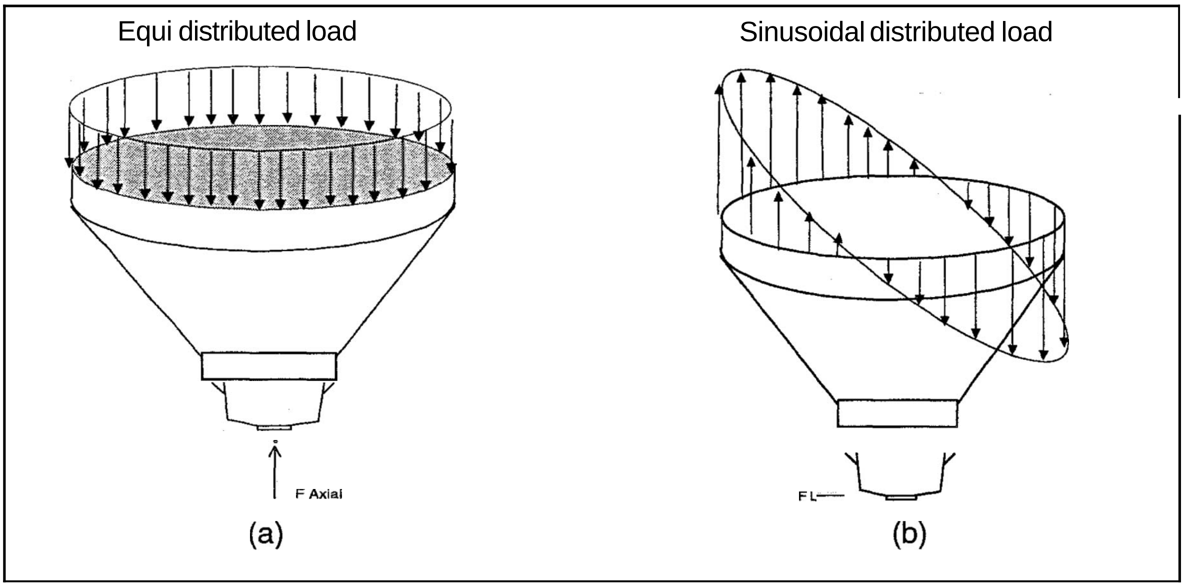

Figure 3-37 Axial and lateral Vulcain load

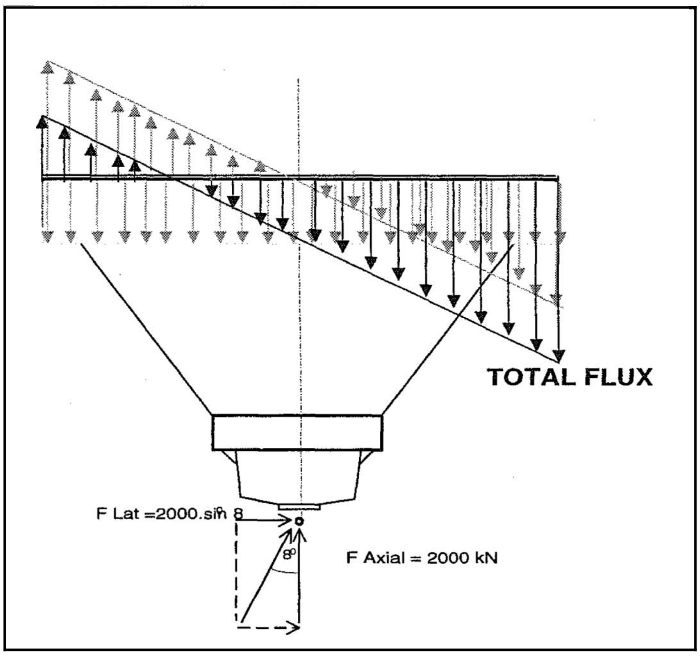

Figure 3-38 Free body diagram of the Vulcain load

The interface with the tank (RIE) requires that the total flux load shall remain below a certain value. Otherwise, the thin walled tank cylinder will buckle. This requirement determines the boundary conditions which will be analyzed.

3.6.1.2 DAAR loads

The loads introduced by the EAP's are transferred to the Box structure via the DAAR lugs. Hence, they are called DAAR loads. These loads have a dynamic nature since they tend to change during the different operational life phases

The lugs have a fixed position as depicted in figure 3-39. With the position co-ordinates the angles of the struts have been defined (Figure 3-39).

The angle χ is for all of the long struts (N11, N12, N21, N22) the same and has a value of approximately 11°
The short struts (N13, N23) have an angle δ which has a value of approximately 36°
The nominal loads are:
- Short struts: traction: -110 kN ≤ F ≤ 110 kN
  Compression: -140 kN ≤ F ≤ 140 kN
- Long struts: traction: -310 kN ≤ F ≤ 310 kN
  Compression: -85 kN ≤ F ≤ 85 kN

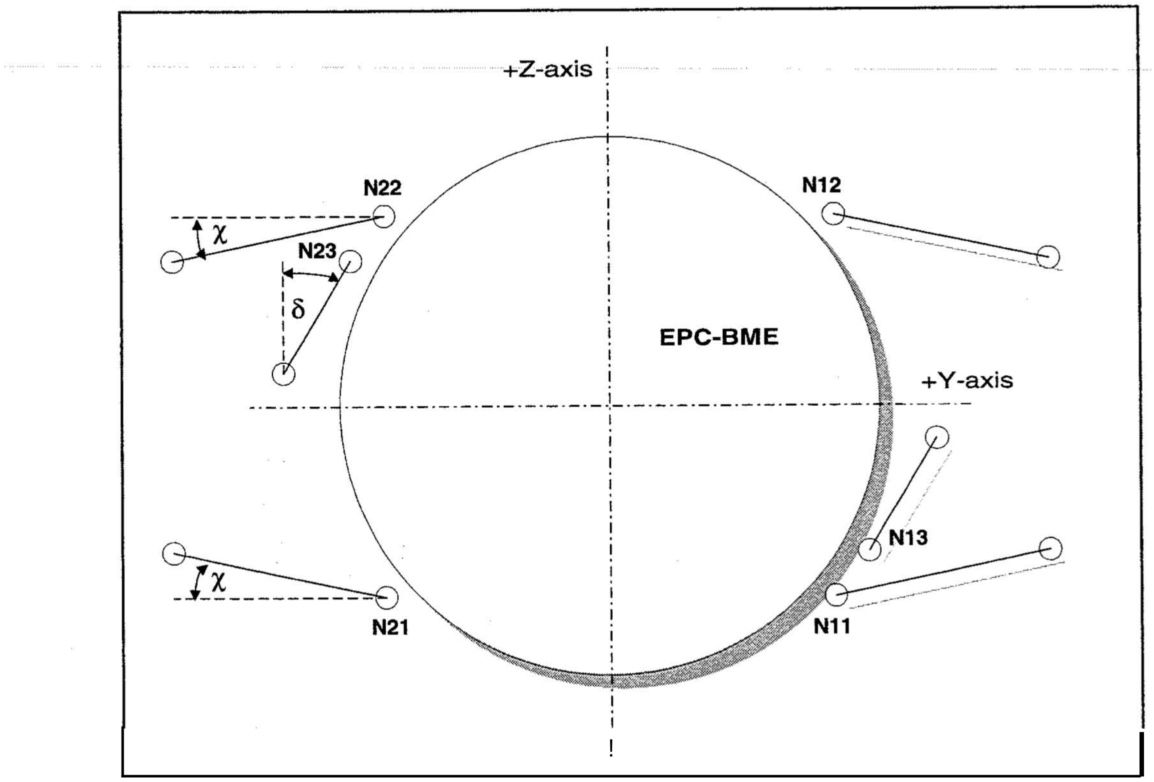

Figure 3-39 Sketch of the top view of the BME with DAAR loads

3.6.1.3 Simplification of the loading case

As stated on section 3.1, the main objective of the detailed finite element modelling is to verify the applicable strength and stiffness requirements of the ARIANE **5** EPC-BME. This objective can be obtained by comparing the result of the old FEM analysis with the result of the detailed model.

For the Box structure, a hypothetical load case is used in order to verify the model with respect to the radial component of the DAAR loads. In this load case, 4 static radial loads (each of 1 kN) are applied on the position of long struts (N11, N12, N21, N22). The load case is depicted on figure 3-40. Note, that the 1 kN load is an arbitrary unit load to provide info on the Box deformation and thus on the flexibility at the interface points.

This hypothetical load case also offers a simple load case to calculate by hand.

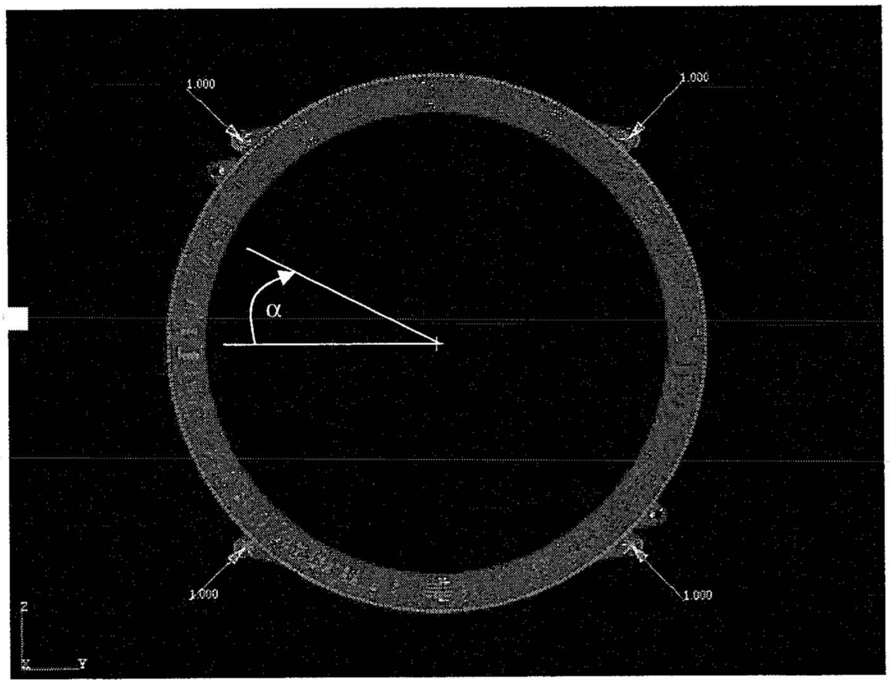

Figure 3-40 The hypothetical load case for the Box structure

NASTRAN input for loading case:

```
$ Nodal Forces of Load Set : force1
FORCE   1    474225 0    999.977 0.    .725317 .688416
$ Nodal Forces of Load Set : force4
FORCE   3    372444 0    999.977 0.    .725317-.688416
$ Nodal Forces of Load Set : force2
FORCE   4    512899 0    999.977 0.    -.688416 .725317
$ Nodal Forces of Load Set : force3
FORCE   5    451451 0    999.977 0.    -.688416-.725317
```

3.6.2 Boundary conditions

As stated on section 3.6.1.1, the interface between the Box structure and the RIE tank determines the boundary conditions which will be analyzed.

Regarding the interface, there are 3 boundary conditions to be analyzed in this project, i.e.:

- Clamped condition
  This boundary condition represents the ideal connection between the Box structure and the RIE tank. There is no displacement in six directions (3 translations and 3 rotations) at the I/F ring.

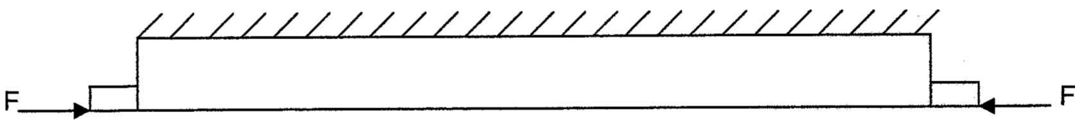

Figure 3-41 Sketch of the Boundary Condition 1 (Clamped)

- Simply supported condition
  This condition represents the bolt connection between the Box structure and the RIE tank. It means there is no translational displacement in three directions.

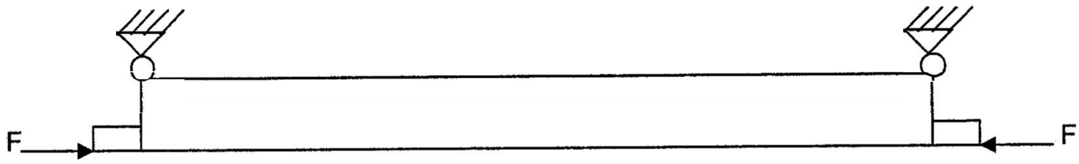

Figure 3-42 Sketch of the Boundary Condition 2 (Simply Supported)

- Roller condition
  This boundary condition is used to analyze the Box structure as one independent structure.

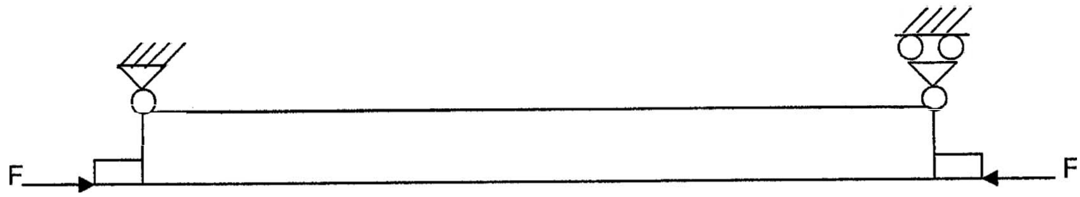

Figure 3-43 Sketch of the Boundary Condition 3 (Roller)

These 3 boundary conditions are applied on the top surface of the Top I/F ring.

3.7 Model Check

3.7.1 Mass properties and volume

This check is performed in order to calculate the mass of the Box structure and the centre of gravity. The result is depicted below.

```
*******************************************************************************
*                          MASS PROPERTIES REPORT                             *
*******************************************************************************
MSC.Patran 2004
File: /mcae/sms/A5BOX-Hasto/boxwork.db
Date: 04-Mar-05
Time: 13:49:23

Scalar Properties:
         Volume            Mass
       0.245835 [m3]     688.338257 [kg]

Center of Gravity in Coordinate Frame:
Comp   Ref. Cartes.        Frame 0
   X       0.238341       0.238341
   Y       0.003904       0.003904
   Z       0.006702       0.006702
```

3.7.2 Rigid body check

NASTRAN ground check performs a grounding check analysis on the stiffness matrix to expose unintentional constraints by moving the model rigidly. NASTRAN moves the whole model to a specific location not to define. This check states if the energy level of the model stays the same. The output given by NASTRAN is shown below.

```
*********************************************************************************
*** USER INFORMATION MESSAGE 7570 (GPWG1D)
RESULTS OF RIGID BODY CHECKS OF MATRIX KGG      (G-SET)  FOLLOW:
PRINT RESULTS IN ALL SIX DIRECTIONS AGAINST THE LIMIT OF  9.876147E-01
DIRECTION      STRAIN ENERGY      PASS/FAIL
---------      -------------      ---------
1              f.059085E-05       PASS
2              9.589770E-07       PASS
3              5.037650E-07       PASS
4              3.214807E-06       PASS
5              2.307127E-06       PASS
6              1.542420E-06       PASS
```

3.8 FEM Analysis Result

3.8.1 Boundary Condition 1

The first boundary condition to be analyzed is the clamped condition. This condition represents the ideal condition of the connection between the Box and the RIE tank.

It means there is no displacement in six directions (3 translations and 3 rotations). These boundary conditions are applied on the top surface of the Top I/F ring.

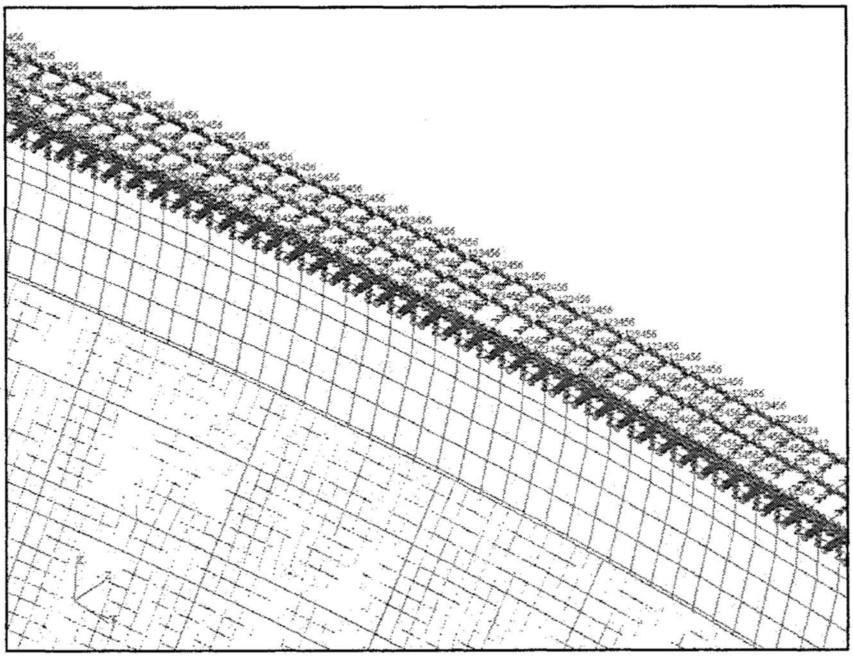

Figure 3-44 Snapshot of boundary condition 1

NASTRAN input for the boundary condition 1:

```
$ Loads for Load Case : Default
SPCADD  2     1
LOAD    2     1.    1.    t     1.    3     1.    4
              1.    5
$ Displacement Constraints of Load Set : BC1
SPC1    1     123456  2349192 2349200 2349208 2349216
SPC1    1     123456  2349337 THRU    2349344
SPC1    1     123456  23496152349616234962l 23496222349627234962 8
        2349633234963423497782349780234978223498392349840234984l
        234984323498442349845234995323499542349957234995823499 61
        2349962235007023500722350074235013l 2350132235013323501 35
.....
        2454083 2454084 2454085 2454087 2454088 2454089 2454197 2454198
        2454201 2454202 2454205 2454206 2454314 2454316 2454376 2454377
        2454380 2454381 2454489 2454490 2454493 2454494
```

The result to be taken is the displacement of the node 25890, which is positioned on the $a = 0$ (Figure 3-40). The complete displacement is depicted on figure 3-45.

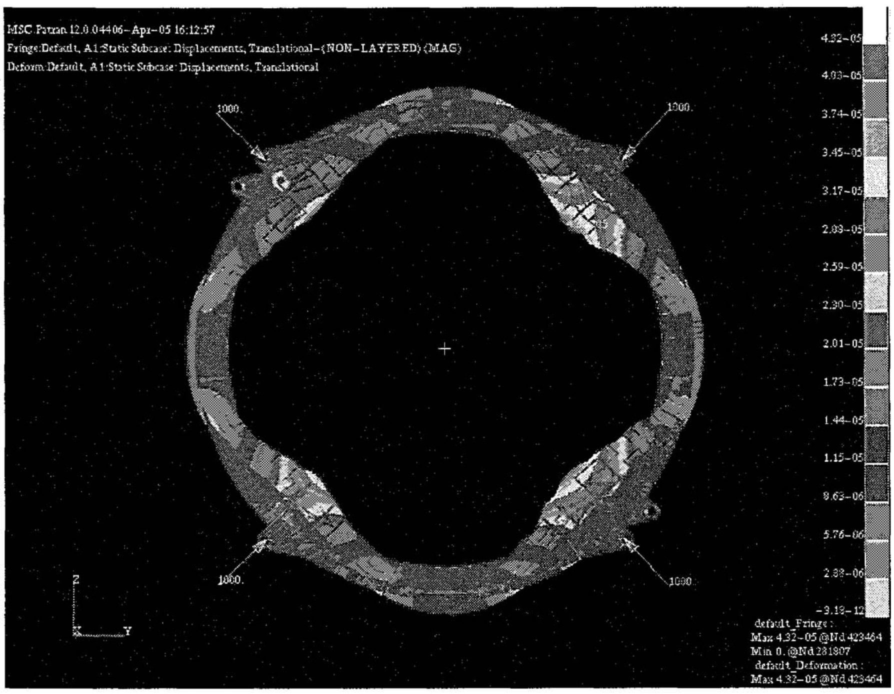

Figure 3-45 Displacement of the Box with Boundary Condition 1

For the node 25890 :

POINT ID.	TYPE	T1	T2	T3	R1	R2	R3
25890	G	4.136380E-07	-7.537186E-06	--1.003746E-07	-1.512259E-05	1.982258E-06	4.756718E-05

As shown above, the displacement of the node 25890 ($a = 0$) in y-direction is **-7.54** x 10^{-6} m.

3.8.2 Boundary Condition 2

The second boundary condition to be analyzed is the simply supported condition. This condition represents the bofts connection between the Box and the RIE tank.
It means there is no rotational displacement in three directions. These boundary conditions are applied on the top surface of the Top I/F ring.

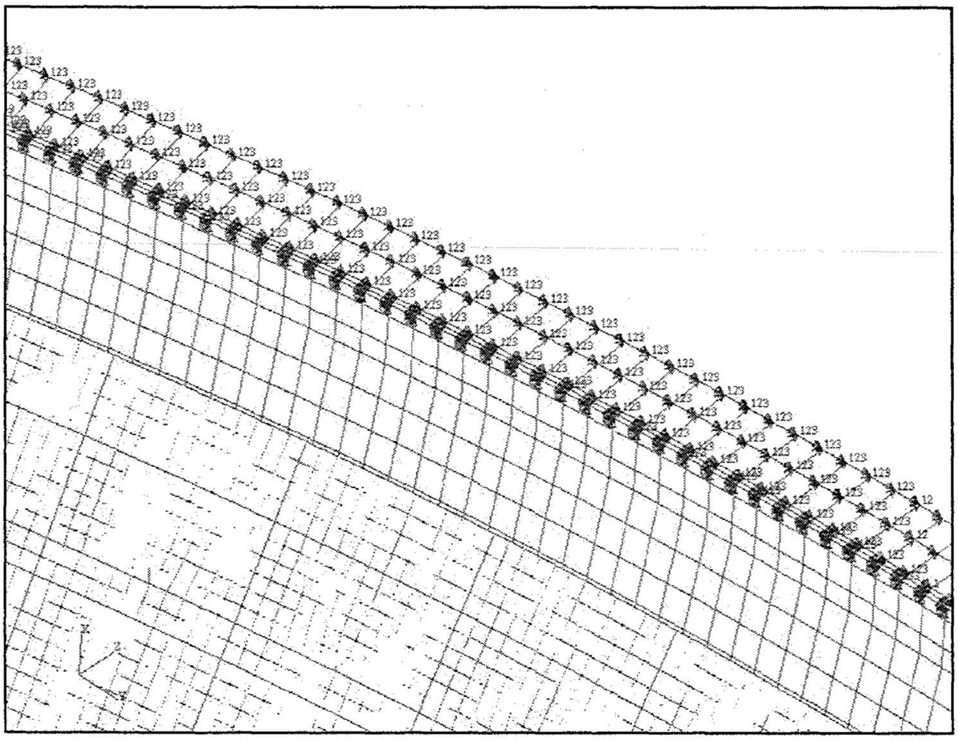

Figure 3-46 Snapshot of boundary condition **2**

NASTRAN input for the boundary condition 2:

```
$ Loads for Load Case : Default
SPCADD  2    1
LOAD    2    1.    1.    1    1.    3    1.    4
        1.   5
$ Displacement Constraints of Load Set : BC2
SPC1   1    123    2349192 2349200 2349208 2349216
SPC1   1    123    2349337 THRU   2349344
SPCI   1    123    2349615 2349616 2349621 2349622 2349627 2349628
        23496332349634234977823497802349782234983923498402349841
        23498432349844234984523499532349954234995723499582349961
        23499622350070235007223500742350131 23501322350133 2350135
        23501362350137235024523502462350249235025023502532350254
.....
        24540832454084245408524540872454088245408924541972454198
        2454201 24542022454205245420624543142454316245437624543 77
        24543802454381 2454489245449024544932454494
```

The result to be taken is the displacement of the node 25890, which is positioned on the a = 0 (Figure 3-40). The complete displacement is depicted on figure 3-47.

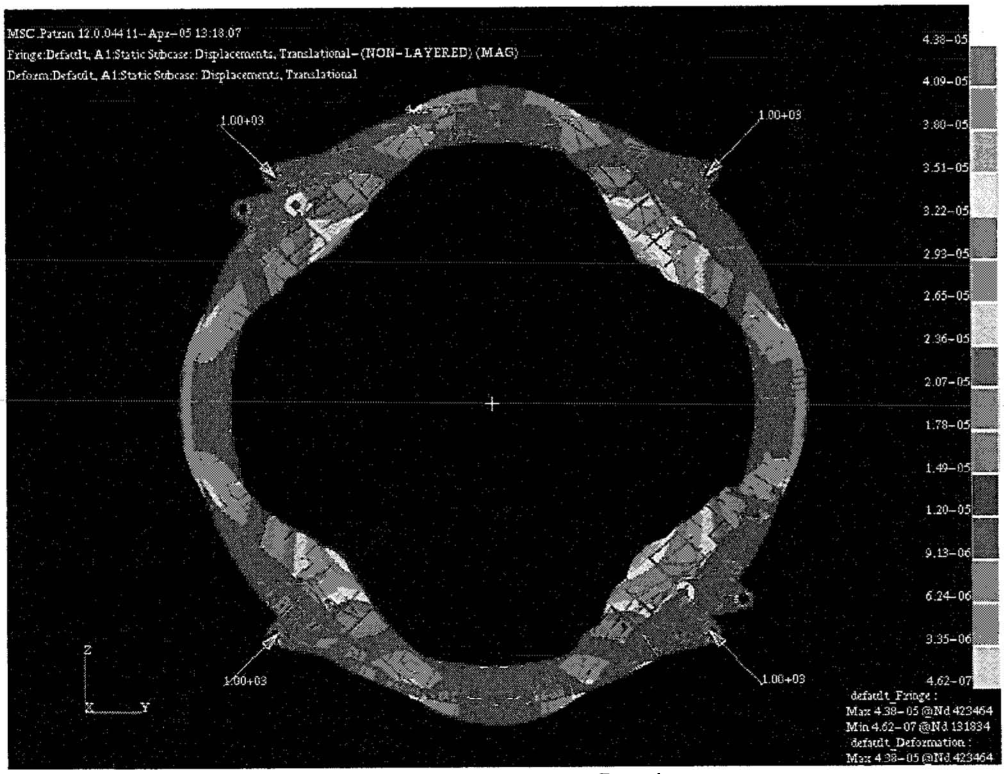

Figure 3-47 Displacement of the Box with Boundary Condition 2

For the node 25890 :

POINT ID.	TYPE	T1	T2	T3	R1	R2	R3
25890	G	4.032148E-07	-6.651802E-06	-2.702797E-08	-1.149399E-05	5.505870E-07	4.017109E-05

As shown above, the displacement of the node 25890 (a = 0) in y-direction is ***-6.65*** x 10'' m.

3.8.3 Boundary Condition 3

In the FEM model, this boundary condition is modelled with two set of displacement constraints. The first set is translational constraint in the x-direction (roller supported) along the top I/F ring, while the second set gives simply supported boundary condition on the position of a = 0. These sets are depicted on figure **3-48** and 3-**49.**

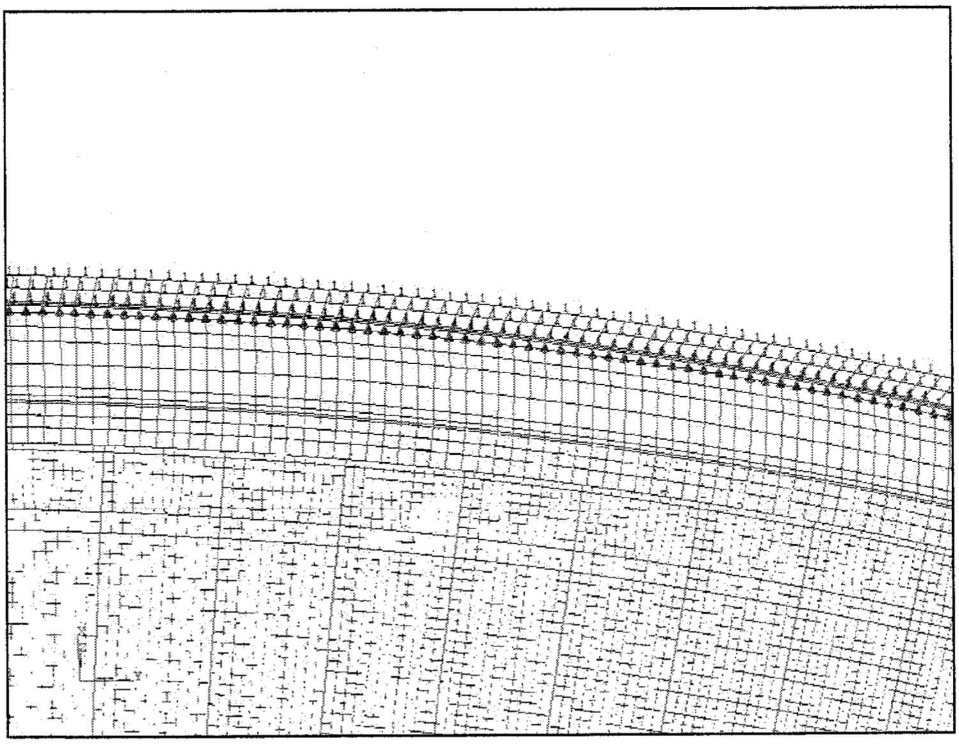

Figure 3-48 Roller supports along the Top I/F ring

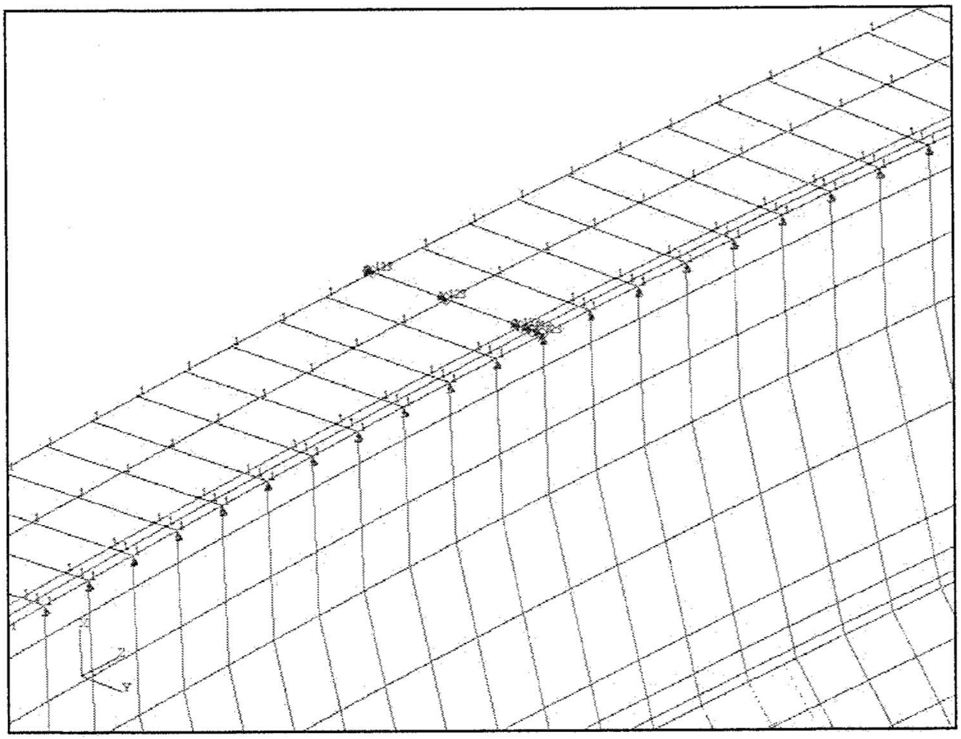

Figure 3-49 Simple supports at the position of $\alpha = 0$

NASTRAN input for the boundary condition 3:

```
$ Loads for Load Case : Default
SPCADD  2    1    3
LOAD    2    1.   1.   1    1.   3    1.   4
             1.   5
$ Displacement Constraints of Load Set : BC3a
SPC1    1    1    2713282 2713294 2713306 2713318 2713387 2713388
         2713389271339027134032713404271340527134062713802 2713803
         2713808 2713809 2713814 2713815 2713820 2713821 2714082 2714084
         2714086 2714095 2714096 2714097 2714099 2714100 2714101 2714236
......
         2812496 2812497 2812500 2812501 2812614 2812616 2812618 2812627
         2812628 2812629 2812631 2812632 2812633 2812768 2812769 2812772
         28127732812776281277728128902812892281290428129052812908
         28129092813044281304528130482813049
$ Displacement Constraints of Load Set : BC3b
SPC1    3    123   27632142763223276322727633722763373
```

The result to be taken is the displacement of the node 25890, which is positioned on the a = 0 (Figure 3-40). The complete displacement is depicted on figure 3-50.

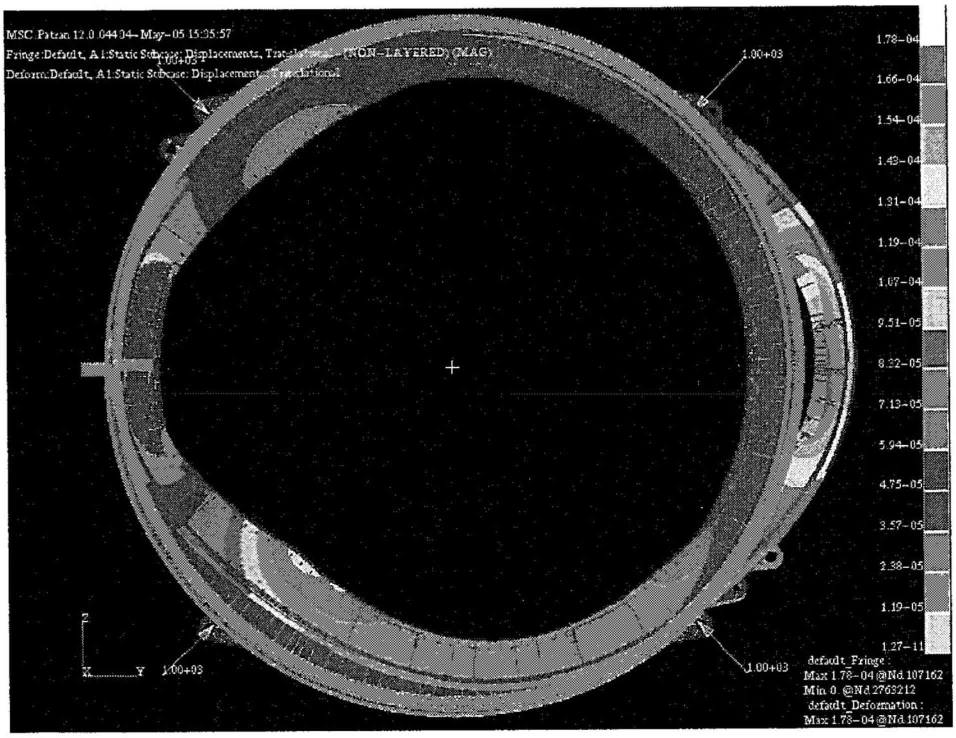

Figure 3-50 Displacement of the Box with Boundary Condition 3

For the node 25890 :

POINT ID.	TYPE	T1	T2	T3	R1	R2	R3
25890	G	3.071231E-07	-3.054821E-06	1.235018E-07	-2.471899E-05	-1.092375E-05	1.621947E-04

As shown above, the displacement of the node 25890 (a = 0) in y-direction is -1.05 x 10^{-5} m. 3;

3.9 Crosscheck with original FEM model

After the detailed FEM of the Box structure has been made, the next step to be taken is to verify with the old FEM model (version A5-v6A). Hence, a crosscheck should be made.

In order to do the crosscheck, the version A5-v6A FEM model is modified. Parts to be calculated are exactly the same parts which are modelled in this report. Thus, the other parts, i.e.: Cone, Cross, LBS, and the brackets are deleted from the version A5-v6A model.

Then, the same loading case and boundary conditions (as described on section 3.6) will be applied to the version A5-v6A model. The comparisons between the results are shown on the table 3-9. The results are also compared with the result from hand calculation (Appendix E.)

Table 3-9 The comparison of the analysis results

Nr.		Displacement (m)		
		BC1	BC2	BC3
1	Hand Calculation	7.816E-06	7.816E-06	3.705E-06
2	New FEM model	7.537E-06	6.652E-06	3.055E-06
3	Version A5 - v6A	7.500E-06	6.613E-06	3.050E-06
	difference 1 vs 2 [%]	3.57	14.90	17.54
	difference 1 vs 3 [%]	4.05	15.40	17.96
	difference 2 vs 3 [%]	0.49	0.59	0.44

Example calculation of the difference:

- Difference 1 vs 2 for BC1:

$$\text{Difference} = \frac{(\text{Displacement by New FEM model} - \text{Displacement by hand calculation})}{\text{Displacement by hand calculation}} \times 100\%$$

$$\text{Difference} = \frac{(7.816\text{E-}06 - 7.537\text{E-}06)}{7.816\text{E-}06} \times 100\% = 3.57\ \%$$

3.10 Conclusion of the FEM analysis

Based on the results shown in table 3-9, it can be concluded:

- The new model has bigger error based on the hand calculation than the old model (version A5-v6A). It is reasonable, because the old model has much more simplification. Thus, the old model is more similar to the hand calculation (which is using uniform cross section).
- The new detailed model does not give significantly different result. It is shown that the differences of the results between the old model and the new model are below 1%.
- The old model (version v6A) still can be used as the basis of calculation process. Furthermore, the new more detailed model provides a better basis for calculating new stiffness/stresses, etc. as a result of new loads.
- The new, more detailed model provides a better basis for calculating the effect of new designs, such as for instance the skirt design. The skirt could be used as an attractive design solution for preventing unwanted loads due to aerodynamic buffeting.

4. Skirt Design

After one of the project's goals (the detailed finite element model of the BME Box structure) has obtained, the next step to be taken is to achieve another project's goal, i.e. the design concept of additional skirt with the optimum dimension in order to minimize the mass increase.

This section describes the design requirements for the skirt and the design concept generation process.

4.1 Design Requirements for the Skirt

Requirements are the starting point for the design activities. The generation of the requirements is a dynamic rather than a static design process. Consequently, changes in the basis are allowable during the design process. In this section the requirements of the skirt will be proposed which the skirt concepts must be fulfilled. The top 10 requirements are listed below and defined consecutively on the next sub-chapters.

- Cost reduction
- Reduce buffeting
- Fulfil the functional requirements of the BME as the existing EPC-BME does
- Respect to the geometrical constraints
- Respect to the external interfaces
- Internal Interfaces perturbation
- Consider the environmental constraints
- Strength performances
- Stiffness performances
- Mass

4.1.1 Cost Reduction

In order to remain competitive on the launcher market, the BME must be at a much lower cost than existing BME. Cost reduction must decrease up to 25% from ARIANE 5, P3 production batch (-30% from P1 batch price, *Internal Technical Notes*; Ref. 6). This cost reduction is the most impotiance requirement. Therefore this point will be the first consideration when generating the concepts. This is also governing other requirements. Adding the skirt offers cost reduction in sense of thermal protection.

4.1.2 Buffeting Problems

As described on section 2.1.1, buffeting loads occur during the first part of the flight (180 seconds into flight). The buffeting loads are caused by aerodynamic currents, being instable at subsonic speeds.

During the first part of the flight, which occurs in atmospheric environment, there is an aerodynamic flow along the surface of the ARIANE 5. At the position of the BME, the smoothly flowing, laminar airflow is disrupted, due to the shape of the BME. This phenomenon is called turbulence, Hence, the flow is called turbulent flow. The variable pressure cause unpleasant vibration on the lower structure, mainly on the Vutcane engine.

The main idea of the skirt design concept is to reduce the buffeting problem.

4.1.3 Functional Requirernents

The existing BME has several functions to accomplish its mission. The functions have been explained in chapter 1. All major functions are not subject to change when the evolution of the BME is envisaged.

Therefore, as well as its predecessors, the BME with skirt must also fulfill the following main functions:

- Vulcain Engine Steering support: to provide the anchorage and enable the load transfer of the servo actuator for steering of the Vulcain engine. The actuators are attached to the cross via two actuator brackets
- Load transfer paths from Vulcain engine to EPC
- Fuel lines and equipment supports: to provide the support for and the load transfer from the fuel lines and equipment. Same description and position as the existing BME
- Withstand LBS Disconnection Load
- Load Transfer from Lower Booster Attachment: The booster bars which are connected to the DAAR lugs have the function to ensure the lower mechanical connection between the boosters and the cryogenic main stage and to transfer the loads at the lower attachment of the EAP into EPC

4.1.4 Geometrical Constrains

Since the BME has to be built between the tank and a defined position by the engine, the available space of envelopes is considered limited for those structures. This constraint must be met when generating the new concepts. Each concepts must respect to the geometry constraints.
The existing BME (ARIANE 5) has the geometry envelope as shown on figure 4-1. Then, refer to the main dimension at table 1-2 and from the figure 4-1 can be shown the main dimension of the existing BME. Then for the skirt concepts, the basic geometry of existing BME wili be frozen and can not allow to be changed. The envelope will be as depicted on figure 4-2.

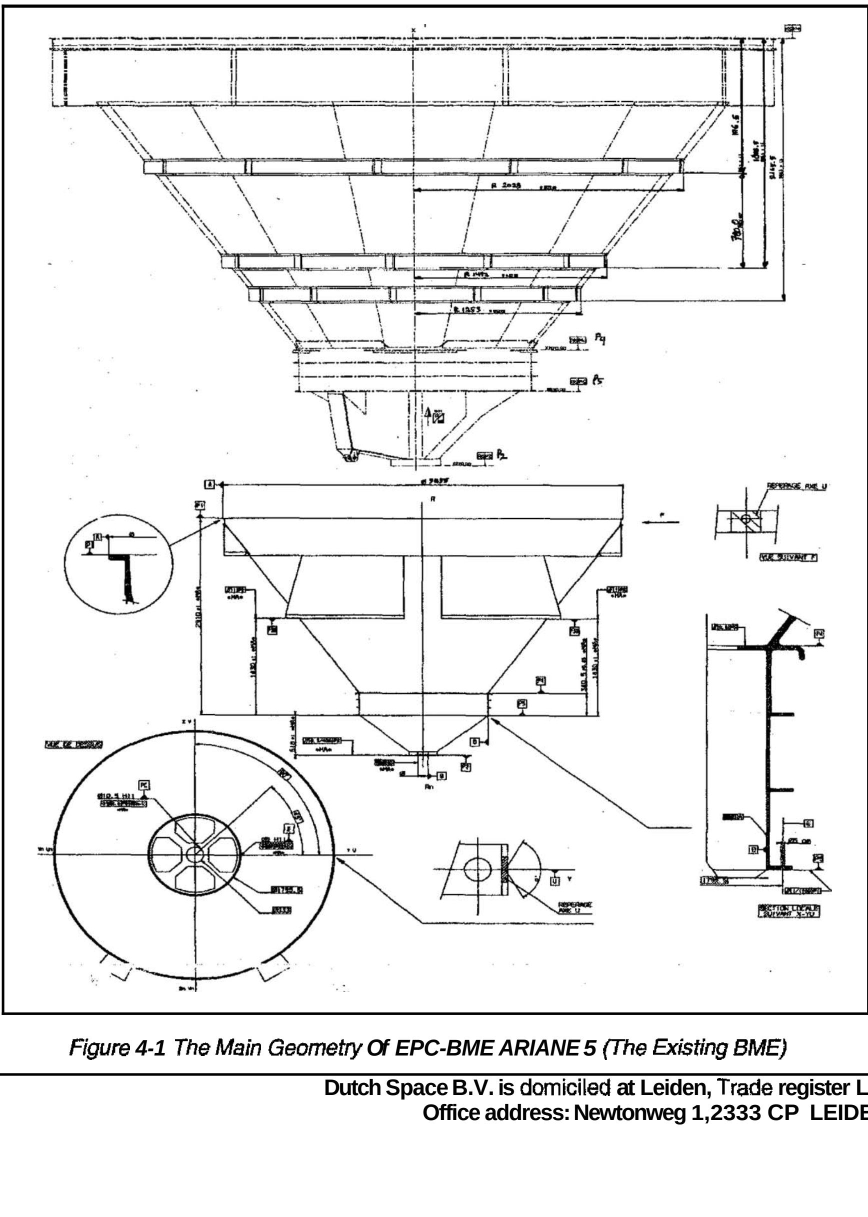

Figure 4-1 The Main Geometry Of EPC-BME ARIANE 5 (The Existing BME)

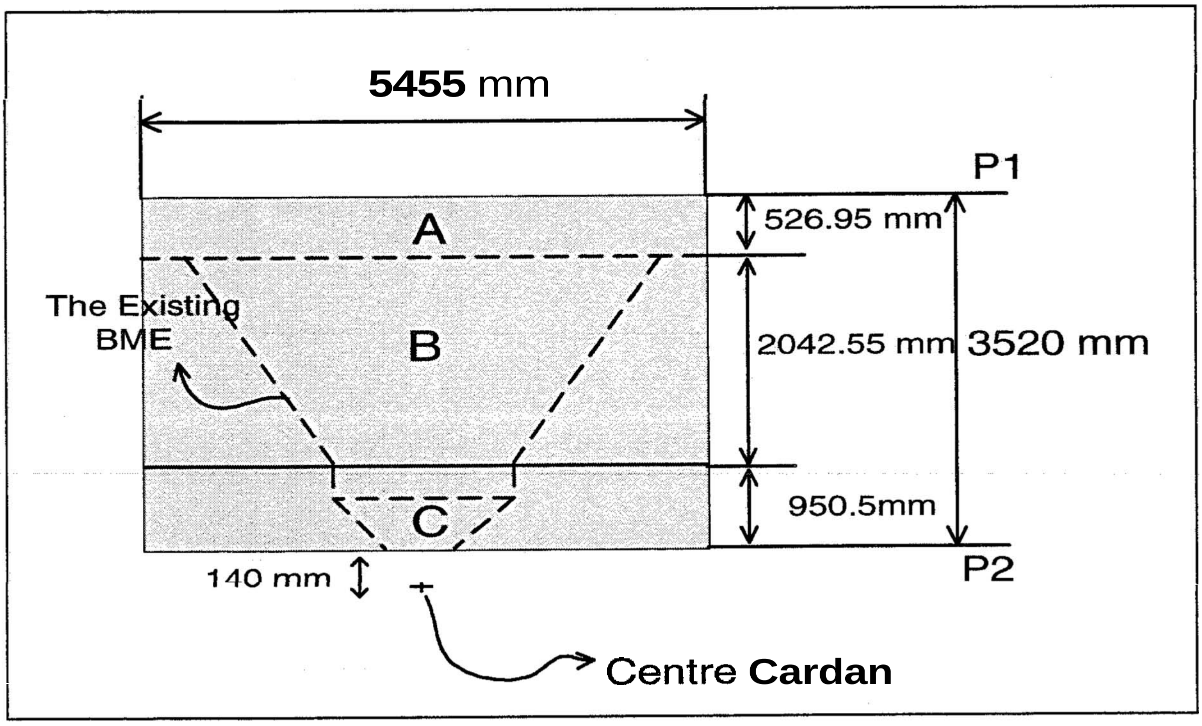

Figure 4-2 Envelope of the New Concept Design

4.1.5 External Interfaces

External interfaces define all adjacent structures/parts which are connected to the BME and which correlate with the BME functions. All those structures must be respected and fixed in terms of envelopes and position once concept generation is started. The BME is surrounded by the following main structures:

- RIE tank
- EAP boosters
- Vulcain engine

Table 4-1 The Interfaces between fhe BME and all adjacent ctructures

I/F	Connection	Dimension/number
BME to RIE-tank	RIE flange	360 equidistant M8 bolts. Diameter 9mm.
BME to EAP Boosters	DAAR lugs	6 struts
BME to engine	Engine adapter	Engine frame to engine adapter with 12xM16 bolts

The skirt concept design must not violate these interfaces.

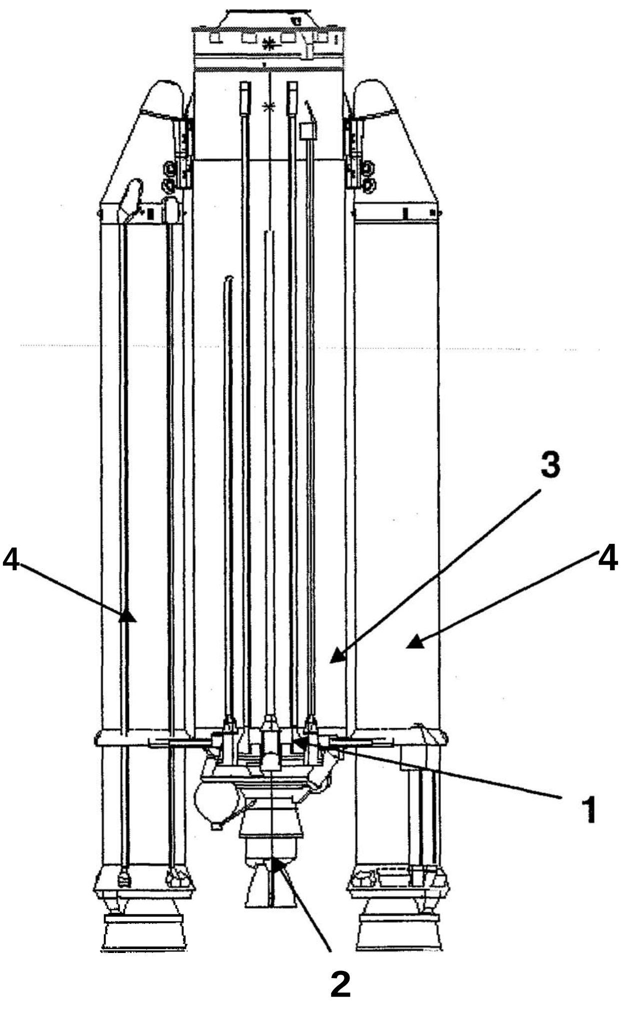

(1 BME
(2) Vulcain Engine
(3) RIE
(4) EAP Booster

Figure 4-3 External Interfaces of *the BME*

The complete external interfaces and the envelopes are described on Appendix ***C.***

4.1.6 Internal Interfaces

The internal interfaces are kept fixed either in geometry or position. The internal interface means all the equipments and lines, which are connected or assembled within the envelope of the structure. Several attachments of equipment and lines must be attached to the main structure of the BME as well. These interfaces are not intended to infiuence the main load. Because there are a lot of equipments, lines and brackets attached within the existing cone section, only the most important equipments are taken into account to simplify the process. Otherwise, it will be confusing and scattered by the complexity of many equipments and lines. It has not been necessary to consider the secondary equipments at upper leve!. Therefore, it is only concentrated on the equipments and lines that take the biggest portion on their envelopes. This assumption arises from the thought that if the major equipments and lines can be situated properly and fixed inside the concepts, then other smaller or secondary equipments and lines can be organized easily and consecutively in order as well.

The major equipments are:

- SSHel
- $HeHP_2$
- GAM
- SCR

And the major propellant lines are:

- LOx
- LH_2
- EPSO
- EPSH

The complete description of the major equipments and lines are depicted on Appendix C.

Accessibility inside the BME structure is necessary to provide access for inspection purposes and for installation of secondary equipments. These activities are done after the structural assembling process of the BME main structure. A maximum of 2 man holes are allowed. The dimension of the hole is flexible as long as it is fit enough to allow one man entrance.

4.1.7 Environmental Constraints

Akin to the BME, the skirt has to perform its functions subjected to a certain environment.

<table>
<tr><th rowspan="2">Phase</th><th></th><th></th><th colspan="3">Natural Environment</th><th></th><th></th></tr>
<tr><th>Situation</th><th>Maximum duration</th><th>Pressure (mbar)</th><th>Temperature (°C)</th><th>Hygrometry (%)</th><th>Salinity</th><th>Rain</th></tr>
<tr><td>Storage</td><td rowspan="3">Hangar in Europe</td><td rowspan="3">1 year</td><td rowspan="15">950 to 1050</td><td rowspan="7">-10 to 45</td><td rowspan="10">< 60</td><td rowspan="10">No</td><td rowspan="11">No</td></tr>
<tr><td>Removal form storage</td></tr>
<tr><td>Provisional acceptance</td></tr>
<tr><td>Transportation to the integrator</td><td>Container</td><td rowspan="2">2 months</td></tr>
<tr><td>Final acceptance</td><td rowspan="3">Hangar in Europe</td></tr>
<tr><td>Awaiting assembly</td><td>3 years</td></tr>
<tr><td>Integration and receipt</td><td>9 months</td></tr>
<tr><td>Storage in Europe</td><td rowspan="2">Container outside</td><td rowspan="8">15 months</td><td>-10 to 45</td></tr>
<tr><td>Transportation from Europe to Guyana</td><td rowspan="2">18 to 33</td></tr>
<tr><td>Storage in Guyana</td><td>Container under shelter</td></tr>
<tr><td>Assembly launcher BIL/BAF</td><td>Hangar in Guyana</td><td>23 to 27</td><td rowspan="5"><100</td><td rowspan="5">Yes</td></tr>
<tr><td>Transfer to launch area</td><td rowspan="4">External climate Guyana</td><td rowspan="4">18 to 33</td><td rowspan="4">Yes</td></tr>
<tr><td>Preparation of launch before fuelling</td></tr>
<tr><td>Possible aborted launch</td></tr>
<tr><td>New preparation of launch after aborted launch</td></tr>
<tr><td>Launch</td><td></td><td></td><td></td><td>Ref.A2 3.5.1</td><td></td><td></td><td></td></tr>
</table>

Table 4-2 Natural Environment

4.1.8 Strength

Even though the skirt is not a load carrying part, the addition of it will give impact to the loading condition of the existing BME. The skirt has to withstand loads due to its own mass as well.
Consequently, there should be requirements for the strength performance of the skirt. These requirements are listed below.

1. Pressure difference
   The blast wave and the aerodynamic forces cause pressure difference (Ap) between inside and outside the skirt with a magnitude of 0.01 bar. The skin of the skirt should be able to withstand this pressure.

2. Vulcain loads
   The Vulcain engine gives thrust load of 2×10^6 N in axial direction and 2.784×10^5 N in lateral direction. These loads will not be carried by the skirt. But, this report will analyze the impact of the skirt to the existing BME considering these loads.

3. Gravitafionat loads
   The main load to be carried by the skirt is the load due to its own mass. This load is influenced by the force of gravity which occurs during the ARIANE 5 flight. The maximum magnitude in axial direction is 5g and in the lateral direction is ± 3g. The thickness of the skirt and the stiffeners will be optimized based on these loads.

The total loading condition for the skirt is depicted on figure 4-5 below.

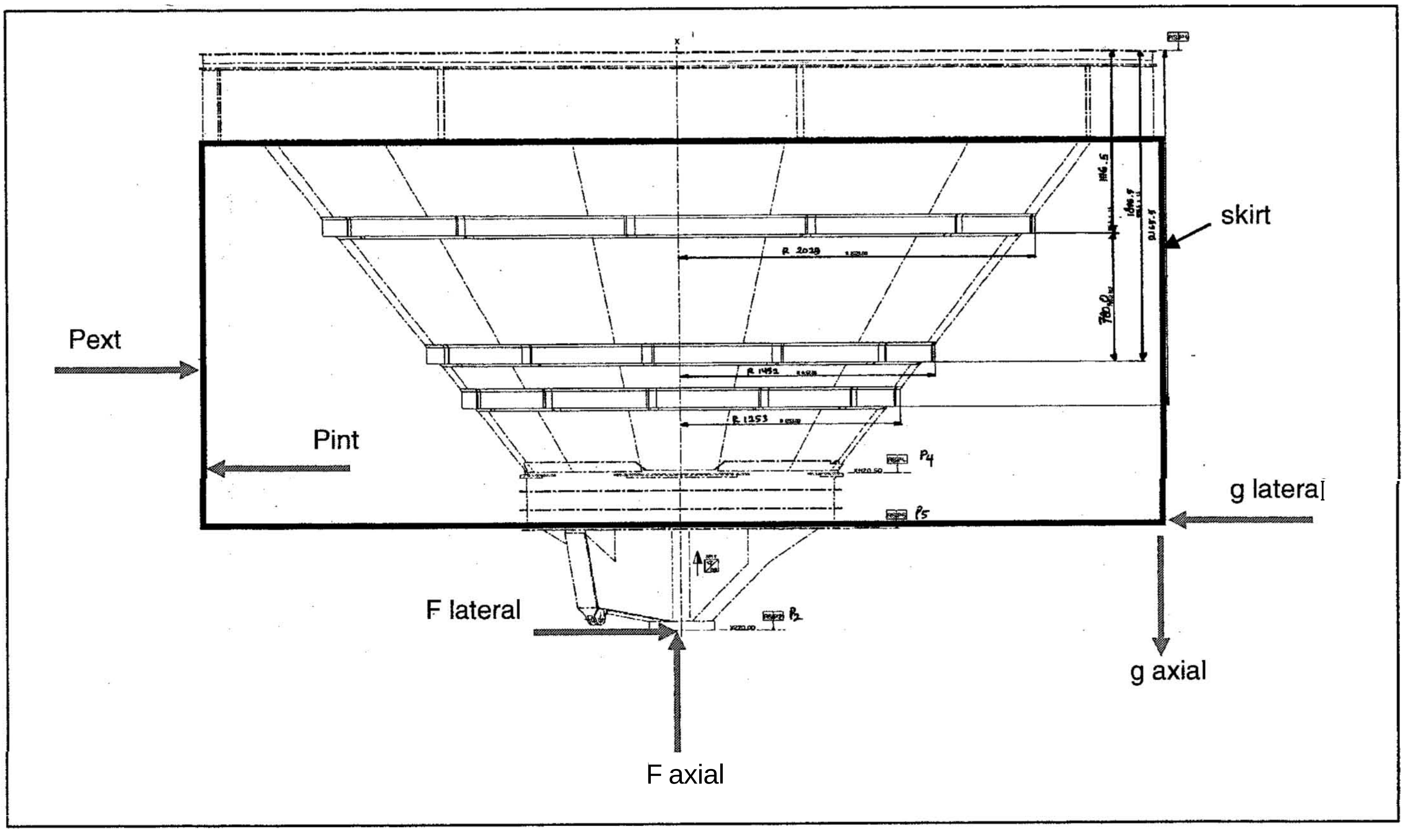

Figure 4-5 Loading case for the skirt

The strength shall be calculated and tested for a temperature of 20°C and it's requirements have to be satisfied until limit load. There are two important strength criteria in the skirt structure which must be satisfied:

a. No material yielding is allowed
b. tnstability (buckling) may not occur

Two safety factors have to be taken into account in case of verification by analysis:

- Yield load = J_E x lim load, J_E=1 . I
- Ultimate load = J_R x lim load, J_R=1.25

4.1.9 Stiffness

This requirement is one of the most important technical performance requirements. To generafe the concepts this criteria is decided to be more importance than the strength criteria. Since the skirt can be assumed as being subjected to compression, the requirements for light-weight structure and stability of the structure (thus the stiffness) will determine the strength.

Stiffness shall be calculated and tested at room temperature 20^0 C and its requirements have to be satisfied until limit load. There are **2** stiffness criteria in the centre cardan which must be satisfied:

a. The axial stiffness of the centre cardan. The stiffness which is occurred in the same direction of axial load introduction.The stiffness (k) can be expressed as the reverse of flexibility (f).

„f = 1/ k_{ax}

The axial flexibility requires: f axial flexibility ≤ 4.5 x 10^{-9} m/N

In other word the stiffness will be : k of the BME ≥ **2.2X** 10^8 Nlm

b. The transversal (lateral) stiffness. The stiffness due to the lateral load effect of the thrust load. This stiffness is calculated in the worst condition. The flexibility in lateral prescribes :

f lateral flexibility ≤ 17 x 10^{-9} m/N , it means the lateral stiffness (k_{lat}) ≥ 5.9 x 10^7 N/m

The stiffness requirement must be calculated within these following boundary conditions:

- The force is subjected to the centre cardan (0, **0, 0**) in axial and transversal direction
- No other load is applied than to the centre cardan
- The skirt is clamped at the level of the flanged connection with the tank

4.1.10 Mass

Since the mass is frequently directly related to cost, higher mass will result in lower production and development cost for the overall launcher performance. Since launching a structure into space is very expensive and the BME is not a payload, the structure (EPC-BME) will be separated from the upper structure after extinction of the Vulcain engine. It is better if the mass of less important structures could be diverted into more payload rather than other supporting structures. The target mass of the BME (excluding lines and equipment should be less than **2000** kg representing the main load carrying structure (Internal technical notes; ref. **5).**

Nevertheless, the mass target is not the primary goal. It is likely to be a spin-off in the design changes. Therefore it needs further study. If the impact on performance is marginal, an increase in the mass of a subsystem can be acceptable. In particular if the accompanied drop in the recurring cost of this sub-system is significant **(see** figure 4-6).

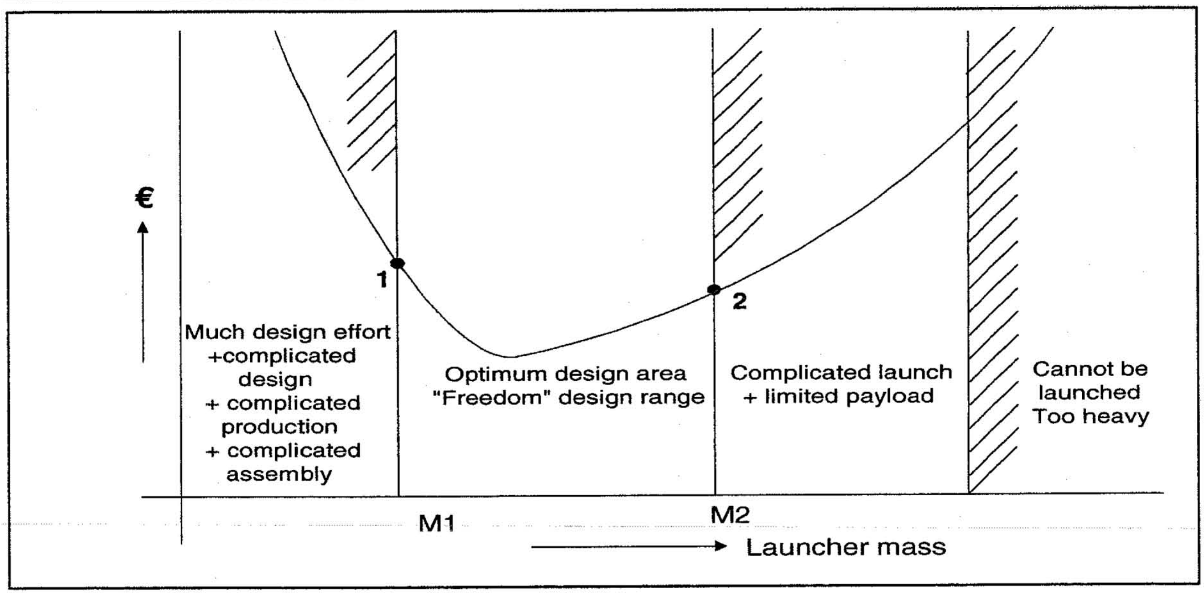

Figure 4-6 Design cost versus mass graph

4.2 Design Concept Generation

The ideas of the Cone-Skirt concept is to reduce buffeting problem and maintain the configuration of the equipment as it is. The Cone-Skirt concept comes as a resuit of comprehensive studies which have been conducted at Dutch Space.

Thus, in order to have a good understanding of the Cone-Skirt concept, initia1 step to be taken on the design concept generation is to review the results of previous studies which have been conducted in Dutch Space.

4.2.1 Result from previous studies

Regarding each part of the EPC-BME, there are many design options which can be explored. Indeed, there are many studies already done in Dutch Space in order to redesign the EPC-BME. Some concepts give a breakthrough result, some lead to another design option.

The results of previous studies can be summarized into 4 design concepts, which are described on the next subsection.

4.2.1.1 Existing BME Cone with Skirt (Cone-Skirt concept)

The main idea of this concept is to keep and maintain the configuration of the equipment as it is. This concept also maintain the original load path.

Advantages:

- Better thermal protection for the equipment
- Can overcorne the buffeting problem
- Easy to manage the equipments installation

Disadvantages:

- Increases the complexity factor
- Requires a stiff and strong skirt

The additional skirt does not function as load carrying structure. Thus, the mass will not be significantly increased. However, this must be confirmed by the load analysis report.

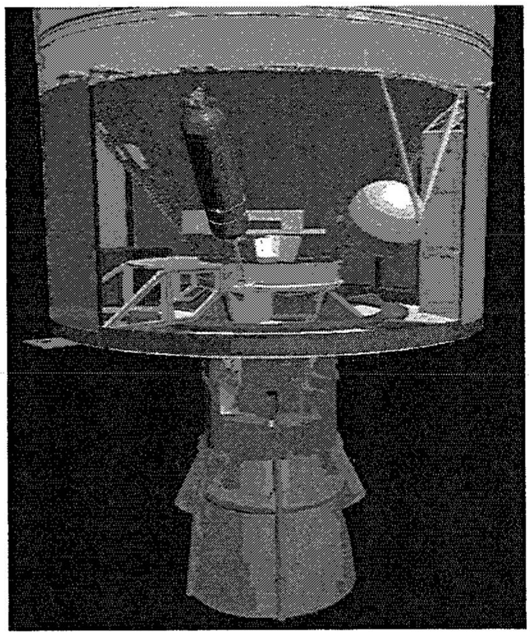

Figure 4-7 Existing BME Cone with Skirt concept

4.2.1.2 Load Carrying Cylinder and Cross with "Low" DAAR lugs

The characterization of this concept is to make the structure more efficient. This is done by combination of the cylindrical skirt and the main structure. The DAAR lugs will be moved down to the P2 level attached near the Cross. This idea solves the high lateral load occurring on the cylindet wall.

Advantages:

- Reduce buffeting
- Easy to manage the equipments installation
- Better thermal protection for the equipments

Disadvantages:

- The DAAR which is moved down requires modification of the Boosters attachment points
- Mass could be very high due to change in original load path (i.e. less efficient)

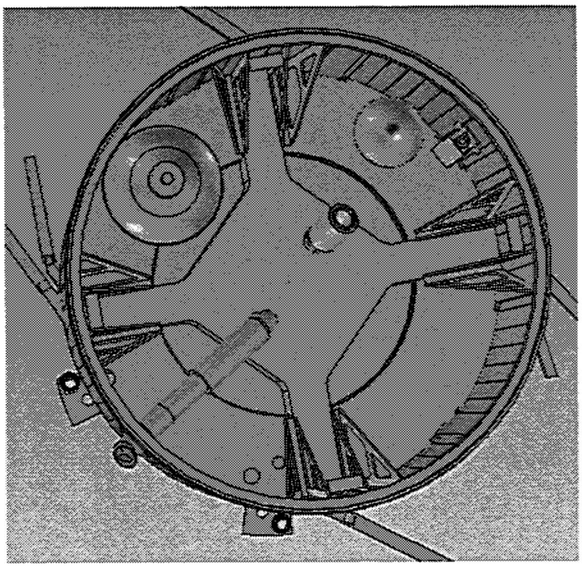

Figure 4-8 Load Carrying Cylinder and Cross with Low DAAR lugs

4.2.1.3 Load Carrying Cylinder and Cross with "High" DAAR lugs

This concept is similar to the concept described on section 4.2.1.2 in terms of shape. In this concept, the DAAR lugs remain at the same positions with the existing BME. Consequently, this concept also maintains the Box structure. However, the Cone structure is absent.

Advantages:
- Reduce buffeting
- Easy to manage the equipments installation
- Better thermal protection for the equipments

Disadvantages:
- Load transfer will not be so efficient
- Installation of the secondary equipments could be a problern
- Mass is very high due to change in original load path and due to an inefficient ring structure to resist the DAAR loads
- As cone is absent, hence no axial/radial stiffness. Therefore, this concept needs a very stiff box structure.

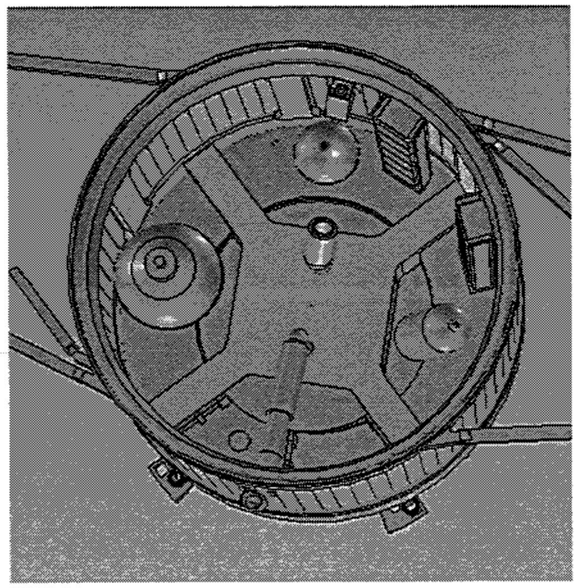

Figure 4-9 Load Carrying Cylinder and Cross with High DAAR lugs

4.2.1.4 Tubular Struts

This concept idea is to reduce the mass by using struts instead of cone panels. The struts are assurned to have lighter weight and simplify the model. The DAAR lugs are still introduced at the Top I/F Ring.

Advantages:
- Efficient on load transfer
- Low mass

Disadvantages:
- Installation of the secondary equipments is a problern
- Increases the number of parts
- Could influence high torsion on the struts structure

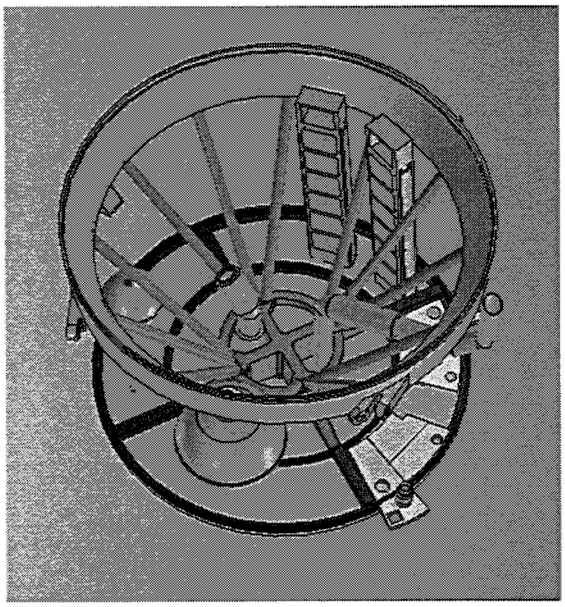

Figure 4-10 Tubular struts concept

4.2.1.5 Conclusion of previous studies

All of the design concepts described above are already analyzed using the complexity factor. The results are shown on the table 4-3 below.

Table 4-3 Result of previous studies

Nr.	Concept	Complexity Factor	Relative to Existing BME (%)
1	Existing BME	50.6	100.00
2	Existing BME with Skirt	57.9	114.43
3	Cylinder and Cross with Low DAAR	48.3	95.45
4	Cylinder and Cross with High DAAR	57.1	112.85
5	Tubular Struts	56.3	111.26

Then the conclusions of the previous studies are:

- Adding skirt to the existing BME increases complexity by 14%
- Only concept 3 has a complexity factor lower than the existing BME
- Concept 4 and 5 are onty slightly less complex than concept 2
- Concept 3 is about 17% less complex than concept 2
- Cylinder and Cross with low DAAR is the least complex but will increase in cornplexity for the LOX and other prirnary interfaces and the mass will be two times higher.
- With a lower and upper torsion box the Cylinder and Cross with high DAAR offers little advantage because of the relative high mass increase.
- The Tubular Strut concept theoretically offers a small advantage but is even more problematic regarding support structure for the primary ***and*** secondary interfaces that is 30% of the cost of the existing BME
- The existing BME accommodates all the current interfaces and is open to further (low risk) value engineering development
- A skirt around the existing BME offers significant advantages not yet accounted for, such as simpler TP (Thermal Protection)

4.3 Skirt design concept generation

Based on the result of the previous studies, the Cone-Skirt concept offers significant advantages. The major primary load carrying structures are to be kept and maintained in this concept. Therefore, the Cone-Skirt concept should be taken forward into detailed study.

This part describes the skirt design concept generation process.

For the skirt design concept, there are 4 aspects to be analyzed, i.e.:

- Shape of the skirt
- Stiffener
- Concept of the bottom part
- Level of the bottom part attachment

Each of the aspects will be discussed in the next sub-section.

4.3.1 Shspe of the skirt

The shape is the most important aspect of the skirt since it will give the aerodynamic effect to the BME. In this study, the main function of the skirt is to reduce the buffeting problem which occurs due to turbulence (see Chapter 3).

There are 3 concepts for the shape of the skirt which will be presented and briefly discussed in the next sub-section. The potential advantages and disadvantages are determined by applying the top ten design requirements (as explained in Chapter 3).

4.3.1.1 Cylindrical

It is a simple shape yet effective. The cylindrical shape reduces the buffeting problem by moving the turbulence away from the BME box. It gives less vibration to the Vulcain engine.

However, there should be a stiffness analysis of this shape due to abruptly surface change on the bottom part.

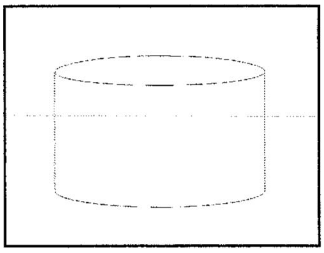

Figure 4-11 Cylindrical Skirt

Potential advantages:
- Simple shape means easy to be manufactured, hence low manufacturing cost
- Offers more space for the equipments than the other concepts
- Easy to make the internal interfaces perturbation

Potential disadvantages:
- Aerodynarnically less effective
- Potentially low stiffness

4.3.1.2 Aerodynamic **Shape**

The purpose of the shape is to eliminate the turbulence, thus also the buffeting problem.

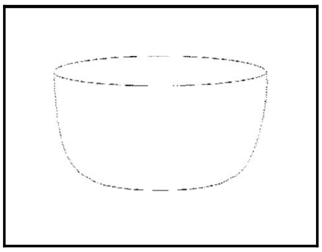

Figure 4-12 Aemdynamic Skirt

Potential advantages:
- Eliminates buffeting

Potential disadvantages:
- High cost due to the difficulty of manufacturing
- Difficult to attach the LBS

4.3.1.3 Stepwise Conical

This shape reduces the buffeting gradually. It also can be manufactured with tower cost, compared to the aerodynamic shape.

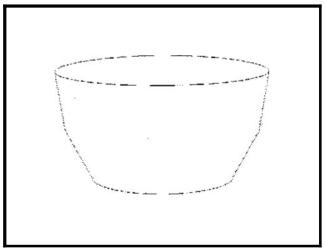

Figure 4-13 Stepwise Conical

Potential advantages:
- Reduce buffeting effectively
- Easy to make internal perturbation
- Low manufacturing cost

Potential disadvantages:
- Difficult to attach the equipments
- Difficult to attach LBS
- The connection between two cone has strong constraints

In order to compare three concepts of the shape, a trade-off matrix is made based on the top ten design requirements. The matrix is shown below.

Requirements	Shape		
	Cylindrical	Aerodynamic	Stepwise Conical
Cost	+	-	+
Reduce buffeting	-	+	0
Respect the geometrical constraint	+	-	-
Internal interfaces perturbation	+	-	0
Respect the external interfaces	+	-	0
Strength performances	0	+	0
Stiffness performances	-	+	0
Mass	0	0	-

The trade-off matrix shows the cylindrical shape has most advantages (plus sign) and only two disadvantages (negative sign). Hence, the cylindrical shape is selected as the shape of the skirt.

4.3.2 Stiffener

One of the design requirements is stiffness performance. Thus, with the intention of increasing the stiffness of the skirt, the use of stiffeners can be applied. This section will discuss some concepts for the stiffener.

There are 3 concepts will be studied, i.e.:
- Hat stiffener
- Blade stiffener
- Honeycomb panels

Some advantages and disadvantages of them are shown on the table below.

Concepts	Advantages	Disadvantages
Hat stiffener 	- high stiffness - low cost	- increase mass
Blade stiffener 	- low cost - low mass	- relative low stiffness
Honeycomb panels 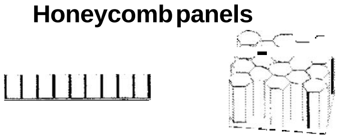	- high stiffness - relatively low mass	- high cost

Then, the trade-off can be determined by applying the design requirements.

Requirements	Concepts		
	Hat Stiffener	Blade Stiffener	Honeycomb panels
Cost	0	+	-
Respect the external interfaces	0	0	-
Strength performances	0	0	+
Stiffness performances	+	0	+
Mass	0	+	0

From the trade-off matrix, it can be concluded that blade stiffener concept is the best concept and should be taken forward into concept design.

4.3.3 Concept design of the bottom part

There are 4 design concepts can be applied for the bottom part of the skirt, i.e.:

- Closed panels
- Panels with holes
- Struts
- Struts and removable panels

Concepts	Advantages	Disadvantages
Closed panels 	- good blastwave protection - low cost - internal thermal protection guaranteed	- vulnerable to buckling - vibration sensitive - too large structure to handle
Panels with holes 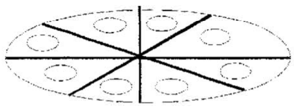	- good blastwave protection - low cost - good internal perturbation - internal thermal protection guaranteed	- high mass -holes reduce stiffness
Beams (open structure) 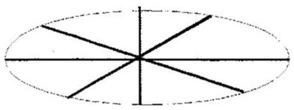	- high stiffness - relatively low mass	-attachment to struts more difficult - internal thermal protection still needed
Beams and removable panels (closed) 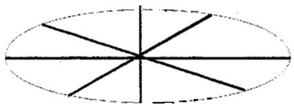	- high stiffness - good blastwave protection - good internal perturbation - internal thermal protection guaranteed	- higher mass

Requirements	Shape			
	Closed panels	Panels with holes	Struts	Struts and panels
Cost	0	-	0	-
Respect the geometrical constraint	-	0	-	0
Internal interfaces perturbation	-	+	+	0
Environmental constraints	+	0	-	+
Strength performances	0	0	0	+
Stiffness performances	-	-	+	+
Mass	0	+	+	-

The trade-off matrix shows that the beams concept and the beams-panels concept have same number of plus-minus sign. Thus, these concepts will be taken into further detailed design.

4.3.4 Level of the bottom part attachment

There is no doubt that the top part of the skirt will be attached to the BME box. Meanwhile, there are two possibilities of the bottom part attachment, i.e.:

- At the level of the interfaces of existing LBS disconnection lines between launcher and platform (P3)
- At the level of interfaces of the attachment Vulcan thermal protection dome with lower cross cylinder (P5)

Level of Attachment	Advantages	Disadvantages
P3 (LBS)	- low mass - low cost	- less space for equipments - ineffective buffeting reduction
P5 (Cross)	- reduces buffeting significantly - more space for equipments	- relatively high mass - relatively high cost

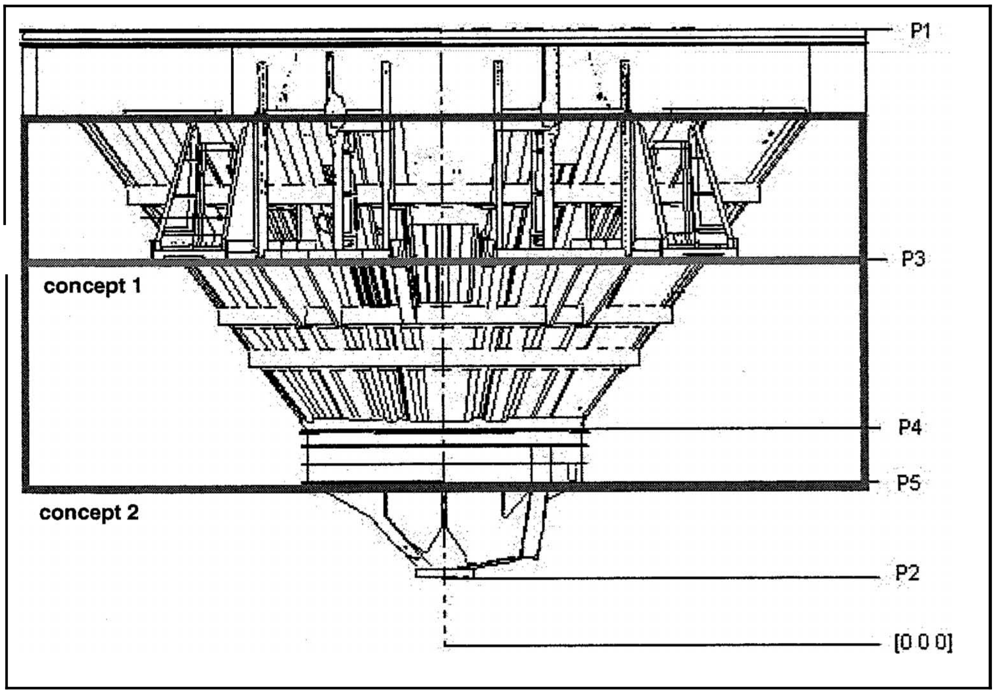

Figure 4-14 Level of Attachment

Requirements	Level of Attachment	
	P3 (LBS)	P5 (Cross)
Cost	+	-
Reduce buffeting	-	+
Respect the geometrical constraint	-	+
Internal interfaces perturbation	0	0
Respect the external interfaces	-	0
Environmental constraints	0	0
Strength performances	0	0
Stiffness performances	0	0
Mass	+	-

The level of attachment will be taken into further design is P5 (Cross). It is decided based on the requirements of reduce buffeting and the geometrical constraint. At level P5, the skirt gives better buffeting reduction and more space for the equipments.

4.4 Summary of the design concept generation

After 4 main design aspects of the skirt have been studied, there are 2 design concepts for the skirt will be taken forward, i.e.:

Cylindrical skirt with blade stiffener, beams bottom part, and attached at level P5
Cylindrical skirt with blade stiffener, beams-removable panels bottom part, and attached at level P5

In the next chapter, detailed analysis of these concepts will be described.

5. Detailed Design Analysis

The design concept generation process gives 2 design concepts which will be analyzed further in this chapter. The concepts are:

- Cylindrical skirt with blade stiffeners, beams bottom part, and attached at level P5
- Cylindrical skirt with blade stiffeners, beams-rernovable panels bottom part, and attached at level P5

The difference between the concepts is only the bottom part concept. One (beams concept) is an open structure, another (beams-removable panels) is a closed structure. Thus, in the next sub chapter, the description is only for the closed structure.

5.1 Description of the concept

As the result of the design concept generation, the skirt is a cylindrical skirt with hat stiffeners and attached at the level of interfaces of the attachment Vulcan thermal protection dome with lower cross cylinder (P5). The basic dimensions of the skirt are listed below:

- Height : 2.38305 m (measured from the box floor to the lower cross cylinder)
- Outer diameter : 5.455 m

The thickness of the skirt will be optimized in the sub-chapter 5.2.

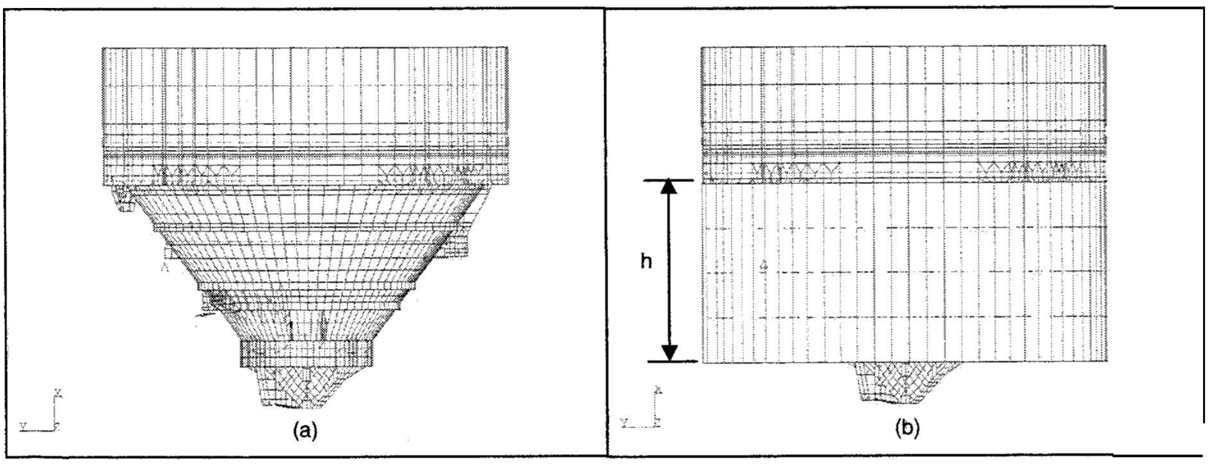

Figure 5-1 The Existing BME. (a) without skirt. (b) with skirt

The top of the skirt is attached to the box floor by rneans of a I/F ring.

In this report, the I/F ring will not be optimized. However, the mass is still taken into account.

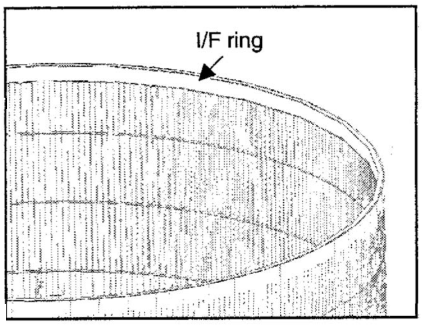

Figure 5-2 The Skirt I/F ring

The concept design for the stiffeners is the blade stiffeners. The thickness of the stiffener and the pitch will be optimized in the sub-chapter ***5.2.***
There is a possibility to add some intermediate rings in order to increase the buckling load of the skirt, with maximum number of 3 intermediate rings. The optimum number of the intermediate rings will be calculated in the sub-chapter 5.2.

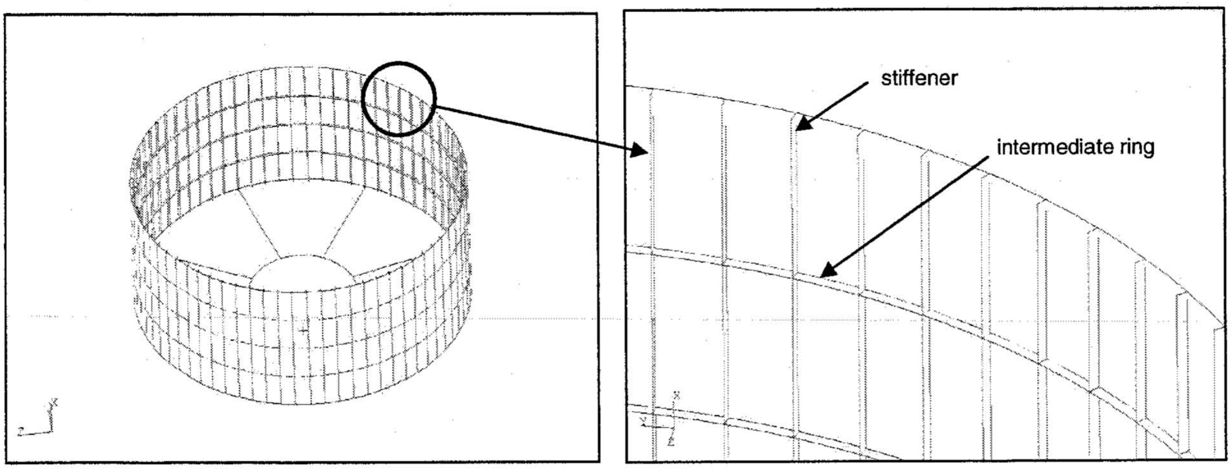

Figure 5-3 The Skirt

The beams in the bottom part are IPE beams. The IPE profile will be optimized in the sub-chapter 5.2.

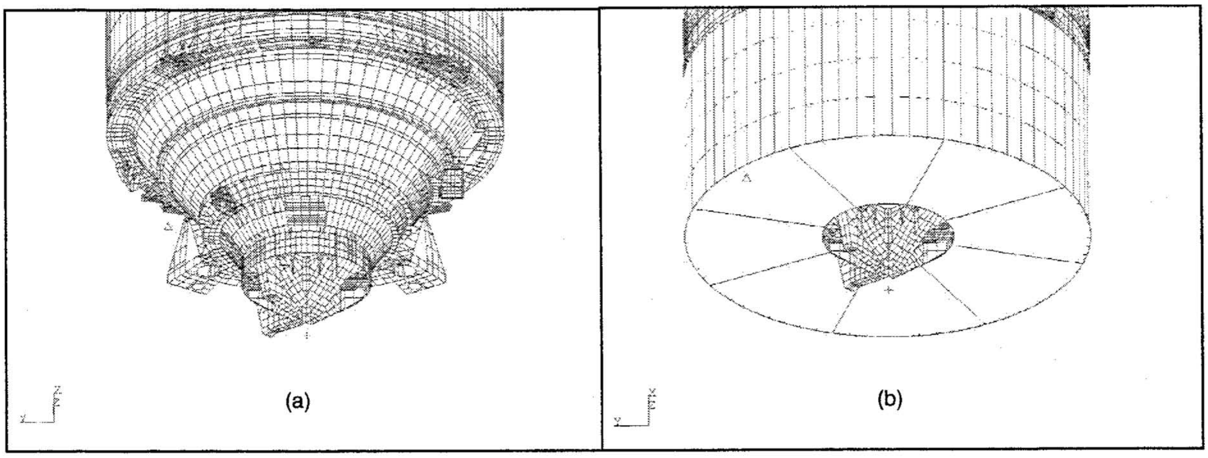

Figure 5-4 The bottom part (a) wiihout skirt. (b) with skirt

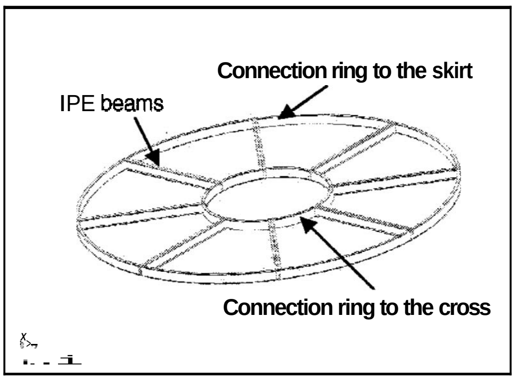

Figure 5-5 The bottom part

5.2 Skirt optimization

The aim of structural optimization is to determine the values of structural design variables in order to minimize an objective function of a structure while satisfying given constraints.

For the skirt concept, the design variables are:

- Skirt thickness (t)
- Stiffener thickness (t_s)
- Stiffener pitch (b)

Due to geometrical constraints, the height of the stiffeners is 40 mm.

The objective of the skirt optimization is to minimize the mass (approximately 200 kg). Meanwhile the constraints are the strength and stiffness performances (as described in the previous sub-chapter).

In the first step of the skirt optirnization, the design variables will be calculated based on condition of the skirt is with no intermediate ring. Thus, the height of the skirt is 2.38305 m (measured frorn the box floor to the cross).

5.2.1 Pressure constraints

Due to the blast wave and the aerodynamic forces (buffeting), there is a pressure difference (Ap) between inside and outside the skirt. The pressure difference is 0.01 bar.
Considering the allowable stress of the skirt material, this loading case gives the minimum thickness for the skirt skin (t).

The cylindrical skirt can be modelled as a pressure vessel. According Gere and Timoshenko (Ext. Ref. 12), the stress on the skin of pressure vessel due to radial pressure is:

$$\sigma = \frac{p \times r}{t}$$

with: σ = stress (N/m^2)
p = pressure (N/m^2)
r = radius of the pressure vessel/skirt (m)
t = thickness of the pressure vessel/skirt (m)

Then, the allowable stress is yield stress / safety factor, or:

$$\sigma_{allow} = \frac{\sigma_{yield}}{1.1}$$

Hence, the minimum thickness for the skirt skin can be calculated with the boundary condition:

$$\sigma \le \sigma_{allow}$$

$$\frac{p \times r}{I} \le \frac{\sigma_{allow}}{1.1}$$

$$t \geq \frac{1.1 \times p \times r}{\sigma_{allow}}$$

Substitute: p with Ap = 0.01 bar = 10^3 N/m^2
r = 2.7275 m
σ_{yield} = 7.1 x 10^7 N/m^2

The minimum thickness is 4.23 x 10^{-5} m.

Because the minimum thickness of a plate that can be produced is 0.03 mm or **0.03** x 10^{-4} m, then the minimum thickness of the skirt skin is **0.03** x 10^{-4} **m.**

5.2.2 Buckling of the stiffener

In order to calculate the stiffness, the skirt can be simplified as plate with stiffeners. For plate with stiffeners, there is a phenomenon called local buckling. Local buckling is a buckling condition which occurs on the stiffeners and the skin before elastic buckling happens on the total structure.

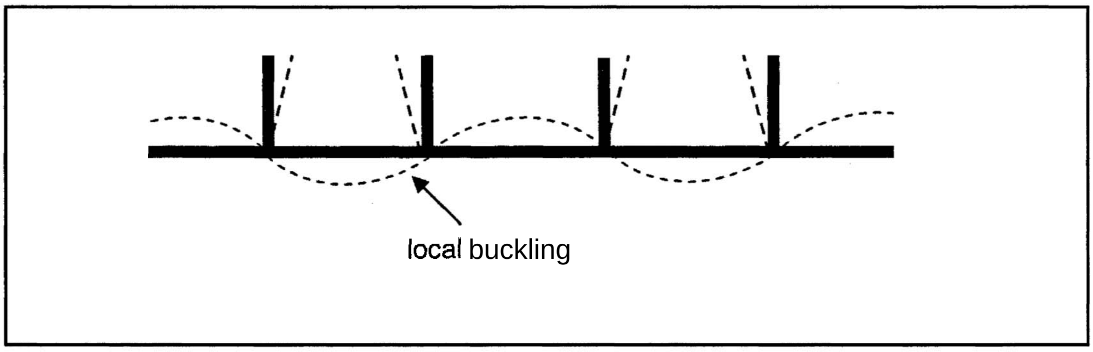

***Figure 5-6** Local buckling on a stiffened panels*

According to Timoshenko (Ext. Ref. 8), the approximate formula for buckling of the stiffeners is:

$\sigma_L = 0.385\ E\ (t_s/h)^2$

with: σ_L = buckling stress (N/m^2) (Stress at which local buckling occurs)
E = Modulus of Elasticity (N/m^2)
t_s = thickness of the stiffener (m)
h = height of the stiffener (m) = **0.04 m**

Substitute E = 7.1 x 10^7 N/m^2 and h = **0.04** m :

$\sigma_L = 1.708 \times 10^{10}\ t_s$

By calculating the actual stress on the skirt (gravitational load is taken into account), which is:

$$\sigma = \frac{F}{A}$$

$$\sigma = \frac{m \times a}{\mathrm{A}}$$

$$\sigma = \frac{\pi \times \rho \times D \times t \times h \times 5g}{\pi \times D \times t}$$

$$\sigma = \rho \times h \times 5g$$

Substitute: p = 2800 kg/m^3
h = 2.38305 m
g = 9.81 m/s^2

σ = 327288.087 N/m^2

With boundary condition which is the buckling stress should be higher than the actual stress, then:

$$\sigma_L \geq \sigma$$

$$1.708 \times 10^{10} \times t_s \geq 3.273 \times 10^5 \ \mathrm{N/m^2}$$

The minimum fhickness for the stiffeners is 0.0044 m or 4.4 mm.

5.2.3 Elastic buckling of the skirt

The skirt area between the stiffeners can be calculated as curved panel.

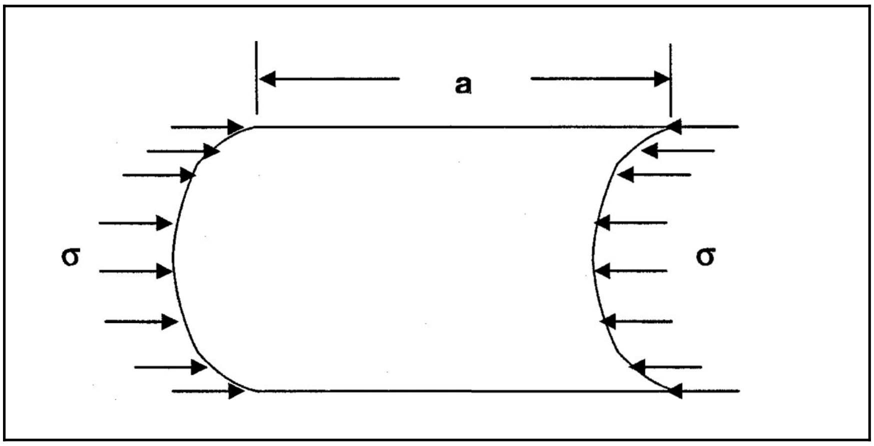

Figure 5-7 Curved panel under uniform compression on curved edge b

According to Roark and Young (Ext. Ref 7), the formula for curved panel under uniform compression on curved edge b is:

$$\sigma' = \frac{1}{6} \times \frac{E}{1-\nu^2} \times \left[\sqrt{12\left(1-\nu^2\right)\left(\frac{t}{r}\right)^2 + \left(\frac{\pi t}{b}\right)^4} + \left(\frac{\pi t}{b}\right)^2 \right]$$

With: o' = critical unit compressive stress at which elastic buckling occurs (N/m^2)
t = thickness of the skirt (m)
E = Modulus of Elasticity (N/m2)
v = Poisson's Ratio
r = radius of the skirt (m)
b = width of panel measured on arc / pitch of the stiffeners (m)

By substituting the known value of E, v, r, and changing s' with s calculated on section 5.2.2, then varying b by changing the number of stiffeners, the minimum thickness for the panels can be obtained.
The table below shows the minimum thickness and estimated mass of the skirt.

n	b (m)	min t (m)	est. mass (kg)
3600	0.0048	0.0004	4246.16
2400	0.0071	0.0005	2864.55
1800	0.0095	0.0007	2183.87
1200	0.0143	0.0011	1523.42
900	0.0190	0.0014	1213.39
800	0.0214	0.0016	1116.75
720	0.0238	0.0018	1043.46
600	0.0286	0.0021	943.55
450	0.0381	0.0028	848.51
400	0.0428	0.0032	829.99
360	0.0476	0.0035	822.99
240	0.0714	0.0052	878.44
180	0.0952	0.0069	997.40
120	0.1428	0.0100	1277.97
90	0.1904	0.0126	1546.52
80	0.2142	0.0138	1666.28
72	0.2380	0.0148	1774.16
60	0.2856	0.0165	1952.62
45	0.3808	0.0186	2176.28
40	0.4284	0.0192	2238.95
36	0.4760	0.0196	2280.81
30	0.5712	0.0200	2327.11
24	0.7141	0.0203	2353.47
20	0.8569	0.0204	2361.64
18	0.9521	0.0205	2363.52
15	1.1425	0.0205	2364.24
12	1.4281	0.0205	2363.08
10	1.7137	0.0206	2361.59

The highlighted row shows the minimum estimated mass for the skirt, which is 822.99 kg. This minimum mass is obtained with minimum thickness of the skirt panels is 0.0035 m or 3.5 mm and 360 stiffeners which are equally distributed.

5.2.4 Iteration process

The result of the first step (no intermediate ring) shows the minimum mass is considerably above the approximated rnass (200 kg). Thus, the next step is to add intermediate ring in order to reduce the actual load and also to reduce the global buckling length.

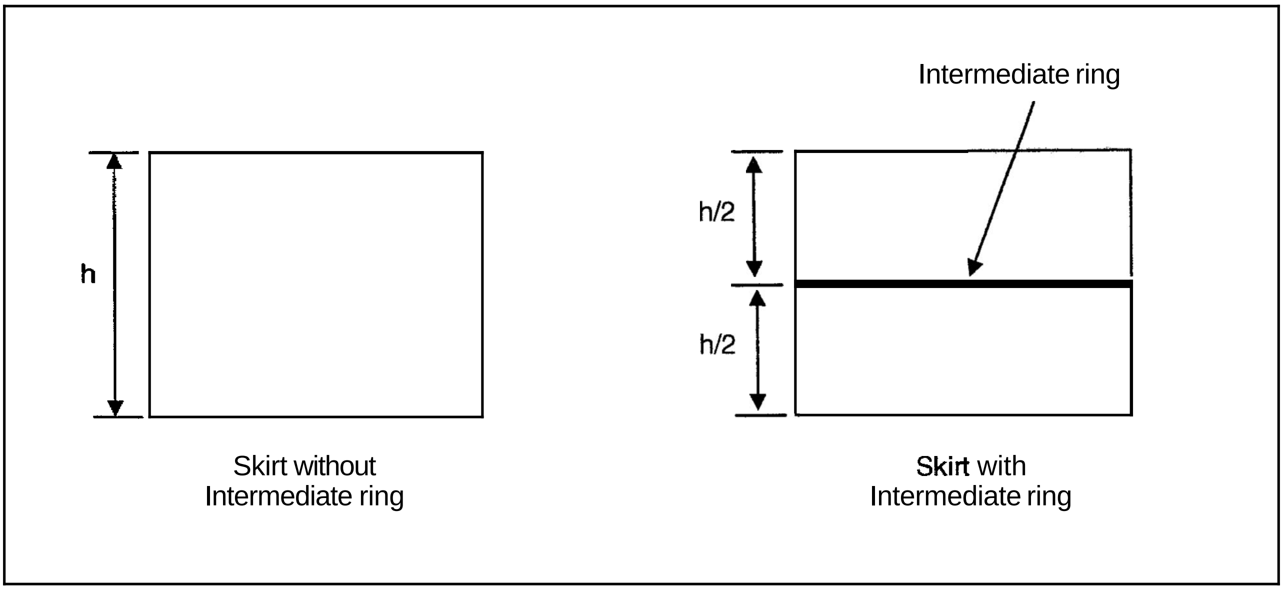

Figure 5-8 Addition of the intermediate ring to the skirt

Because the approximated thickness of the skirt is ≈ 1.5 mm, then the geometry of the intermediate ring has been selected. The cross section of the intermediate ring is depicted on figure 5-9.

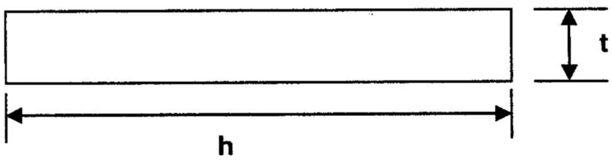

Figure 5-9 The cross section of the intermediate ring

Where: h = 0.04 m = 40 mm
t = 0.003 m = **3** mm

The thickness (t) is selected based on The Engineering Science Data Unit / ESDU (Ext. Ref. 6), while the height (h) is fixed by geometrical constraints. Based on this geometry, the mass of an intermediate ring is 5.76 kg. This value will be taken into account for the skirt optimization.

As calculated on section 5.2.2, the actual stress is:

$$\sigma = \rho \times h \times 5g$$

The equation shows that decreasing the height will result in a lower actual stress. Thus, by increasing the number of intermediate rings, the stress which each panel has to withstand will **be** lower.
After increasing the number of intermediate rings, the calculation on the section 5.2.2 and 5.2.3 is repeated. This iteration process is stopped after reaching the maximum number of the intermediate ring, i.e. 3 rings.

The optimum thickness of the skirt is achieved with the configuration of 3 intermediate rings and 360 stiffeners. The result for the skirt with 3 intermediate rings is depicted on the table below, while the complete table of the iteration process is shown on Appendix B.

With 3 rings

σ = 81822.02 N/m2
min ts = 0.002188 m

n	b (m)	min t (m)	Estimated mass (kg)
2400	0.0071	0.0003	1449.51
1800	0.0095	0.0004	1109.15
1200	0.0143	0.0005	778.85
900	0.0190	0.0007	623.67
800	0.0214	0.0008	575.23
720	0.0238	0.0009	538.44
600	0.0286	0.0011	488.07
450	0.0381	0.0014	439.24
400	0.0428	0.0016	429.02
360	0.0476	0.0017	424.33
240	0.0714	0.0025	441.91
180	0.0952	0.0032	482.76
120	0.1428	0.0041	558.00

The result of the iteration process gives:

- Minimum thickness of the skirt (t) is 1.7 mm
- Minimum thickness of the stiffeners is 2.2 mm

These values can be obtained with:
- Number of stiffeners is 360 which are equally distributed
- The pitch is 47.6 mm

The table shows that the estimated mass is 424.33 kg. This value is still twice the approximated mass. That is the best value can be obtained, since there is a maximum number of intermediate ring which is 3 rings.

5.3 Beams Optimization

In order to minimize the total mass, the beams on the bottom part are also needed to be optimized. The profile to be used for the beam is the IPE profile. Thus, the optimization process is done in purpose to select the IPE profile which gives the minimum mass.

The main load which the beams have to withstand is the load due to the mass of the skirt, in y-direction. Thus, there is a factor of 3g for the load (see figure 4-5). The beams must not buckle with respect to this loading condition. The free body diagram of the beam is depicted on figure 5-9 below.

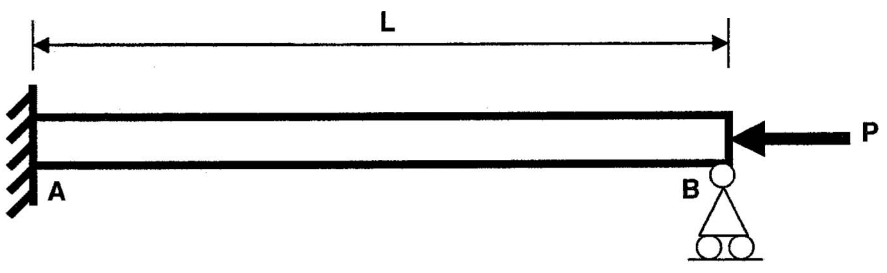

Figure 5-10 Free body diagram of the beam

The end A is the end of the beam which is connected to the cross, therefore modelled as fixed end. The end B which is connected to the skirt, is modelled as pinned end.

Based on Gere and Timoshenko (Ext Ref. 12), the critical buckling load for column fixed at the base and pinned at the top is:

$$P = \frac{20.19 \times EI}{L^2}$$

With: P_{cr} = critical buckling load (N)
E = Modulus of Elasticity (N/m^2)
I = moment of inertia (m^4)
L = length of beam (m)

Using L = 1.83 m (based on the geometry of the BME, figure 4-1) and E = 7.1 x 10^{10} N/m^2, and varying I based on the IPE profile data sheet, the value of critical buckling load, Pcr can be obtained. The value of the critica! buckling load then is compared to the actual load of the beam which is:

P = m x 3g

with: P = actual load (N)
m = total mass of the skirt + mass of the beam (kg)
g = gravity constant = 9.81 m/s^2

Because there are 8 beams on the bottom part, the actual load is divided by 8.

P' = P / 8

Buckling does not occur when: P' ≤ P_{cr}

Using the IPE profile data sheet, the estimated mass of the skirt (424.33 kg), and the mass of the intermediate ring, the result of beams optimization is shown on the table below.

Table 5-3 Beams optimization

IPE	mass (kg)	Pcr (N)	Py (N)	STATUS
80	87.83	342.96	1924.57	NOT OK
100	118.57	732.16	2037.65	NOT OK
120	152.24	1361.56	2161.51	NOT OK
140	188.83	2316.37	2296.13	OK
160	231.28	3720.75	2452.29	OK
180	275.19	5651.78	2613.84	OK
200	327.89	8306.40	2807.70	OK
220	383.52	11860.17	3012.33	OK
240	449.39	16655.62	3254.65	OK
270	528.43	24790.75	3545.44	OK
300	617.72	35794.59	3873.92	OK
330	718.73	50395.02	4245.48	OK
360	835.83	69662.44	4676.28	OK
400	970.50	99034.56	5171.69	OK
450	1135.91	144462.87	5780.19	OK
500	1327.67	206375.53	6485.62	OK
550	1551.63	287384.34	7309.52	OK
600	1785.84	394254.33	8171.11	OK

Status OK if P' ≤ P_{cr}

From the table 5-3, the optimum beam is the one with IPE 140 profile (The data is depicted on Appendix F). This profile gives a total mass (8 beams) of 188.83 kg.

5.4 Summary of the Skirt and Beams Optimization

The optimization process for the skirt and beams gives a conclusion that the estimated total mass of the skirt is:

Total mass = mass of the skirt + mass of 3 intermediate rings mass of the beams
= 424.33 kg + 17.28 kg + 188.83 kg
= 630.44 kg

6. The Impact of the Skirt to the Existing BME

After the optimum skirt is obtained, the next step in the design process is to review the result. This chapter describes the impact of the optimized skirt (cylindrical skirt with 3 intermediate rings) to the existing BME.

The main purpose of the skirt is to reduce the buffeting problem on the existing BME. Even though the skirt is not a load carrying structure, the addition of the skirt gives some influences to the stiffness of the BME.

Using FEM model, the impact of the skirt to the stiffness of the BME can be analyzed. By modelling the skirt and attaching it to the old BME model (version A5-v6A), the stiffness of the BME before and after the attachment can be calculated.

The stiffness to be analyzed is the stiffness of the BME due to the Vulcain load in axial and lateral direction.

The reason of using the old FEM model (version A5-v6A) is because the new detailed model of the BME (includes Cross and LBS structure) is not finished yet.

6.1 Axial stiffness

The Vulcain engine gives a force of 2×10^6 N in the axial direction to the BME. This force is applied on the centre cardan.

As stated on part 4.1.9, the required stiffness is 2.2×10^8 N/m

Figure 6-f shows the displacement of the BME without skirt due to axial Vulcain load, while figure *6-2* shows the displacement with the skirt.

Based on the displacement, stiffness with and without the skirt can be calculated as:

$$K = \frac{F}{d}$$

With: K = stiffness (N/m)
F = applied force (N)
d = displacement (m)

The results are shown on table below.

Table 6-1 Result for axial load

	displacement (m)	stiffness (N/m)
without skirt	0.008204	2.438E+08
with skirt	0.008181	2.445E+08

Thus, it can be concluded that the addition of the skirt only slightly increases the axial stiffness of the BME, as expected. Furthermore, the stiffness fulfils the requirement.

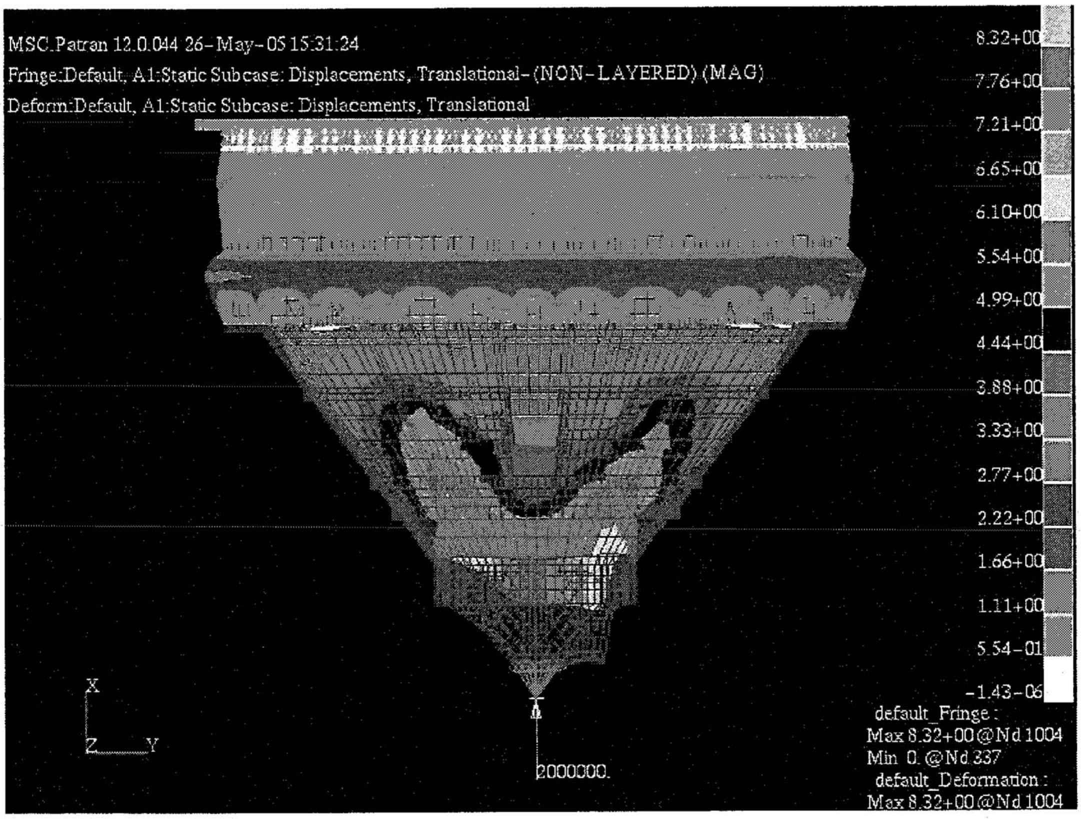

***Figure 6-1** Displacement of the BME without the skirt due to axial load*

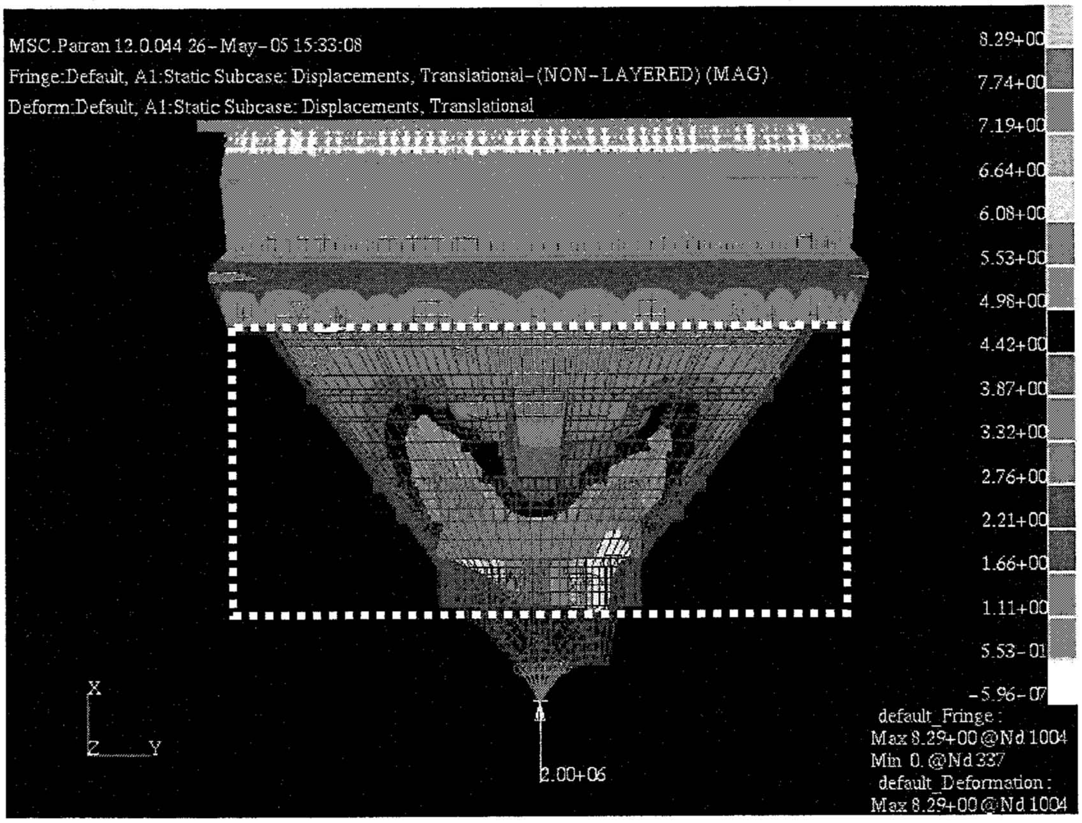

***Figure 6-2** Displacement of the BME with the skirt due to axial load*
(The dashed line is the position of the skirt, which is not shown)

6.2 Lateral stiffness

The Vulcain engine gives a force of 2.78×10^5 N in the lateral direction to the **BME.** This force is applied on the centre cardan.

As stated on part 4.1.9, the required stiffness is 5.9×10^7 N/m

Figure 6-3 shows the displacement of the BME without skirt due to lateral Vulcain load, while figure 6-4 shows the displacement with the skirt.

The calculated stiffness of the **BME** without and with the skirt is depicted on the table below.

Table 6-2 Result for lateral load

	displacement (m)	stiffness (N/m)
without skirt	0.005192	3.85E+08
with skirt	0.004640	4.31E+08

It can be concluded that the addition of the skirt increases the lateral stiffness of the BME. Furthermore, the stiffness fulfils the requirement.

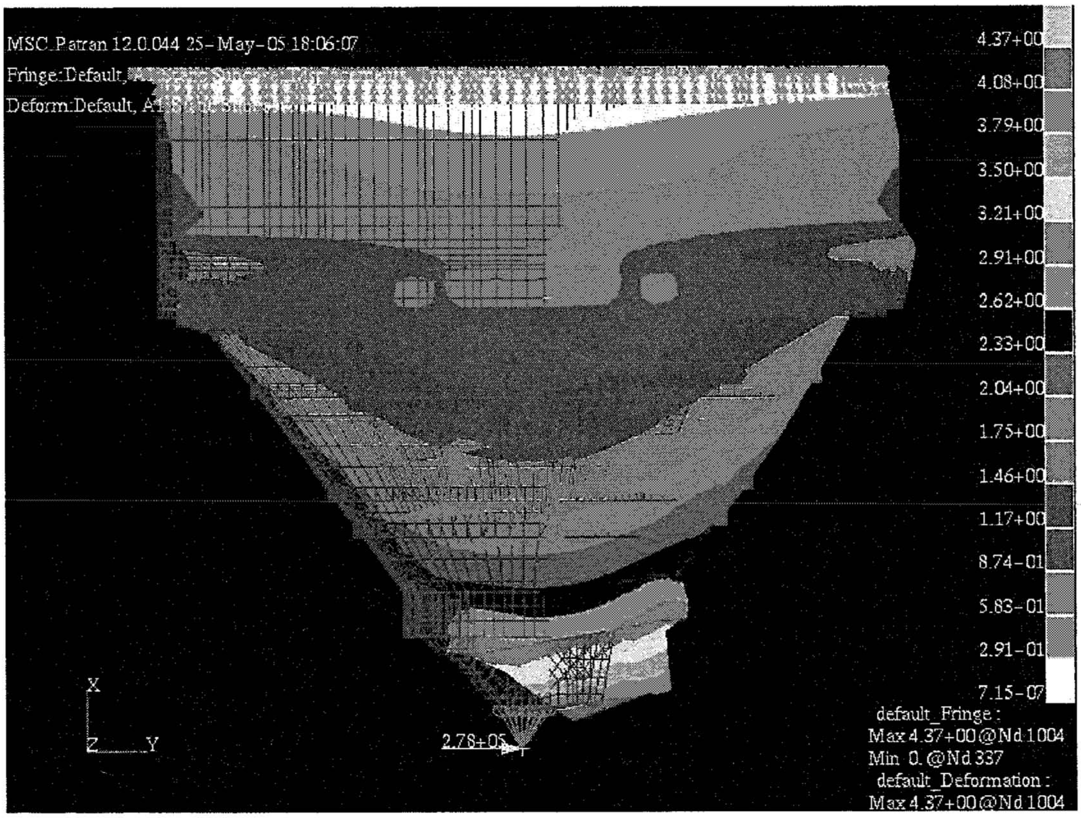

Figure 6-3 Displacement of the BME without the skirt due to lateral load

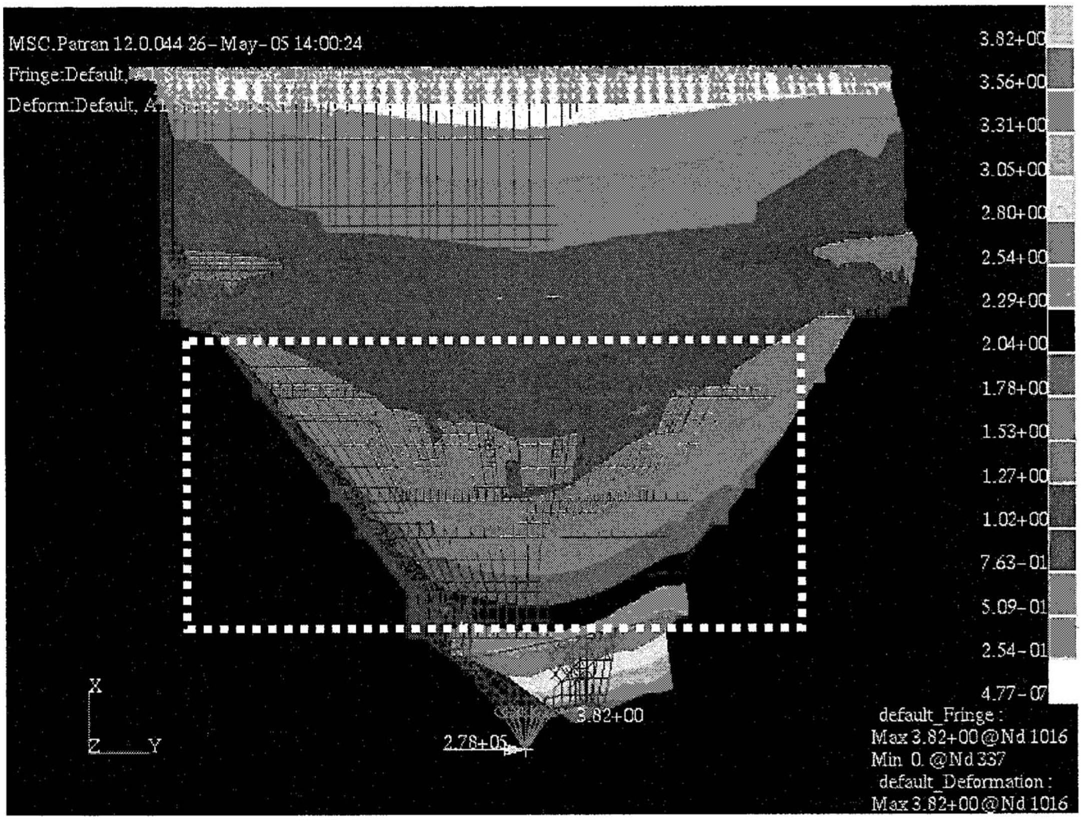

Figure 6-4 Displacement of the BME with the skirt due to lateral load
(The dashed line is the position of the skirt, which is not shown)

7. Conclusions and Recommendations

7.1 Conclusions

Based on the results of the preliminary study as presented above, the following conclusions with respect to the objective of the study can be drawn:

- The new finite element model has bigger error based on the hand calculation than the old model (version A5-v6A). tt is reasonable, because the old model has much more simplifications. Thus, the old model is more similar to the hand calculation (which is using a uniform cross section).
- The new detailed finite element model of the BME Box structure (with DAAR lugs) does not give significantly different result. It is shown that the differences of the results between the old model and the new model are below 1%.
- The old finite element model (version v6A) still can be used as the basis of calculation process. Furthermore, the new more detailed finite element model provides a much better basis for calculating new stiffness/stresses, etc. as a result of new loads.
- The new, more detailed model provides a better basis for calculating the effect of new designs, such as for instance the skirt design.
- Due to geometrical constraints and interfaces with other structures and equipments, the feasible skirt design concept is the cylindrical skirt concept.
- The cylindrical skirt concept can satisfy the stiffness requirements. However, at a considerabte mass of **630.44** kg (excluding thermal protection).
- The addition of the skirt increases the stiffness of the BME in lateral direction.

7.2 Recommendations for Further Study

With respect to the limitation of this study, further study of the EPC-BME ARIANE 2010 is required. Therefore, some recomrnendations are listed below:

- There should be an aerodynamic test for the skirt design concept. This test can be done either by means of wind tunnel or computational fluid dynamics (CFD) software.
- The Cone-Skirt design concept needs more detailed optimization. For instance, the effect of the thermal protection needs to be investigated.
- In order to reduce the skirt mass, a study of skirt design with CFRP or aluminium honeycomb panels shall be done. Honeycomb panel offers high stiffness and low mass structure at relatively high cost.

LIST OF APPENDICES

APPENDIX A THESIS ASSIGNMENT

Assignment
Generation of a new detailed FEM for the AR-5 Engine frame, based on the Cone-Skirt Concept. The expected time involved is 8-9 months, based on experience from Buyung Afrianto

Background
The development of Ariane 5 is proceeding with the present engine frame (see: figure attached). The design has now been made of a cone / box concept. Today, all equipment is now installed inside the cone and poses a considerable integration effort. In this study one of the design concepts to be studied is the so called: Cone-Skirt concept. It uses the maximum amount of existing technology and design features. The major primary load carrying structures are to be kept and maintained in this concept .In addition, it will allow the possibility that all secondary equipment can be installed on the new skirt now on the inside to protect against the blast wave, coming from the SRB's. However, the new skirt must be as light as possible and still support all the required equipment, such as bottles and pressure tanks. The work involved forms part of a larger study in which DS is involved, called AR-2010. The baseline performances should stll be met. Costs should be analysed aswell

Purpose
The purpose of this study is to generate a detailed FEM of the box cylinder structure, based on the latest drawing revisions. The model will need to be checked against the present coarse FEM. A correlation shall be done on the basis of comparing the old and new FEM against specific criteria. The generation of these criteria will be part of the study and will be verified in this study. Hand calculations shall be supported by a complete model of the BME based on Finite Element Modelling (being MSC/ NASTRAN).

The material properties and the thermal coating to protect against the booster heat shall be included in the thermal analyses and the mass budget.

Step for Step Plan
1. Familiarisation about the ARIANE project in general and in detail to investigate and grasp / understand the problem. Survey of existing documentation concerning the ARIANE project.
2. Generation of a functional / requirements specification concerning the FEM. This shall be documented in a design specification, providing all the external interfaces etc and the stiffness, loads and mass requirements.
3. Review of the FEM specification with specialists. Determine the "top 10" design drivers for your concept to be analyzed and document them.
4. Review of detailed drawings on the box-cone structure with the top ring interface. Generation of drawing tree showing latest revisions.
5. Make simple hand calculations based on drawings to demonstrate first order magnitude performance data.
6. Make overall FEM model of the box - cylinder structure with the detailed bracketry with all equipment attached to demonstrate compliance against the functional performance and environmental requirements
7. Perform correlation tests on the new FEM based on criteria for the old FEM model. Refine the new FEM model if needed.
8. Make adequate and concise description of the FEM in accordance with ESA rules ECSS. Check on sensitivity aspects on FEM input data.
9. Final reporting including mass and performance data of FEM with traceablity of FEM schematic description against actual Hardware installed in the box-cylinder structure.
10. Internal presentation and presentation to Technical College Utrecht

Henk Cruijssen
Dirk Spanjer
Floor Maitimo

APPENDIX B INTERFACE CONTROL DOCUMENT

BME - **Interface** Controle **Document**.

Introduction.

For the Ariane-5 project the current structural analyses of the Bati Moteur Equipe (BME) are carried out with a MSC-NASTRAN model which was created in the late eighties. The way in which the model was created was rather coarse w.r.t today standards. This had to do with the limited computer resources and power by the time the model was created. As the design changed, the model was updated, resulting in higher model versions and in 1994 the model was correlated with a structural test. The result of this update was model version 04. Nowadays four different model versions are used. This is caused by the fact that the current design comprises two versions: the P2.1 series and the P2.2 series (the latter one is also referred to as the PA-version). Furthermore the more powerful Vulcan II engine is introduced. All possible design options are reflected in the different MSC-NASTRAN models.

As stated above, the currently used FEM is rather coarse. Because of the fact that generation of a complete new FEM of the BME is very time consuming, and consequently, expensive and the fact that the current model is a with a hardware test correlated model, changing the current model is not possible.

For the generation of the FEM of the Ariane 2010 however another approach is chosen. It is thought that it is not very useful to stick to updates of the current (outdated) model. It is better to create a complete new model with a sufficient fineness and consequently accuracy, and reflecting the latest design changes. Nevertheless creating such a FEM remains very laborious and time-consuming. Therefore the following approach is adopted. The BME-model is split up in four main parts. Each main part is modeled by somebody else. In order to keep the model generation costs as low as possible, students will perform the task, of course supervised by DS-analysts and people.

However the individual FEMs need to be coupled afterwards. In order to be able to do so, appointments and requirements are needed to smooth the coupling process. Especially at the Interfaces between the four main parts a clear definition of the number and location of the nodes is required; otherwise coupling becomes far more difficult. These requirements and appointments are described in the under laying document.

Division of BME in four **main parts.**

The following table gives the division in main parts and the responsible student.

Division of the BME in four **main parts** and responsible **person**		
BME-main pari	Student	From Insitute
BME-BOX/Cylinder	Hasto Nugroho	HTS-Utrecht
BME-Cone	Guo Yunyan	HTS-Utrecht
%ME-Cross	Timon Duurkoop	HTS-Eindhoven
BME-LBS	Tim Garritsen	TU-Delft

Phvsical Units to be used.

All geometry, element and material properties must be defined in the SI-system (Systerne International). This means that the following basic 'units' have to be used.

Length in meters [m]
Mass in kilograms [kg]
Time in seconds [s]

Derived units are for example:

Force in Newton's [N] = [kg*m/s^2]
Stress, Pressure, Young's modulus etc, in Pascal [Pa] = [N/m^2]

Used Coordinate-, Element-. Node-, Property- and Material-numbers.

All used numbers in a FEM related to a main part must be located in a certain range. This is necessary to avoid the problem of duplicate numbers once all models are combined to one overall model.

Numbering ranges of the main parts FEMs		
BME-main part	**Student**	**Numbering Range (from - to)**
BME-BOX/Cylinder	Hasto Nugroho	1.000.000 -1.999.999
BME-Cone	Guo Yunyan	2.000.000 -2.999.999
BME-Cross	Timon Duurkoop	3.000.000 -3.999.999
BME-LBS	Tim Garritsen	4.000.000 -4.999.999

Note: It is possible in PATRAN to define a certain numbering offset afterwards

Used Coordinate Svstems.

Each main part must have its own 'basic' coordinate system. All used coordinate systems in a rnain part must directly or indirectly refer to this particular basic coordinate system. This has the advantage that relocation of the main part at an arbitrary location in space is simply a matter of changing the data defining the basic coordinate system of a main part.

Note: If not present it is possible in PATRAN to define such a basic coordinate system afterwards.

Compatibility at the Interfaces.

The several main parts do interface at certain locations. In order to be able to couple the models to one overall model, it is necessary that at both sides of an interface the number of nodes and their location match with each other. This document does not define that number and location. It is only stated that it is required that at the interfaces the node distributions at both sides match. Therefore it is stated that the first one who has defined his cide of the interface, determines this Interface-node distribution. All others who have to model their side of the same interface have to conform themselves to this firstly defined node distribution.

Use of PARAM cards.

In MSC-NASTRAN several PARAM cards can be used to direct the analysis or to request special outputs. An example is the 'PARAM, GRDPNT,0' card which calcuiates and presents the implemented rigid body mass properties with respect to a certain node. However, due care should be taken with the use of these PARAM cards, because it can result in completely wrong or useless results. An example is the 'PARAM,BAILOUT,-1' card. This PARAM forces the analysis to continue, even when errors are detected. An example is a static analysis of a model (SOL 101), for which not all rigid body motions are constrained. In fact a solution is not possible (the stiffness matrix is singular). Nevertheless, by use of 'PARAM,BAILOUT,-1' the analysis continues and produces answers, but they are useless. This PARAM card must only be used to debug the model in case of errors. The actual analysis should be carried out without this PARAM activated. Quite often this requirement is not fulfilled and analyses are performed with this option.

APPENDIX C EXTERNAL AND INTERNAL INTERFACES OF THE BME

C.1. External Interfaces

External interfaces define all adjacent structures/parts which are connected to the BME and which correlate with the BME functions. All those structures must be respected and fixed in terms of envelopes and position once concept generation is started. The BME is surrounded by the following main structures:

- RIE tank
- EAP boosters
- Vulcain engine

I/F	Connection	Dimension/number
BME to RIE-tank	RIE flange	360 equidistant M8 bolts. Diameter 9mm.
BME to EAP Boosters	DAAR lugs	6 struts
BME to engine	Engine adapter	Engine frame to engine adapter with 12xM16 bolts

(1) BME
(2) Vulcain Engine
(3) RIE
(4) EAP Booster

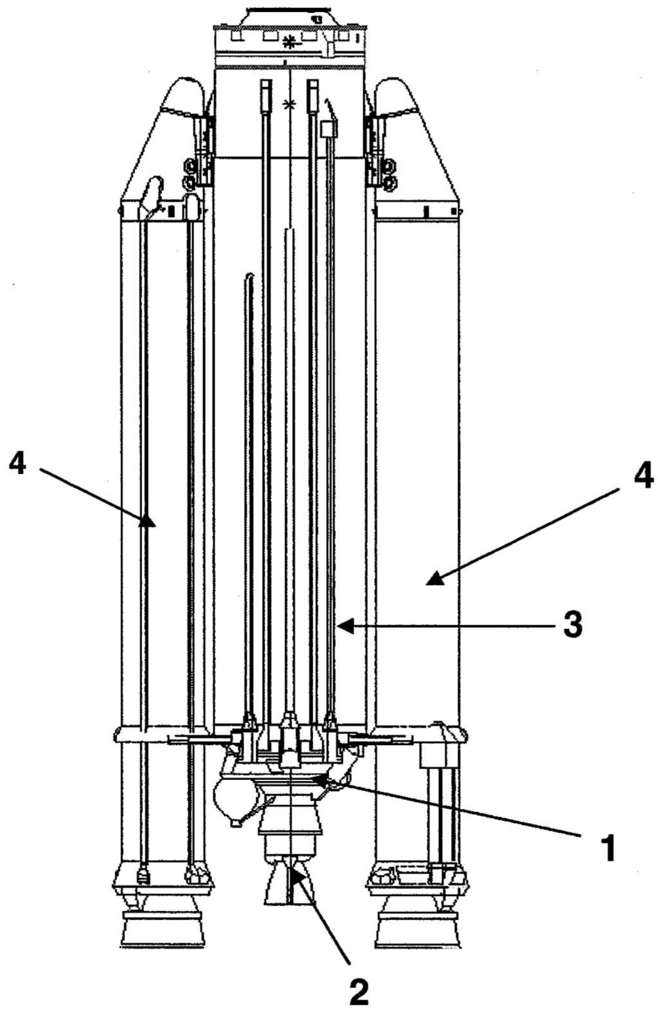

Figure C-1 External Interfaces of the BME

C.1.1 RIE tank

The concept design must consider the envelope of the RIE tank (also named cryogenic tank), because the lower part of this structure protrudes inside the BME at Box structure. For the existing BME, the top interface ring which is part of the Box assembly is the mechanical interface between the BME and the RIE. The connection is performed by 360 equidistant M8 bolts. For this purpose the ring has 360 holes of diameter 9mm. The bolts are placed at a pitch diameter of 5435 mm.

C.1.2 EAP boosters

The boosters are connected by 3 struts to the BME via the DAAR lugs. The DAAR lugs, which are an integral part of the box floor segments, transfer the booster loads in plane of the box floor. A detail of the DAAR lug is shown in figure C-3

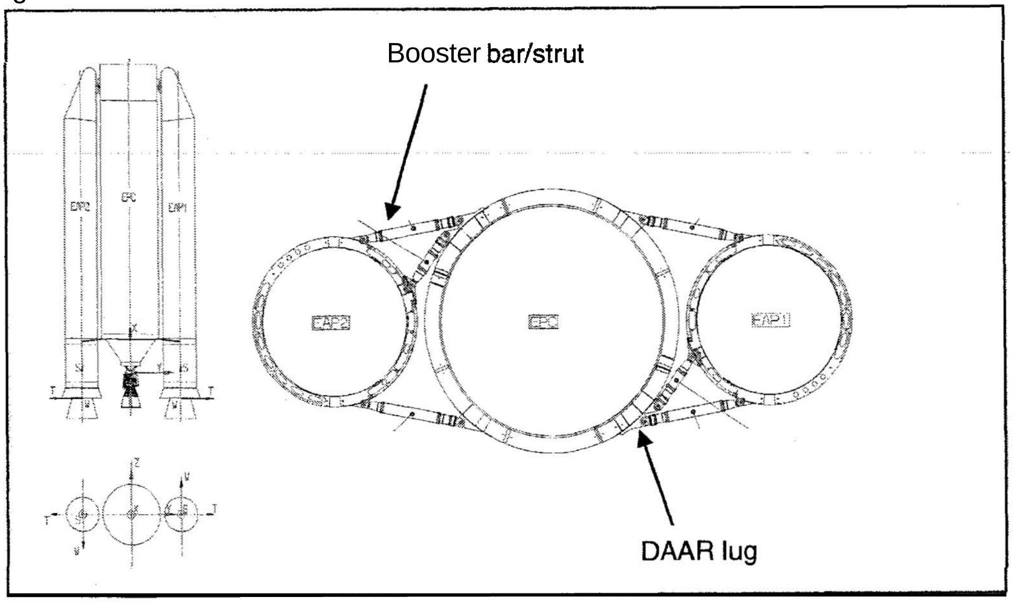

Figure C-2 Interfaces of the EAP Booster

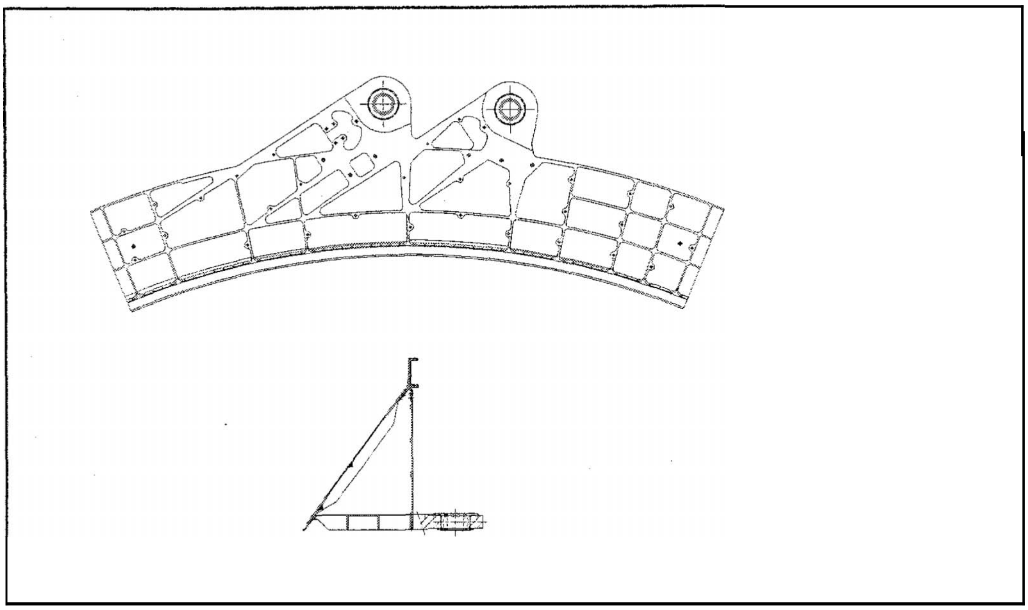

Figure C-3 DAAR lug

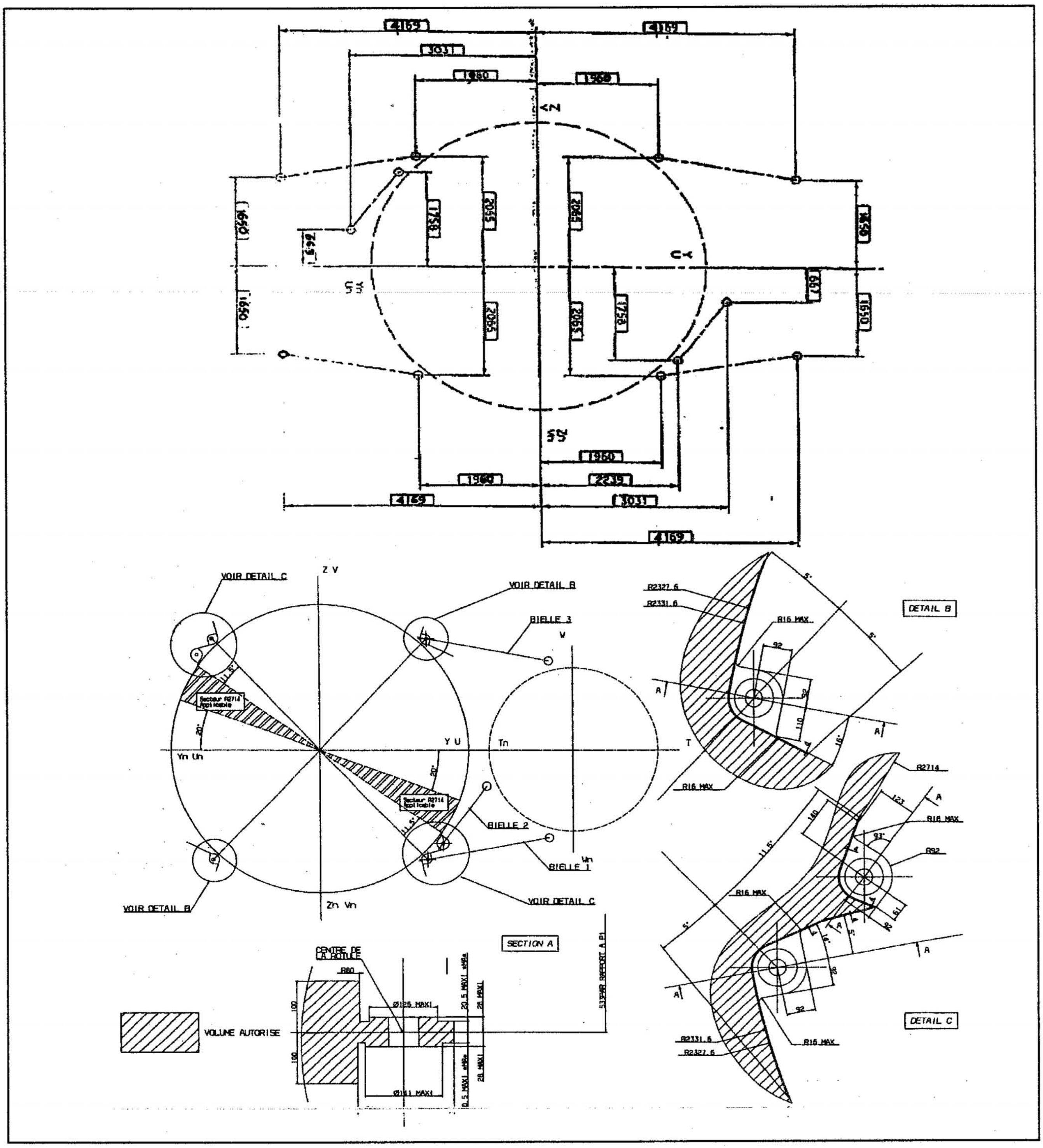

Figure C-4 DAAR lugs position

The location and positioning of the DAAR lugs are still considered fixed with respect to the BME structure.

C.1.3 Vulcain engine

The engine adapter is an integral pari of the centre column of the Cross and is the mechanical interfaces with the Vulcain engine. The engine frame is bolted to the engine adapter with 12xM16 bolts. The interfaces flange is equipped with 12 inserts with MJ16x 1.5 thread. The interfaces are shown below:

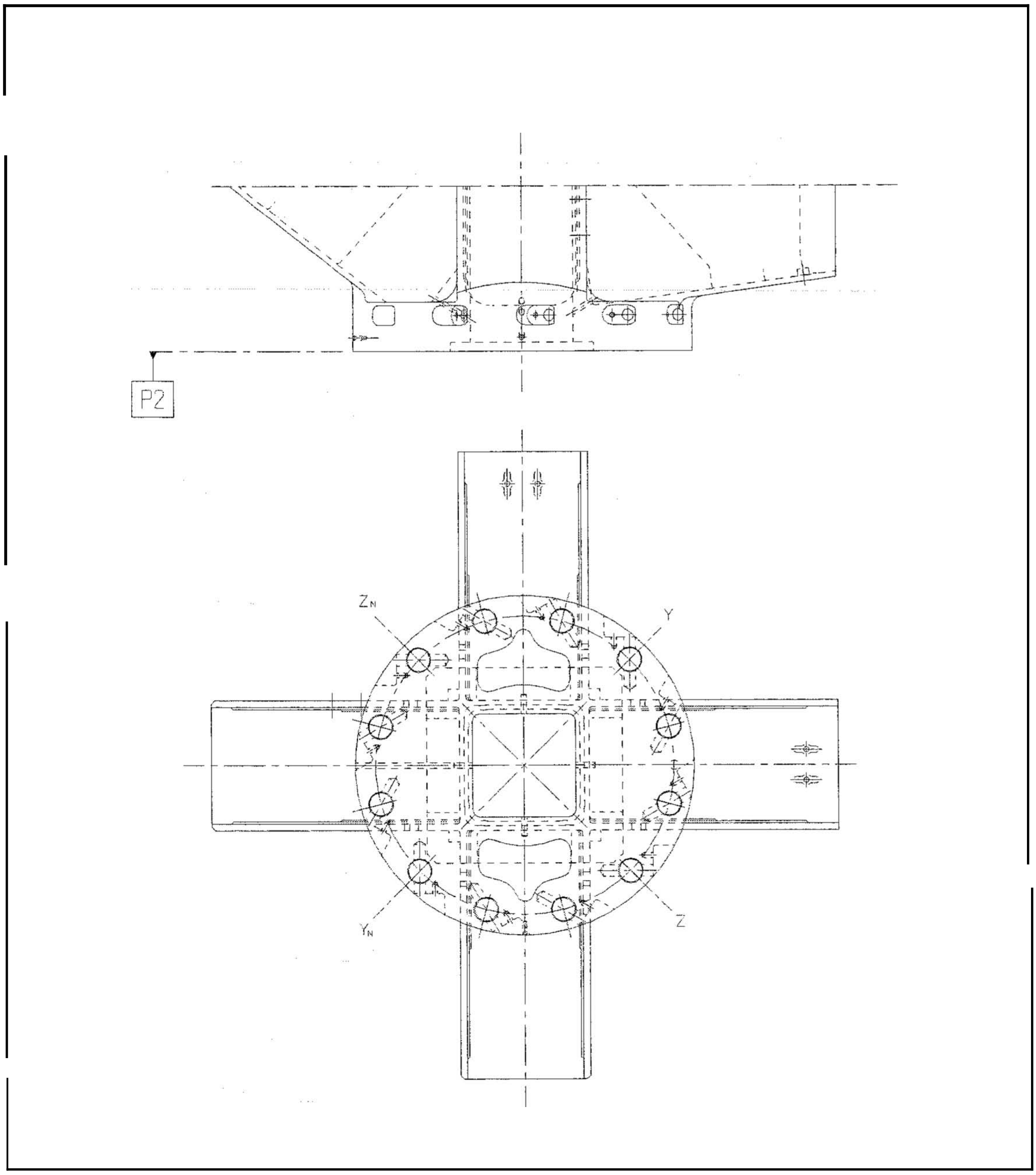

Figure C-5 Vulcain Engine Interfaces

C.2 Internal Interfaces

The internal interfaces are kept fixed either in geometry or position. The internal interface means all the equipments and lines, which are connected or assembled within the envelope of the structure. Several attachments of equipment and lines must be attached to the main structure of the BME as well. These interfaces are not intended to influence the main load. Because there are a lot of equipments, lines and brackets attached within the existing cone section. Only the most important equipments are taken into account to simplify the process. Otherwise, it will be confusing and scattered by the complexity of many equipments and lines. It has not been necessary to consider the secondary equipments at upper level. Therefore, it is only concentrated on the equipments and lines that take the biggest portion on their envelopes. This arises from the thought that if the major equipments and lines can be situated properly and fixed inside the concepts, then other smaller or secondary equipments and lines can be organized easily and consecutivety in order as well. The major equipments are:

- SSHel
- $HeHP_2$
- GAM
- SCR

And the major propellant lines are:

- LOx
- LH_2
- EPSO
- EPSH

Accessibility inside the BME structure is necessary to provide access for inspection purposes and for installation of secondary equipments. These activities are done after the structural assembling process of the BME main structure. A maximum of 2 man holes are allowed. The dimension of the hole is flexible as long as it is fit enough to allow one man entrance.

C.2.1 Major Equipments

C.2.1.1 SSHel

SSHel is the liquid helium sphere. There is only 1 SSHel in the BME.

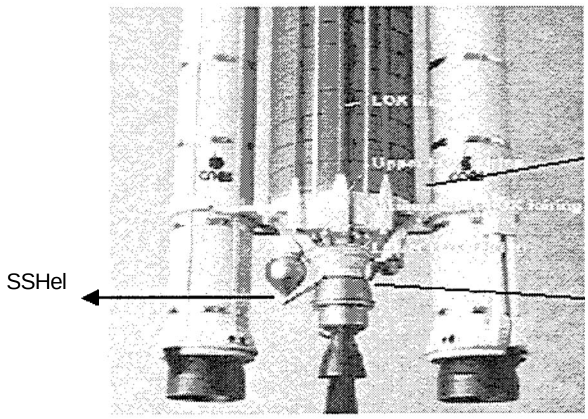

Figure C-6 SSHel on The BME

The envelope is defined at A5 EF-1232000-C-01-ASET **ed** 1 **rev** 1 ; **tome** 1 (*Internal Technica1 Notes ; reference 10*) **can be seen** below :

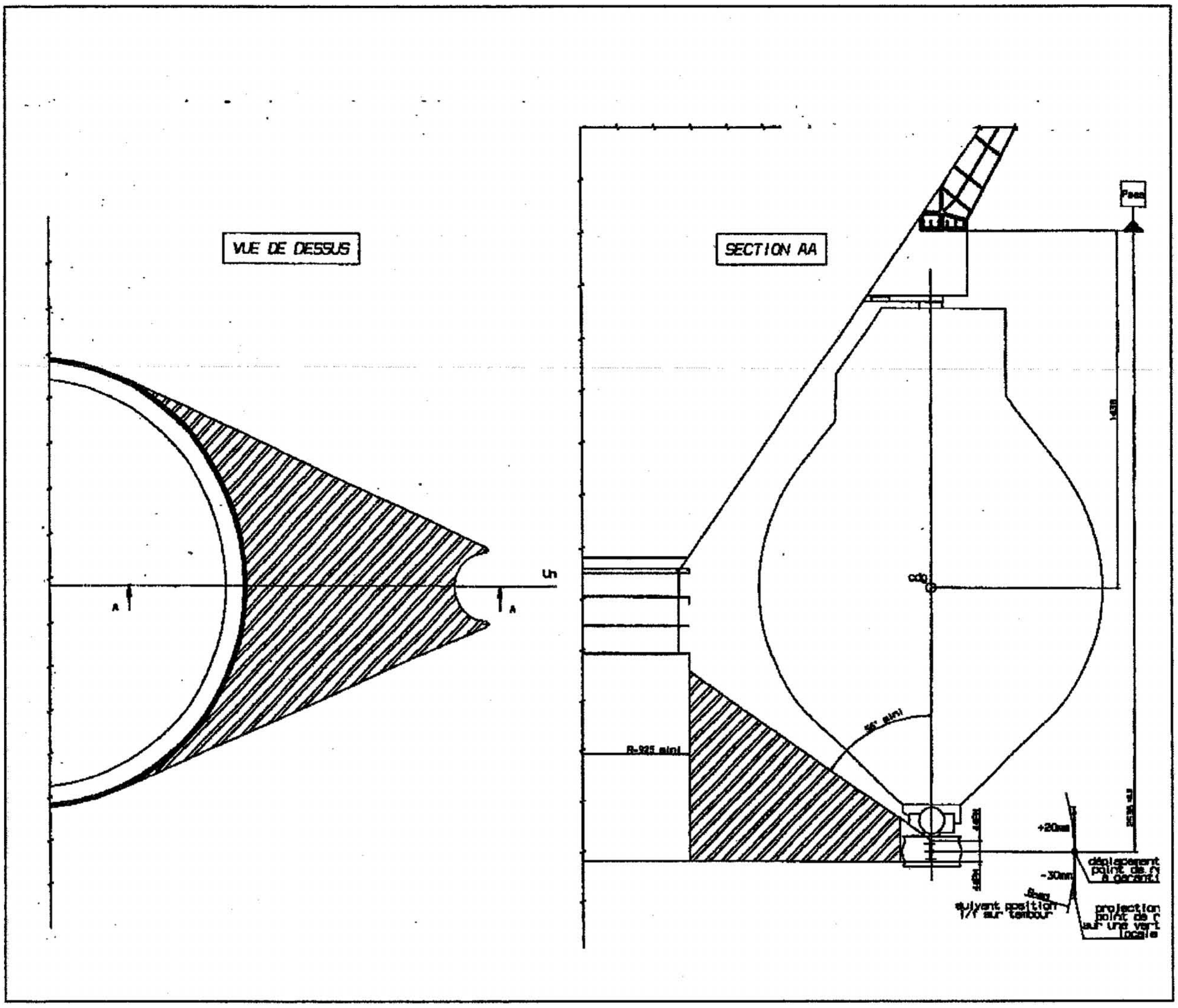

Figure C-7 SSHel Envelope

C.2.1.2 HeHP sphere

HeHP is a high pressure helium sphere. The amount of this spheres in the existing BME design were based on 2 spheres. The envelope of the HeHP as depicted at A5 EF-1232000-C-01-ASET ed 1 rev 1 ; tome 1 (*Internal Technical Notes* ; *reference 10)* shown on figure 3-12.

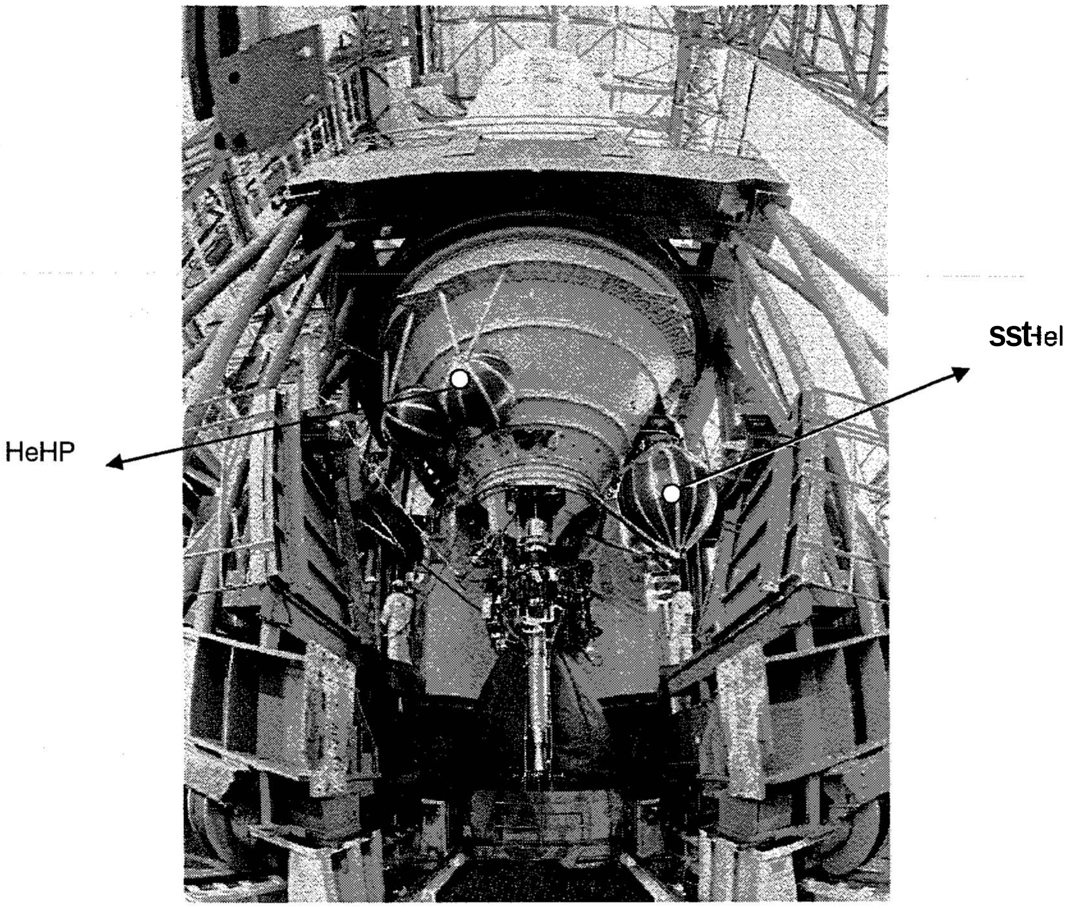

Figure C-8 The Existing HeHP and SSHel

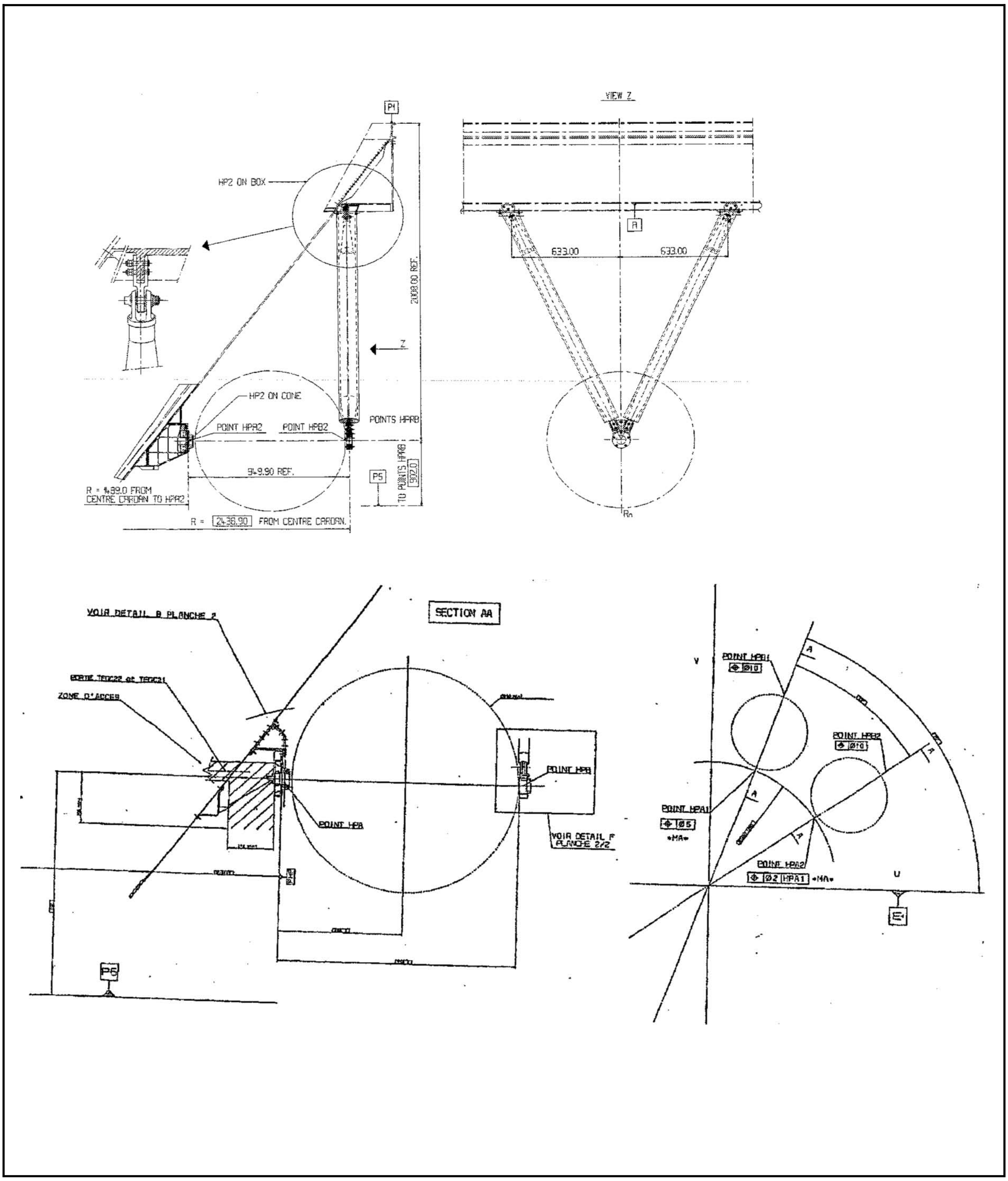

Figure C-9 Envelope Of HeHP On The Existing BME

C.2.1.3 GAM

The GAM stands for Group of activation motor, that is a hydraulic interface to support **flexible device.** There is 1 GAM in the existing BME and its supports are attached to the Cone and Box **structure.**

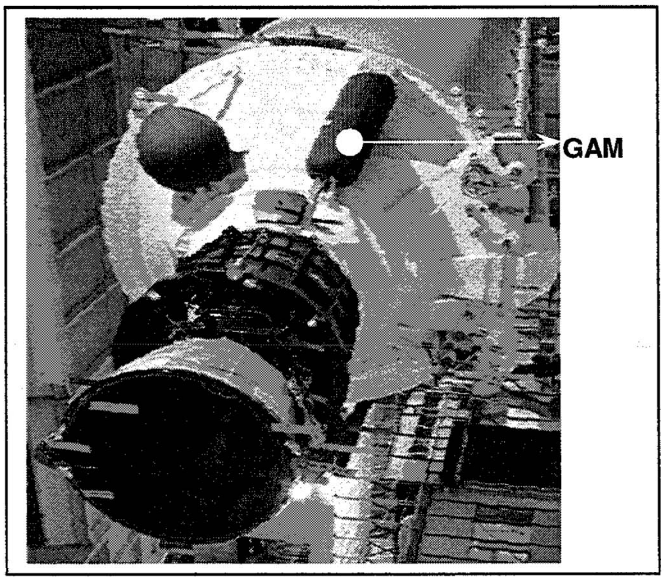

Figure C-10 GAM ***on the BME structure***

For the envelope refer to A5 EF-1232000-C-01-ASET ed 1 rev 1 ; tome 1

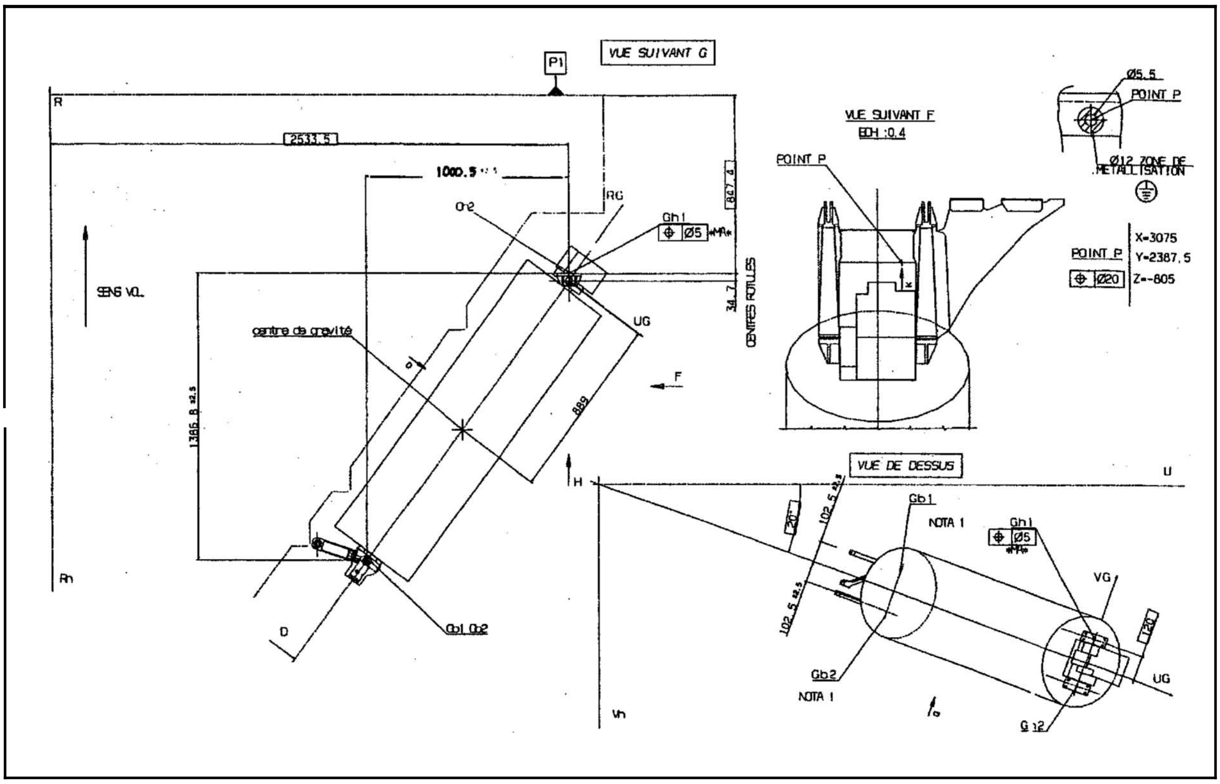

Figure C-11 GAM ***Envelope In The Existing BME***

C.2.1.4 SCR

Even though the SCR is secondary equipment supports, it takes a big portion and fixed positian in the BME. It consists of a support below the Box, three supports on the Cone, and four supports on the cross. The purpose is to counter undesired torsion moments around the launcher x-axis due to large fuel quantities teaving the tank (i.e a "whirle").

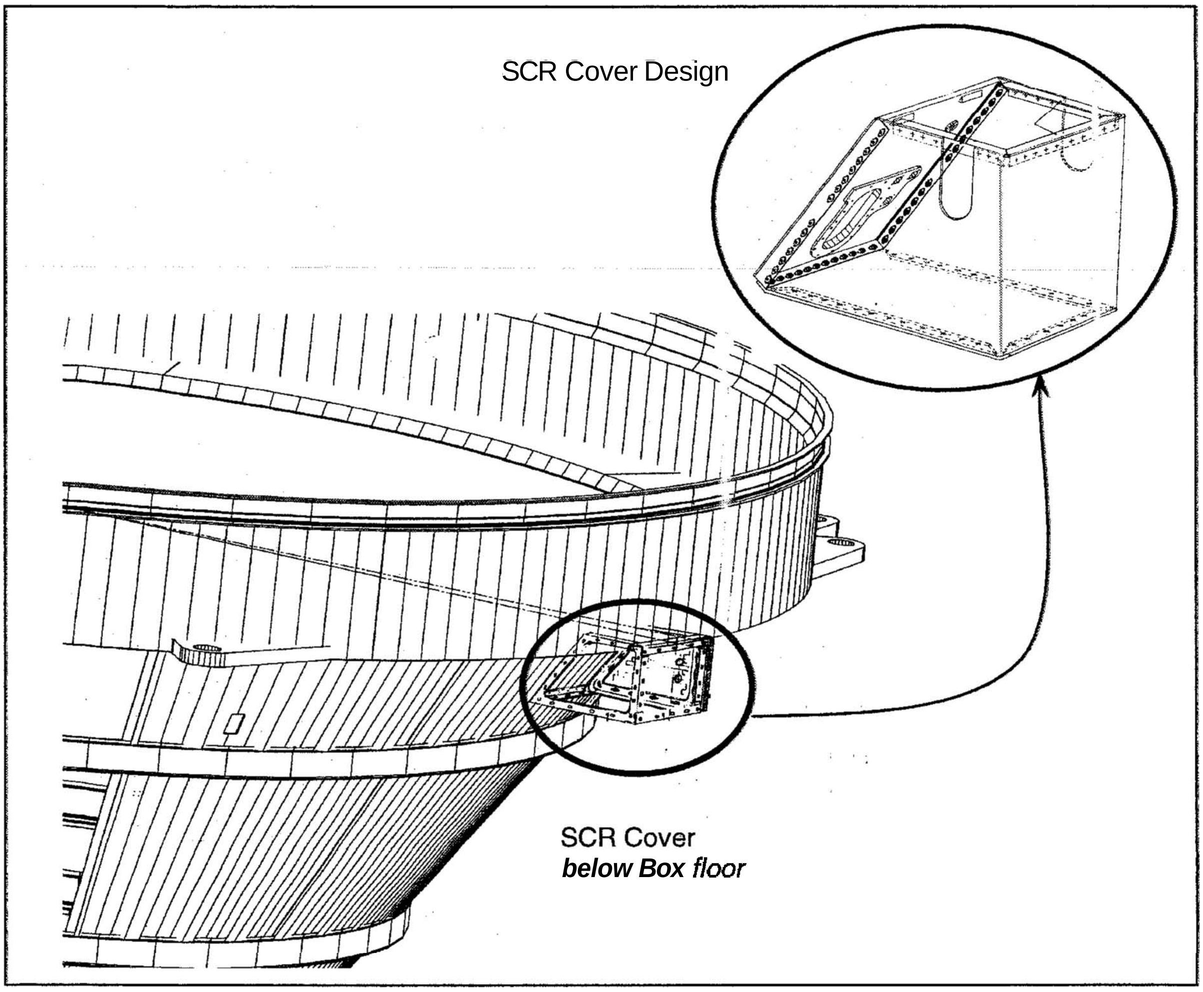

Figure C-12 SCR on The BME Structure

For the envelope refer to A5 EF-I232000-C-01-ASET ed 1 rev 1 ; tome 1, as shown on figure C-I3.

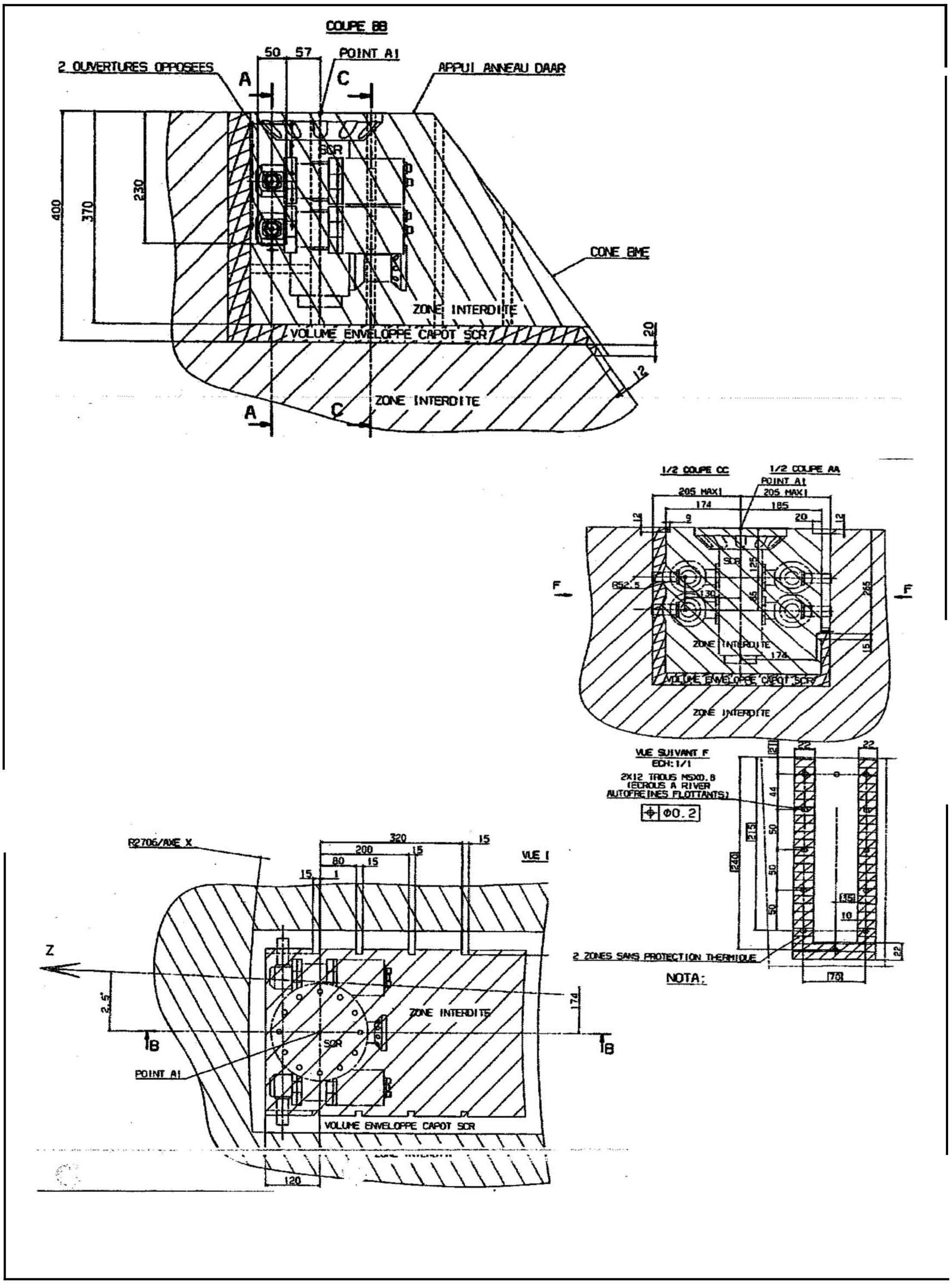

Figure G-13 Envelope of the SCR

C.2.2 Major lines

Position : Routing of LH2 and LOx lines : are fixed as indicated in A5 EF-1232000 – C-01-ASET edition 1 (*Internal Technical Notes* ; *reference 10)*

C.2.2.1 LOx

Feed line for oxygen propellant.
Envelope : A5 EF-1232000-C-01-ASET ed 1 rev 1 ; tome 1 *(Internal Technical Notes* ; *reference 10*)

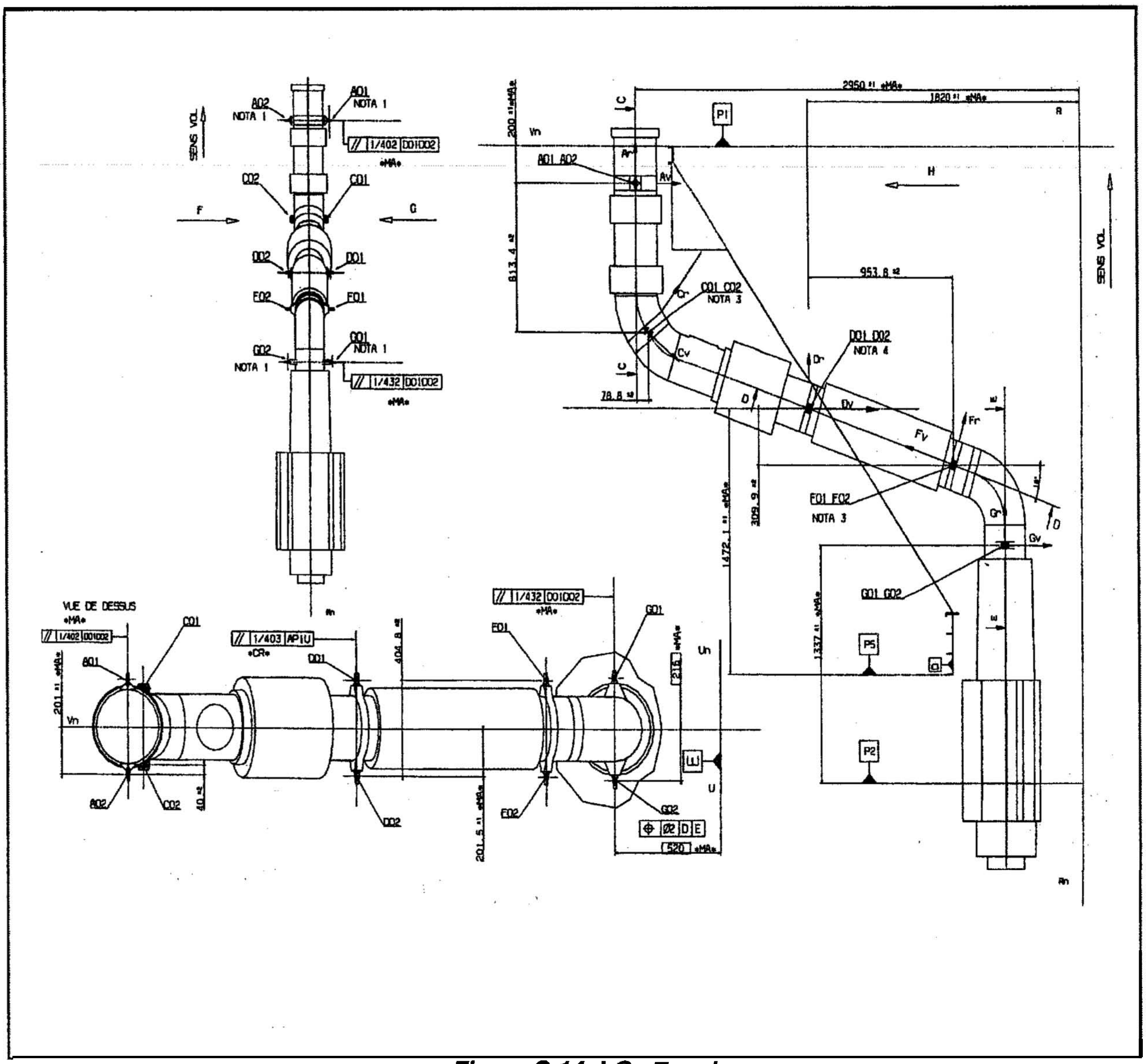

Figure C-14 .LOx Envelope

C.2.2.2 LH_2

Feed line for hydrogen propellant.

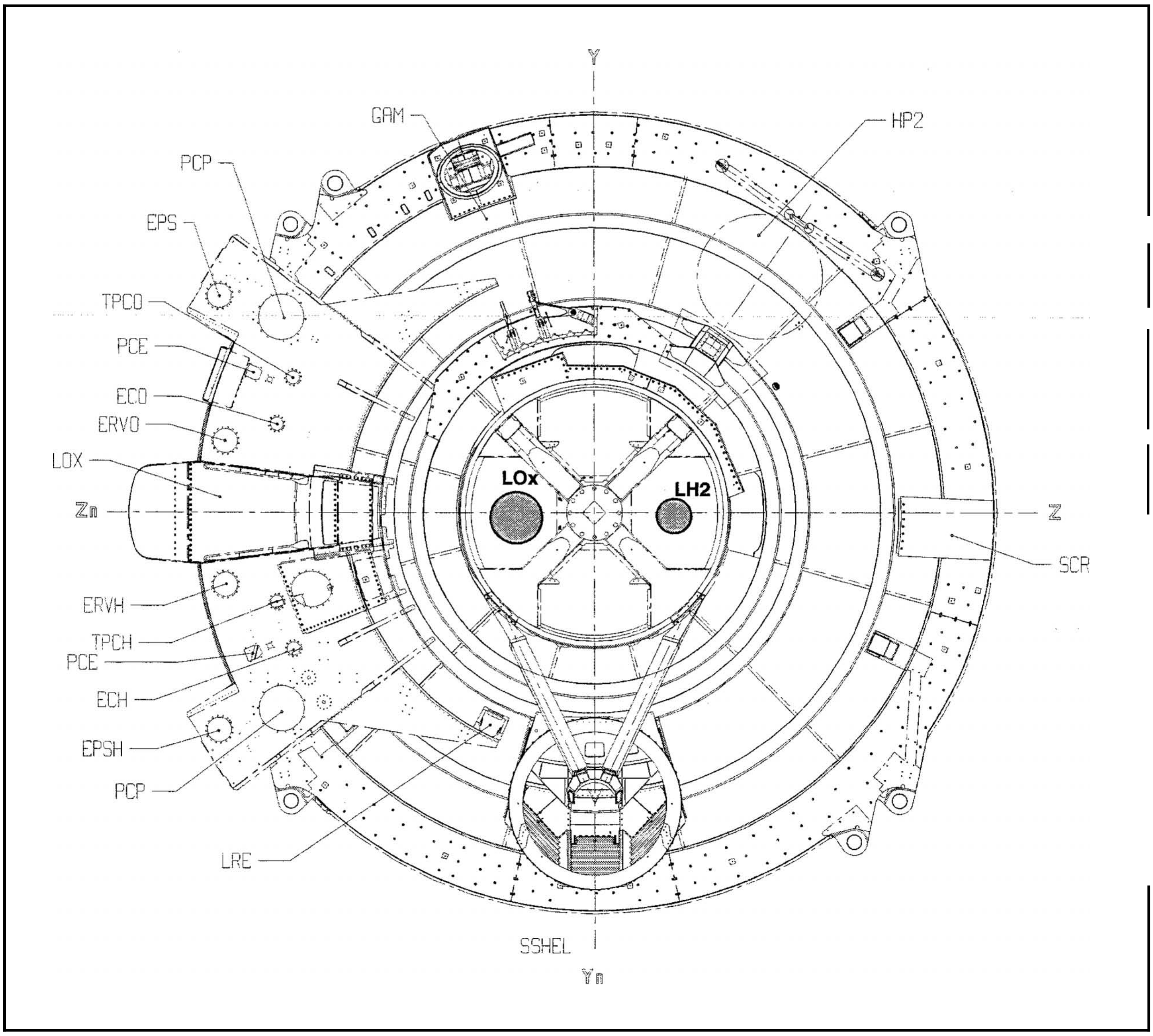

Figure C-15 The Position Of Several Equipments And Lines

Envelope of LH_2 exist on A5 EF-1232000-C-01-ASET ed 1 rev 1 ; tome I shown below:

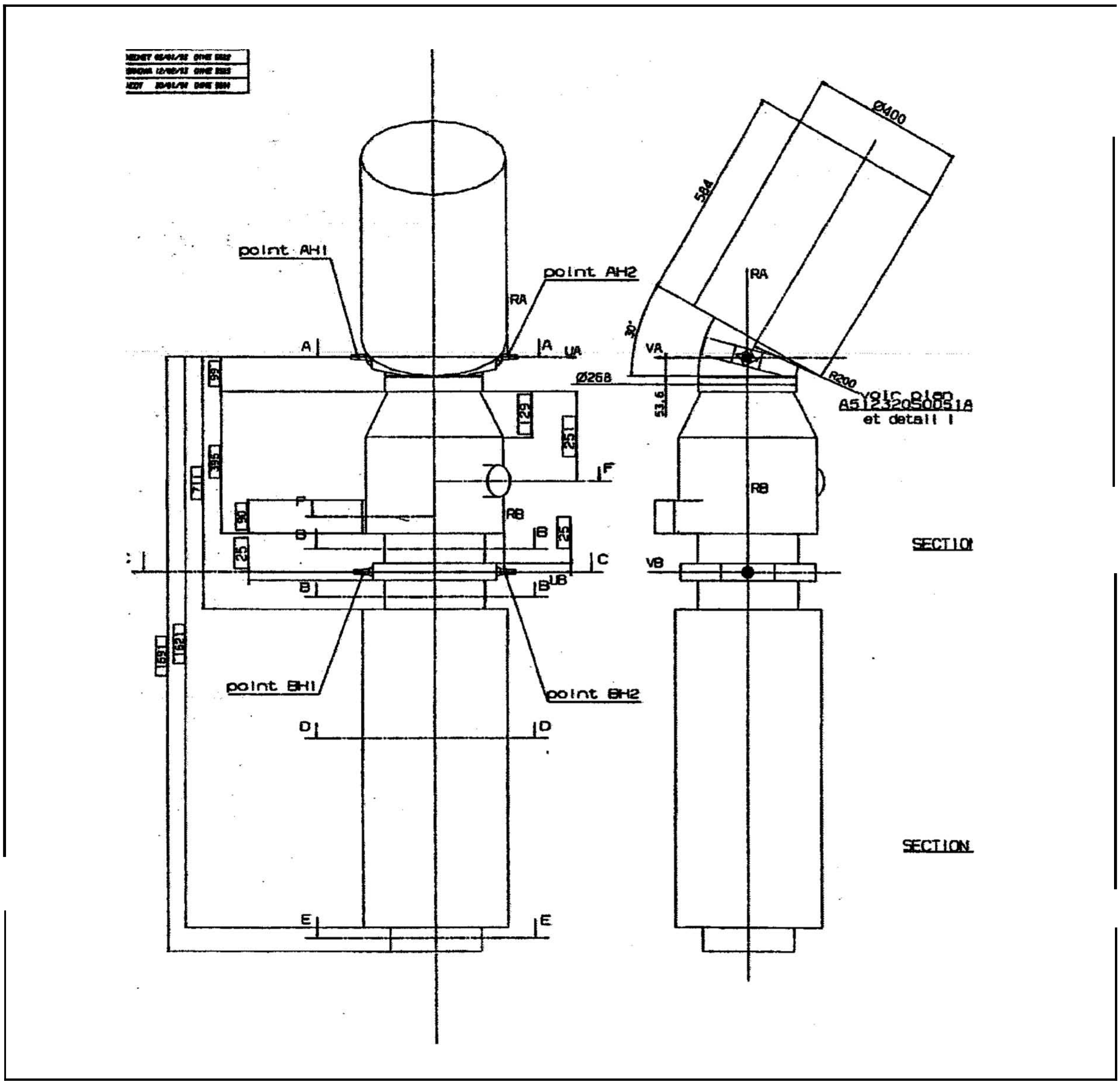

Figure C-16 The Envelope of LH_2

C.2.2.3 EPSO

EPSO is line to increase the pressure of Oxygen.

Position of the EPSO and EPSH

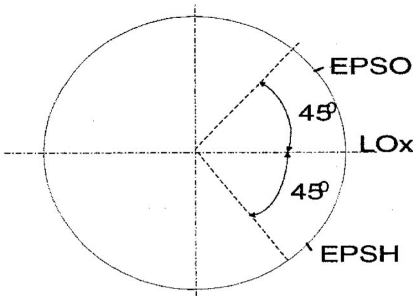

Envelope: A5 EF-1232000-C-01-ASET ed 1 rev 1 ; tome 1

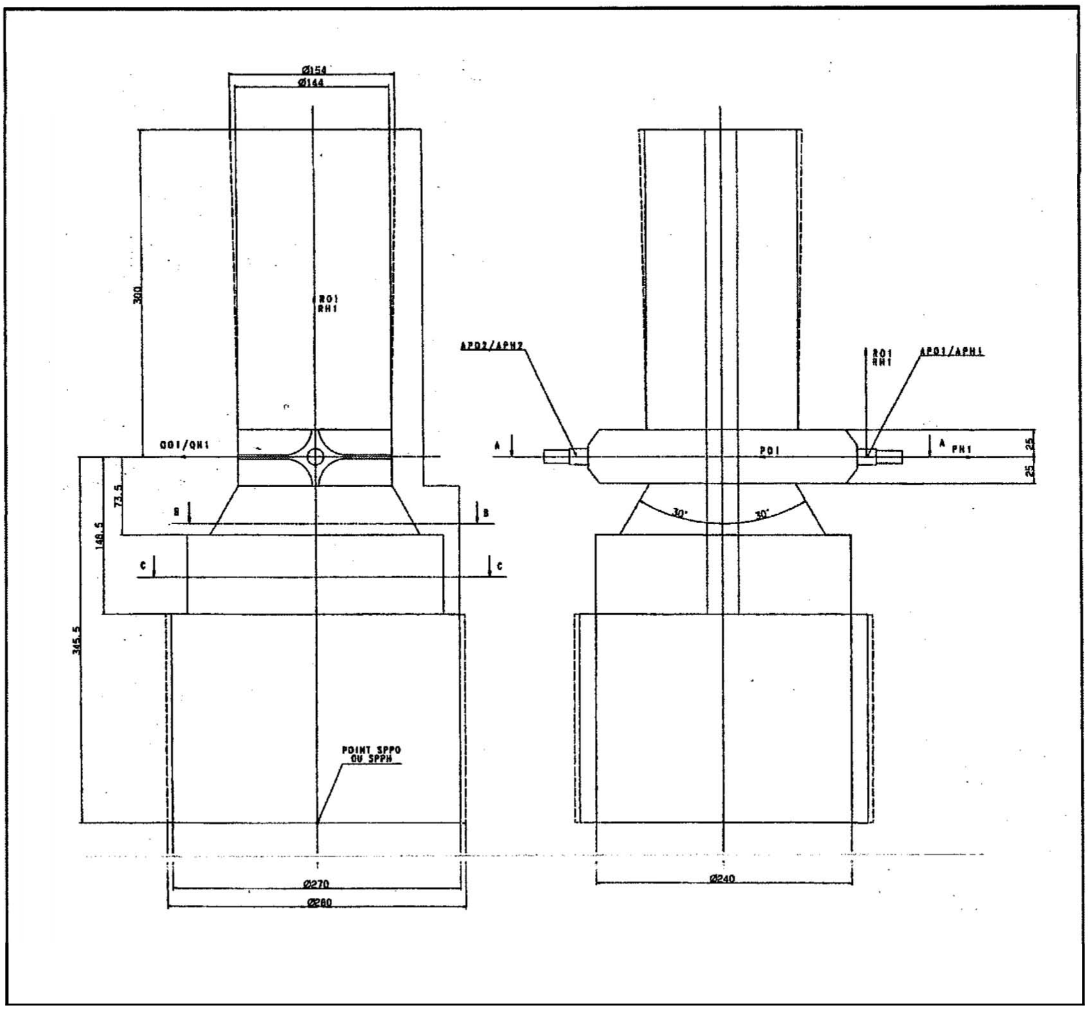

Figure C-17 Envelope of EPSO

C.2.2.4 EPSH

EPSH is line to increase the pressure of Hydrogen.
Its envelope is same as EPSO line.

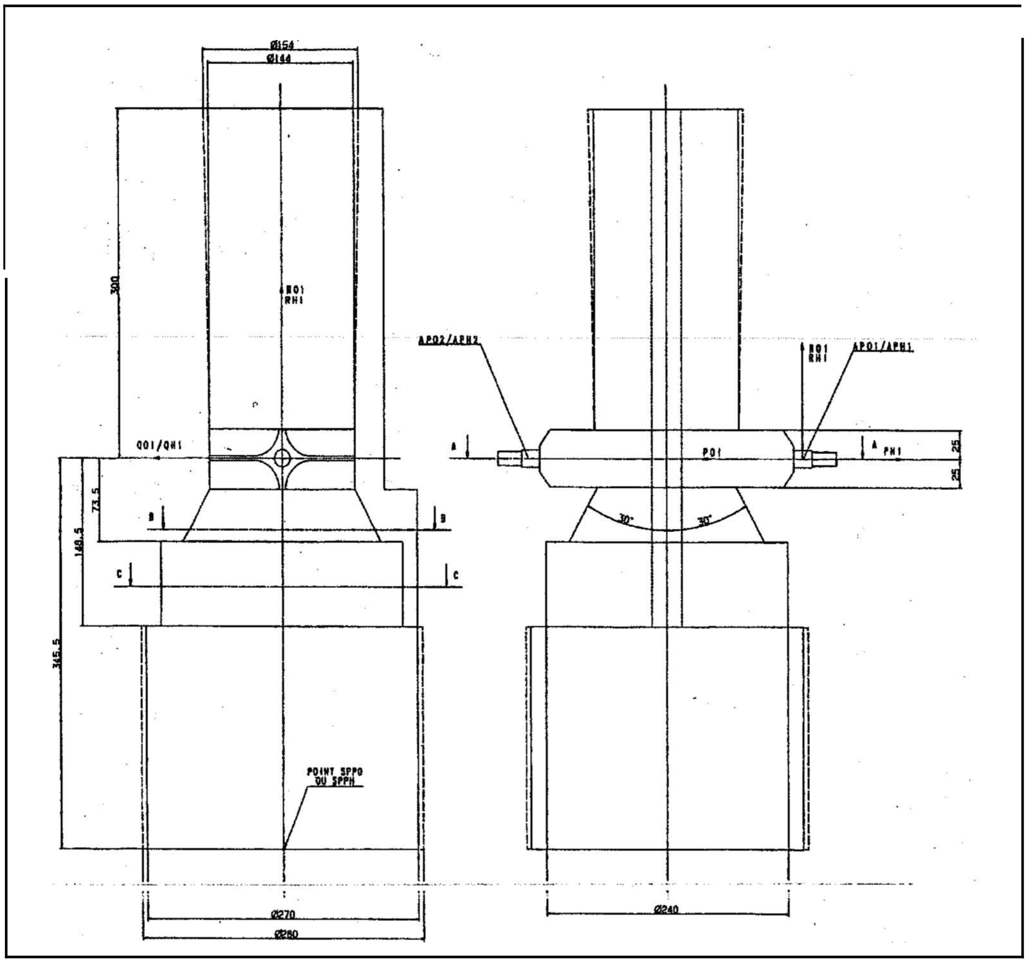

Figure C-18 Envelope of EPSH

APPENDIX D ELEMENT TYPE FOR FINITE ELEMENT MODELING

D.1 Plate Element

The element library of NASTRAN gives the user a wide range of plate elements that could be used to represent the surfaces of the LBS FEM. To make a selection of these plate elements, the most important elements are described. A selection is made to point the best plate element for the purpose of making the mesh of the LBS structure.

The CQUAD4, the CQUADX CQUAD8 and CQUADR represent the CQUAD (plate element with 4 sides) element family. All CQUAD elements are basically derivatives of the CQUAD4 element. The CQUADX element is basic CQUAD4 element but the user can define how many grid points this element may have with a maximum of 9. The CQUADR element uses a torsion stiffness perpendicular to the surface of this element, so called drilling DOF. The phenomenon of using a torsion moment is the reason why the CQUADR element provides better answers for non-rectangular elements when running static analysis. However, MSC also states that the CQUADR is not fully implemented for other types of analysis, such as buckling and non-linear. Therefore, the CQUADR element will not be used. The CSHEAR element is a CQUAD-like element, which onty defines a shear panel element.
The CQUAD4 element is a basic plate element that is commonly used within Dutch Space. This element represents forces and moments like figure D-l shows. This element will be used to represent the mesh.

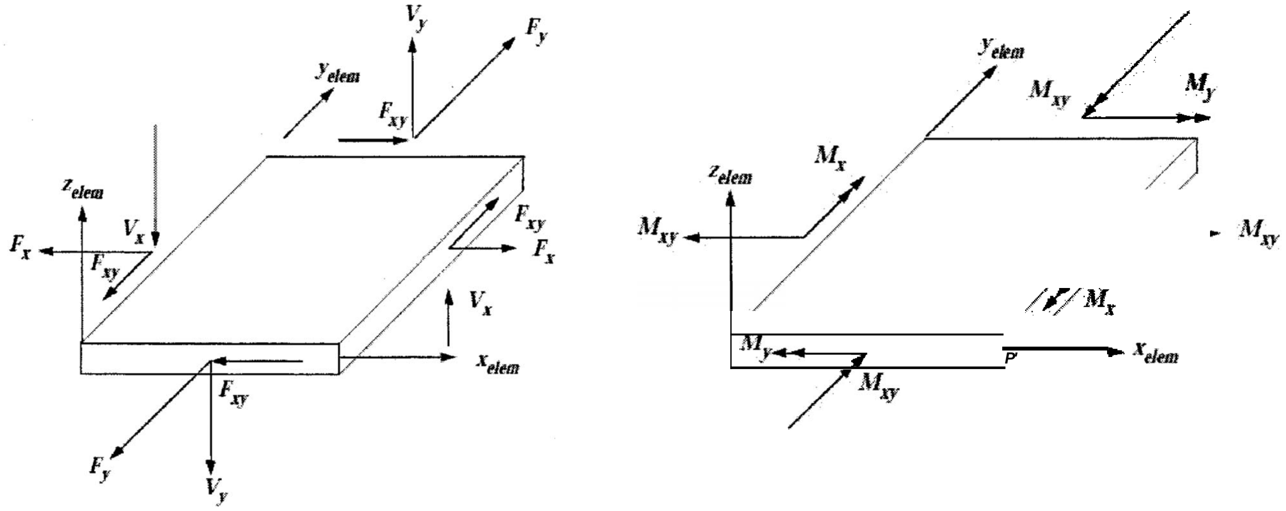

Figure D-1 Forces and Moments on a plate element

The CTRIA element have the name to be slightly "stiffer" than CQUAD elements because their geometric definition. The CTRIA (three sides and three nodes) elements will be used as less as possible at toad introduction points due to the extra stiffness these elements introduce. The CTRIA element family consists of actually the same element types as CQUAD, i.e. CTRIA3, CTRIAR, CTRIA6. If a CTRIA element is used, it will be the "standard" CTRIA3 element.

D.2 Solid Element

Sotids (for instance hexagonal) are 3D finite elements. The disadvantage of these elements is that they need more computing resource. In the future with more computing resource, the disadvantage of time consuming calculation of solid elements will be reduced. A reason for applying CHEXA solid elements is that their cross section can directly be obtained from CAD drawings. This is a time saving operation in the modelling sequence.

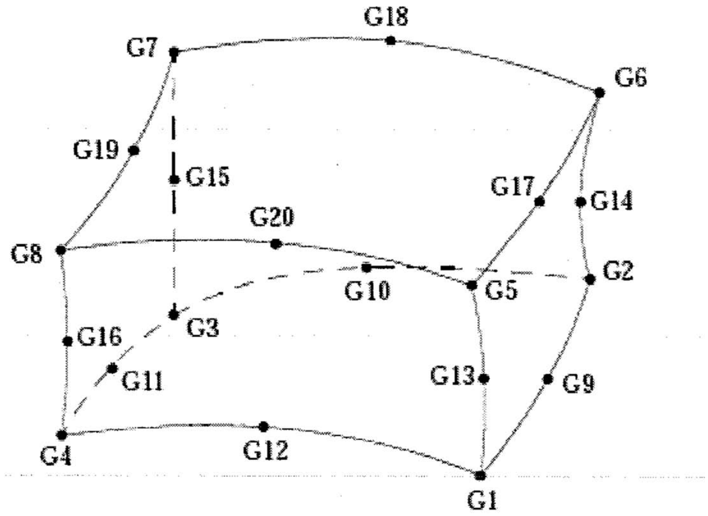

Figure D-2 Solid element

APPENDIX E HAND CALCULATION

E.1 Displacement of a ring due to radial force

In order to verify the result of the FEM model, a theoretical calculation should be made. For the Ariane 5 EPC-BME Box, the calculation is made based on a ring which loaded with radial load and clarnped on a point. The structure is depicted below.

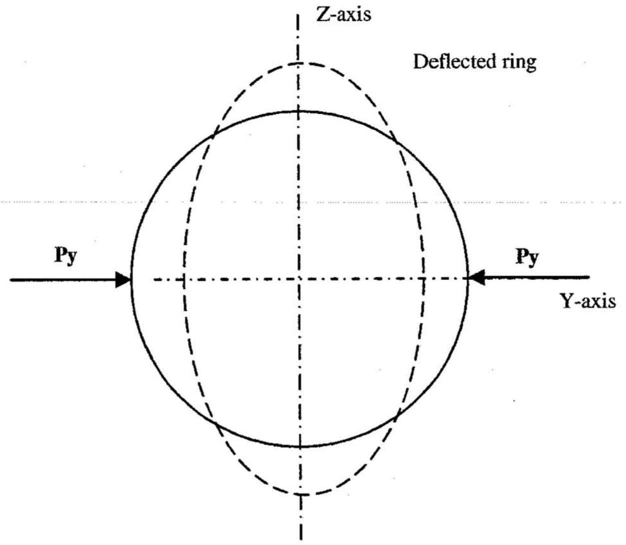

Figure E-l The simple ring structure

Due to a radial load Py on a single point on a ring i.e. a DAAR lug, a distribution of sheat stress is introduced in the surrounding ring structures. This shear stress is distributed along the ring structure as depicted in figure F-l (internal technical notes; ref. 9).

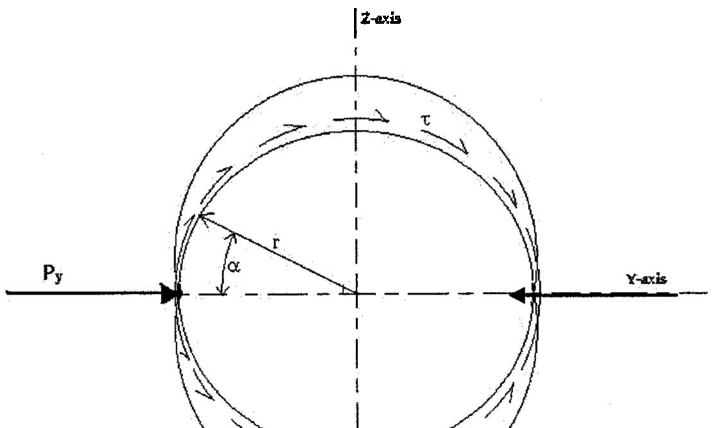

Figure E-2 Shear stress distribution on ring structure

In the figure can be seen that the shear stress maximum at an angle α of +/- 90°. The formula for the shear stress is defined *as:*

$$\tau = \frac{P_y \times \sin\alpha}{\pi \times r} \qquad \text{(E1-1)}$$

A slice of the ring with the reaction forces on node 1 is depicted in Figure E-3.

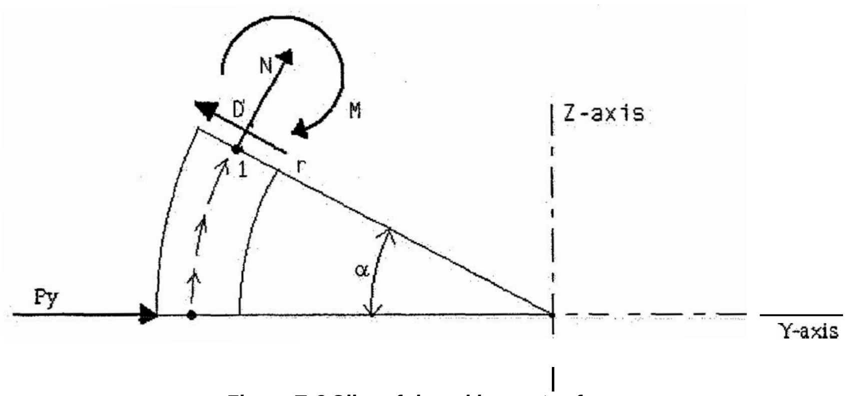

Figure E-3 Slice of ring with reaction forces

The contribution of the shear stress over this girder can be calculated by summing up both the horizontal and the vertical contributions of the shear stress (Figure E-4). This is done by formulating an integral for these two contributions and solving this with the use of the computer software *MathCAD.*

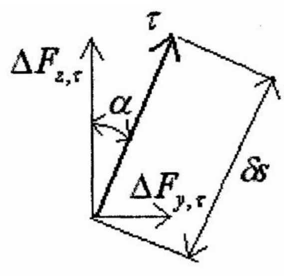

Figure E-4 Horizontal and vertical contributions of the shear stress

The equation for the vertical contribution is:

$$\Delta F_{z,\tau} = \int_0^{+\alpha} \cos\alpha \times \tau \times \delta s$$

With substitution of $\delta s = r \times \delta\alpha$ this equation is:

$$\Delta F_{z,\tau} = \int_0^{+\alpha} \cos\alpha \times \tau \times r \times \delta\alpha \qquad \text{(E1-2)}$$

The equation for the horizontal contribution than is:

$$\Delta F_{y,\tau} = \int_0^{+\alpha} \sin\alpha \times \tau \times r \times \delta\alpha \qquad \text{(E1-3)}$$

Substitution of equation E1-1 in E1-2:

$$\Delta F_{z,\tau} = \int_0^{+\alpha} \cos\alpha \times \frac{P_y \times \sin\alpha}{\pi \times r} \times r\,\delta\alpha$$

$$\Delta F_{z,\tau} = \frac{P_y \times \sin^2\alpha}{2 \times \pi}$$

Substitution of equation E1-1 in E1-3:

$$\Delta F_{y,\tau} = \int_{0}^{+\alpha} \sin a \; x \frac{P, x \sin a}{\pi \times r} x \; r\delta\alpha$$

$$\Delta F_{y,\tau} = \frac{\alpha \times P_y}{2x11} - \frac{P, \times \sin\alpha \times \cos\alpha}{2\times\pi}$$

Then the force applied on the ring will be

- In vertical direction:

$$F_{z,\tau} = -\frac{P_y \times \sin^2 \alpha}{2\times\pi} \qquad \text{(E1-4)}$$

- In horizontal direction:

$$F_{y,\tau} = \frac{P_y}{2} - \frac{\alpha \times P_y}{2\times\pi} + \frac{P_y \times \sin\alpha \times \cos\alpha}{2\,x\,n} \qquad \text{(E1-5)}$$

To determine the turnover of the moment M in the ring first an equation for the turnover of the transverse force D must be stated. This can be done by deducing the transverse force D from the reaction forces on node 1 (Figure E-5).

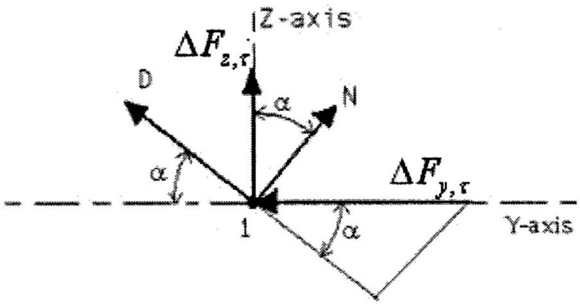

Figure E-5 Angle of D in respect to reaction forces on node 1

With the insight of this figure the equation for the transverse force D will be:

$$D = \sin\alpha \times \left(-\frac{P_y \, x \sin^2 a}{2\times\pi}\right) - \cos\alpha \times \left(\frac{P_y}{2} - \frac{\alpha \times P_y}{2\times\pi} + \frac{P_y \times \sin a \, x \cos a}{2x11}\right) \qquad \text{(E1-6)}$$

The equation for the normal force will be:

$$N = \cos\alpha \times \left(-\frac{P_y \times \sin^2 \alpha}{2\times\pi}\right) + \sin\alpha \times \left(\frac{P_y}{2} - \frac{\alpha \times P_y}{2\times\pi} + \frac{P_y \times \sin\alpha \times \cos\alpha}{2\times\pi}\right) \qquad \text{(E1-7)}$$

To calculate the moment over the ring structure the differential equation for the moment as function of the transverse force can be written and solved for M.

$$\frac{\delta M}{\delta s} = D$$

$$\delta s = r \times \delta\alpha$$

Then the input for *MathCAD* is the integral with the upper and lower limits:

$$M = \int_0^a D \times r \times d\alpha + C_1$$

$$M = \int_0^\alpha \left(\sin\alpha \times \left(-\frac{P_y \times \sin^2\alpha}{2\times\pi} \right) - \cos\alpha \times \left(\frac{P_y}{2} - \frac{\alpha \times P_y}{2\times\pi} + \frac{P_y \times \sin\alpha \times \cos\alpha}{2\times\pi} \right) \right) \times r \times d\alpha + C_1$$

$$M = \frac{P_y \times r \times \cos\alpha}{\pi} + \frac{P_y \times r \times (\alpha - \pi) \times \sin\alpha}{2\times\pi} - \frac{P_y \times r}{\pi} + C_1 \qquad \text{(E1-8)}$$

Now the angular deflection can also be determined by stating the differential equation for the angular deflection as a function from the moment and solve this equation with *MathCAD*:

$$\frac{\delta\varphi}{\delta s} = \frac{M}{EI}$$

$$\delta s = r \times \delta\alpha$$

$$\varphi = \int_0^\alpha \frac{M}{EI} \times \delta s + C_2$$

$$\varphi = \int_0^\alpha \frac{\left(\frac{P_y \times r \times \cos\alpha}{\pi} + \frac{P_y \times r \times (\alpha - \pi) \times \sin\alpha}{2\times\pi} - \frac{P_y \times r}{\pi} + C_1 \right) \times r}{EI} \delta\alpha + C_2$$

$$\varphi = \frac{P_y \times r^2 \times (\pi - \alpha) \times \cos\alpha)}{2\times\pi\times EI} + \frac{3 \times P_y \times r^2 \times \sin\alpha}{2\times\pi\times EI} + \frac{\alpha \times r \times (\pi \times C_1 - P_y \times r)}{\pi \times EI} - \frac{P_y \times r^2}{2 \times EI} + C_2 \qquad \text{(E1-9)}$$

To find the integration constants C_1 and C_2 the boundary conditions need to be determined. What is known about the ring is that the angular deflection for α=0° and α=180° is zero (Figure E-2). Thus:

$$\varphi_{\alpha=0^\circ} = 0$$

$$\varphi_{\alpha=180^\circ} = 0$$

There are two unknown constants and two equations thus this can be solved by fill-in α=0° and α=180° in equation E1-9 which provides constants C_1 and C_2:

$$\varphi_{\alpha=0^\circ} = 0 \Rightarrow equation9$$

$$\varphi = \frac{P_y \times r^2 \times (\pi - 0) \times \cos 0)}{2\times\pi\times EI} + \frac{3 \times P_y \times r^2 \times \sin 0}{2\times\pi\times EI} + \frac{0 \times r \times (\pi \times C_1 - P_y \times r)}{\pi \times EI} - \frac{P_y \times r^2}{2 \times EI} + C_2$$

$$C_2 = 0 \qquad \text{(E1-10)}$$

$$\varphi_{\alpha=180^\circ} = 0 v Equation10 \Rightarrow Equation9$$

$$\varphi = \frac{P_y \times r^2 \times (\pi - \pi) \times \cos\pi)}{2 \times \pi \times EI} + \frac{3 \times P_y\ x r^2\ x sinn}{2 \times \pi \times EI} + \frac{\pi \times r \times (\pi \times C_1 - P_y \times r)}{\pi \times EZ} - \frac{P_y \times r^2}{2 \times EI} + 0$$

$$0 = \frac{\pi \times r \times (\pi \times C_1 - P_y\ x r)}{\pi \times EI} - \frac{P_y \times r^2}{2 \times EI}$$

$$C_1 = \frac{3 \times P_y \times r}{2 \times \pi} \quad \text{(El-11)}$$

Since the constants C_1 and C_2 are now determined graphs can be made for the equations of the moment and the angular deflection. Substitution of equation El-11 in E1-8 results to the equation for the moment:

$$M = \frac{P_y \times r \times \cos\alpha}{\pi} + \frac{P_y \times r \times (\alpha - \pi) \times \sin\alpha}{2 \times \pi} - \frac{P_y \times r}{\pi} + \frac{3 \times P_y \times r}{2 \times \pi} \quad \text{(E1-12)}$$

Substitution of equations E1-10 and El-11 in equation E1-9 results to the equation for the angular deflection:

$$\varphi = \frac{P_y \times r^2 \times (\pi - \alpha) \times \cos\alpha)}{2 \times \pi \times EI} + \frac{3 \times P_y \times r^2 \times \sin\alpha}{2 \times \pi \times EI} + \frac{\alpha \times P_y \times r^2}{2 \times \pi \times EI} - \frac{P_y \times r^2}{2 \times EI} \quad \text{(EI-13)}$$

The displacement over the ring can also be determined for this load case by stating the differential equation for the displacement and solving this with *MathCAD*:

$$\varphi = \frac{\delta f}{\delta s}$$

$$\delta s = r \times \delta\alpha$$

$$f = \int_0^{\alpha} \varphi \times r \times \delta\alpha + C_3$$

$$f = \int_0^{\alpha} \left(\frac{P_y \times r^2 \times (\pi - \alpha) \times \cos\alpha)}{2 \times \pi \times EI} + \frac{3 \times P_y \times r^2 \times \sin\alpha}{2 \times \pi \times EI} + \frac{\alpha \times P_y \times r^2}{2 \times \pi \times EI} - \frac{P_y \times r^2}{2 \times EI} \right) \times r \times \delta\alpha + C_3$$

$$f = -\frac{2 \times P_y \times r^3 \times \cos\alpha}{\pi \times EI} + \frac{P_y \times r^3 \times (\pi - \alpha) \times \sin\alpha}{2 \times \pi \times EI} + \frac{P_y \times r^3 \times (\alpha^2 - 2 \times \pi \times \alpha - 8)}{4 \times \pi \times EI} + C_3 \quad \text{(E1-14)}$$

To determine the integration constant C_3 the boundary conditions for the displacement have to be defined. The boundary condition for the displacement is:

$$f_{\alpha = 180^\circ} = -f_{\alpha = 0^\circ}$$

Thus,

$$-\frac{\pi \times P_y \times r^3}{4 \times EI} + C_3 = \frac{4 \times P_y \times r^3}{\pi \times EI} - C_3$$

$$C_3 = \frac{P_y \times r^3}{\pi \times EI} \times \left(\frac{16 - \pi^2}{8} \right) \qquad \text{(E1-15)}$$

Substitution of equation E l -15 in equation E1-14 results to the equation for the displacement:

$$f = \frac{P_y \times r^3}{\pi \times EI} \times \left[(-2 \times \cos\alpha) + \left(\frac{(\pi - \alpha) \times \sin\alpha}{2} \right) + \left(\frac{(\alpha^2 - 2 \times \pi \times \alpha - 8)}{4} \right) + \left(\frac{16 - \pi^2}{8} \right) \right] \qquad \text{(E1-16)}$$

E.2 Moment of Inertia (I) of the Box Floor (Hand Calculation)

As a result of the non similar cross section area of the box floor, the moment of inertia of the box floor is obtained by analyze 2 selected cross sections.

Cross Section 1:

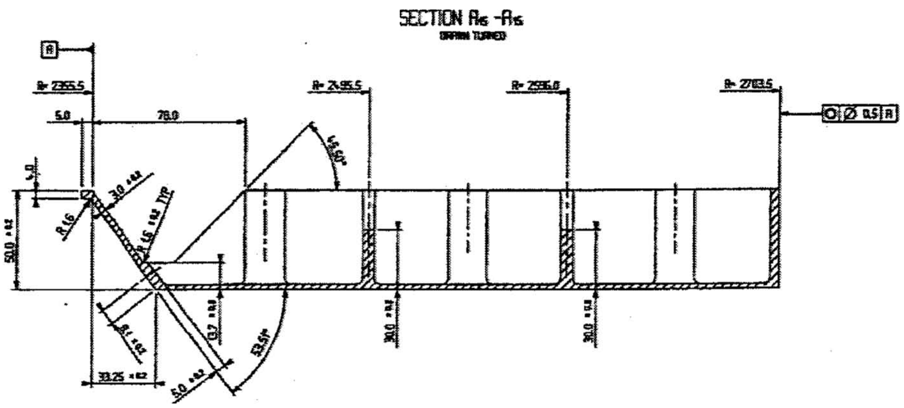

The moment inertia is :

I = 0.00012723 m^4

And analyze only the shaded area, the moment of inertia is:

I = 7.2216 x 10^{-5} m^4

Cross Section 2:

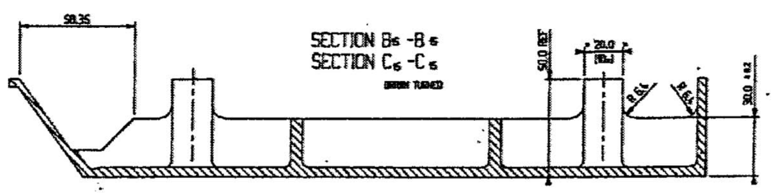

The moment of inertia is:

$I = 2.1525 \times 10^{-5}\ m^4$

And analyze only the shaded area, the moment of inertia is:

$I = 7.2229 \times 10^{-5}\ m^4$

Then the average moment of inertia is:

$I = 7.3299 \times 10^{-5}\ m^4$

E.3 Hand Calculation for Boundary Condition 1 and 2

In the finite element modelling (Chapter 3), there are 3 boundary conditions analyzed. Boundary Condition 1 and 2 can be analyzed as shown below.

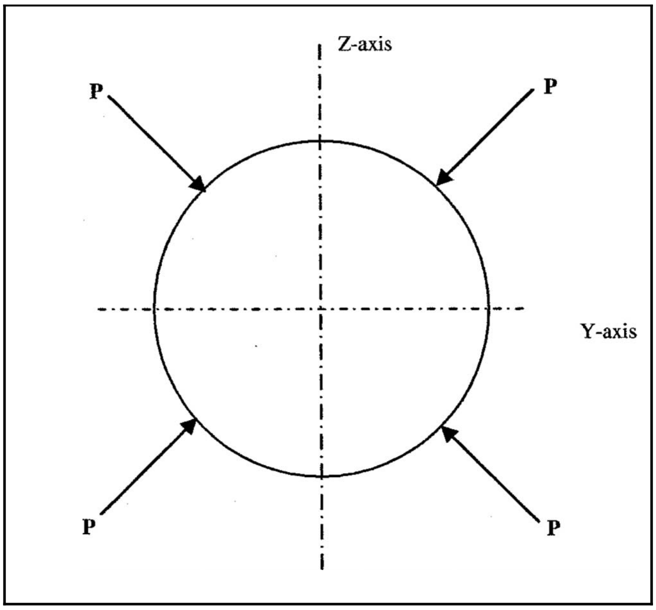

Picture E3-1 Boundary Condition 1 and 2

Using superposition principle, this loading case can be divided into 2 loading cases.

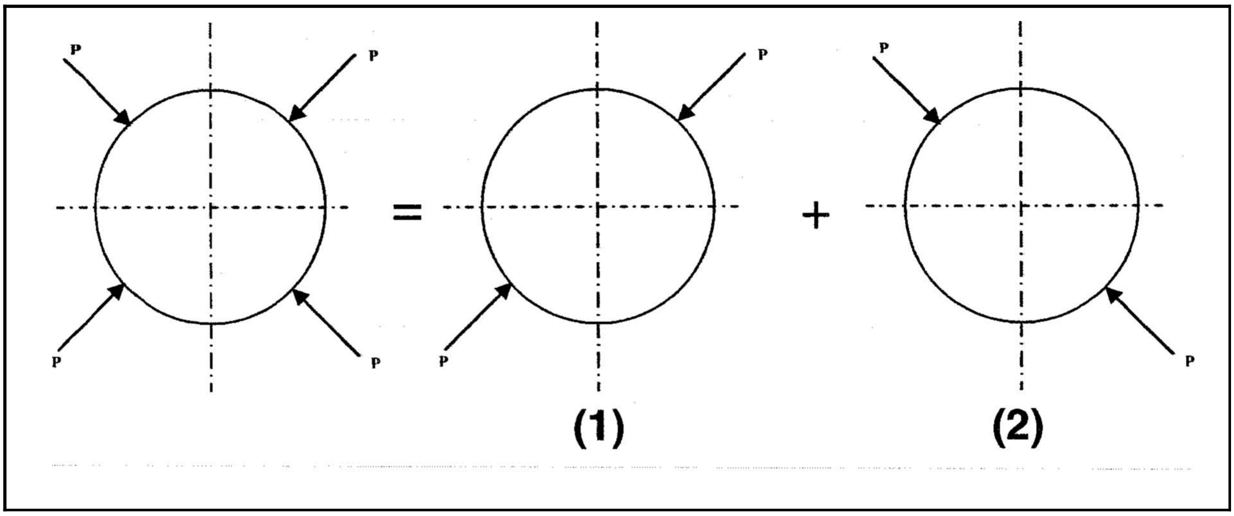

Picture E3-2 Superposition of the boundary condition

The displacement for the case (1) can be obtained by changing a with ***(a-d4)*** in equation (El-16). Meanwhile, the disptacement for the case (2) can be obtained by changing ***a*** with (α-3π/4) in equation (E1-16).

Equation E3-1:

$$f_1 = \frac{P_y r^3}{\pi EI}\left[\left(-2\cos\left(\alpha-\frac{\pi}{4}\right)\right)+\left(\frac{\left(\frac{3\pi}{4}-\alpha\right)\times\sin\left(\alpha-\frac{\pi}{4}\right)}{2}\right)+\left(\frac{\left(\alpha^2-\frac{5\pi\alpha}{2}+\frac{9\pi^2}{16}-8\right)}{4}\right)+\left(\frac{16-\pi^2}{8}\right)\right]$$

Equation E3-2

$$f_2 = \frac{P_y r^3}{\pi EI}\left[\left(-2\cos\left(\alpha-\frac{3\pi}{4}\right)\right)+\left(\frac{\left(\frac{\pi}{4}-\alpha\right)\times\sin\left(\alpha-\frac{3\pi}{4}\right)}{2}\right)+\left(\frac{\left(\alpha^2-\frac{7\pi\alpha}{2}+\frac{21\pi^2}{16}-8\right)}{4}\right)+\left(\frac{16-\pi^2}{8}\right)\right]$$

The exact value of the displacement on a = 0 is the sum of the displacement for the case (1) on a = **45** and the displacement for the case (2) on a = 135, or:

$$f_{\alpha=0^\circ} = f_{1,\alpha=45^\circ} + f_{2,\alpha=135^\circ} \qquad \text{(E3-3)}$$

The material used for the box floor is Al 7075 T7351 and the modulus of elasticity (E) is 7.1 x 10^{10} N/m2. The outer radius of the box (r) is 2.7035 m. Substitute E and r to the equations E3-1 and E3-2, and using the average moment of inertia (I) calculated on section **E.2,** the displacement of the box floor with boundary condition 1 and 2 can be obtained.

The result is: $f_{\alpha=0^\circ} = -7.816\times10^{-6}\,m$

E.4 Hand Calculation for Boundary Condition 3

The Boundary Condition 3 can be analyzed as shown below.

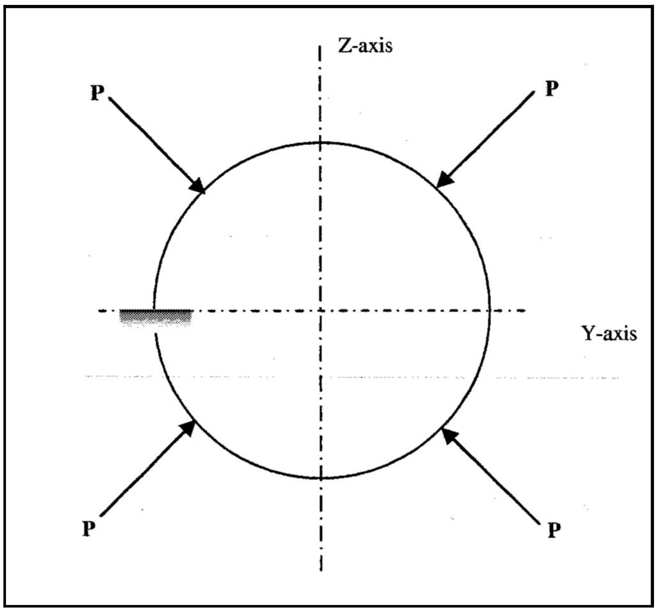

Picture A4-l *Boundary Condition* 3

This condition means that the displacement on a = 0 is zero. The equation for the displacement can be obtained by changing the boundary condition for equation A l-14 with:

$$f_{\alpha=0^\circ} = 0$$

Thus,

$$-\frac{4\times P_y \times r^3}{\pi \times EI} + C_3 = 0$$

$$C_3 = \frac{4\times P_y \times r^3}{\pi \times EI} \tag{A4-1}$$

Substitution of equation A4-1 in equation A l-14 results to the equation for the displacement:

$$f = \frac{P_y \times r^3}{\pi \times EI} \times \left[(-2\times\cos\alpha) + \left(\frac{(\pi-\alpha)\times\sin\alpha}{2} \right) + \left(\frac{(\alpha^2 - 2\times\pi\times\alpha - 8)}{4} \right) + \left(\frac{4}{\pi} \right) \right] \tag{A4-2}$$

Using superposition principle, this loading case can be divided into **2** loading cases.

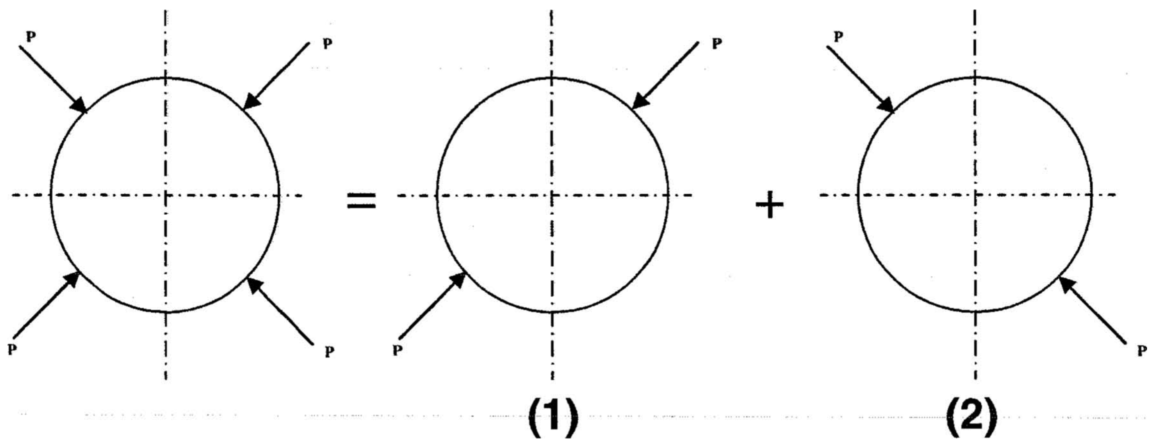

***Picture E4-2** Superposition of the boundary condition*

The displacement for the case **(1)** can be obtained by changing **a** with (α-π/4) in equation (E4-2). Meanwhile, the displacement for the case **(2)** can be obtained by changing a with (α-3π/4) in equation **(E4-2).**

Equation **E4-3:**

$$f_1 = \frac{P_y r^3}{\pi EI}\left[\left(-2\cos\left(\alpha-\frac{\pi}{4}\right)\right)+\left(\frac{\left(\frac{3\pi}{4}-\alpha\right)\times\sin\left(\alpha-\frac{\pi}{4}\right)}{2}\right)+\left(\frac{\left(\alpha^2-\frac{5\pi\alpha}{2}+\frac{9\pi^2}{16}-8\right)}{4}\right)+\left(\frac{4}{\pi}\right)\right]$$

Equation **E3-4**

$$f_2 = \frac{P_y r^3}{\pi EI}\left[\left(-2\cos\left(\alpha-\frac{3\pi}{4}\right)\right)+\left(\frac{\left(\frac{\pi}{4}-\alpha\right)\times\sin\left(\alpha-\frac{3\pi}{4}\right)}{2}\right)+\left(\frac{\left(\alpha^2-\frac{7\pi\alpha}{2}+\frac{21\pi^2}{16}-8\right)}{4}\right)+\left(\frac{4}{\pi}\right)\right]$$

The exact value of the displacement on **a =** 180 is the sum of the displacement for the case (1) on a **= 225** and **the** displacement for the case **(2)** on **a** = **315,** or:

$$f_{\alpha=0^\circ} = f_{1,\alpha=225^\circ} + f_{2,\alpha=315^\circ} \qquad \text{(E4-5)}$$

The material used for the **box floor** is **Al 7075 T7351** and the modulus of elasticity (E) is **7.1** x 10^{10} N/m2. The outer radius of the box (r) is **2.7035** m. Substitute **E** and r to the equations **E4-3** and **E4-4,** and using the average moment of inertia (I) calculated on section **E2,** the displacement of the box floor with boundary condition 1 and **2** can be obtained.

The result is: $f_{\alpha=180^\circ} = 3.705\times10^{-6}\,m$

APPENDIX F SKIRT OPTIMIZATION

Without ring

a = 3.27E+05 N/m2

min **ts** = **0.00438** m

α	n	b (m)	min t (m)	est. mass (kg)
0.1	3600	0.00476	0.00035	4246.16
0.15	2400	0.00714	0.00053	2864.55
0.2	1800	0.00952	0.00071	2183.87
0.3	1200	0.01428	0.00106	1523.42
0.4	900	0.01904	0.00142	1213.39
0.45	800	0.02142	0.00159	1116.75
0.5	720	0.02380	0.00177	1043.46
0.6	600	0.02856	0.00212	943.55
0.8	450	0.03808	0.00282	848.51
0.9	400	0.04284	0.00317	829.99
1	360	0.04760	0.00352	822.99
1.5	240	0.07141	0.00523	878.44
2	180	0.09521	0.00688	997.40
3	120	0.14281	0.00995	1277.97
4	90	0.19042	0.01261	1546.52
4.5	80	0.21422	0.01375	1666.28
5	72	0.23802	0.01478	1774.16
6	60	0.28562	0.01646	1952.62
8	45	0.38083	0.01857	2176.28
9	40	0.42843	0.01917	2238.95
10	36	0.47604	0.01958	2280.81
12	30	0.57125	0.02004	2327.11
15	24	0.71406	0.02034	2353.47
18	20	0.85687	0.02045	2361.64
20	18	0.95208	0.02049	2363.52
24	15	1.14249	0.02052	2364.24
30	12	1.42812	0.02054	2363.08
36	10	1.71374	0.02055	2361.59

With 1 ring

a = 1.64E+05 N/m2
min **ts** = **0.00309** m

α	n	b (m)	min t (m)	est. mass (kg)
0.1	3600	0.00476	0.00025	3008.17
0.15	2400	0.00714	0.00038	2031.25
0.2	1800	0.00952	0.00050	1549.94
0.3	1200	0.01428	0.00075	1082.90
0.4	900	0.01904	0.00100	863.60
0.45	800	0.02142	0.00112	795.21
0.5	720	0.02380	0.00125	743.32
0.6	600	0.02856	0.00150	672.48
0.8	450	0.03808	0.00199	604.65
0.9	400	0.04284	0.00223	591.10
1	360	0.04760	0.00247	585.59
1.5	240	0.07141	0.00364	619.90
2	180	0.09521	0.00473	694.78
3	120	0.14281	0.00659	858.35
4	90	0.19042	0.00797	991.41
4.5	80	0.21422	0.00848	1041.58
5	72	0.23802	0.00889	1081.39
6	60	0.28562	0.00945	1135.44
8	45	0.38083	0.00996	1181.97
9	40	0.42843	0.01007	1190.58
10	36	0.47604	0.01014	1195.01
12	30	0.57125	0.01021	1198.07
15	24	0.71406	0.01025	1197.68
18	20	0.85687	0.01026	1196.05
20	18	0.95208	0.01027	1194.94
24	15	1.14249	0.01027	1193.00
30	12	1.42812	0.01028	1190.82
36	10	1.71374	0.01028	1189.27

With 2 rings

a = 1.09E+05 N/m2

min **ts =** **0.00253** m

α	n	b (m)	min t (m)	est. mass (kg)
0.1	3600	0.00476	0.00020	2462.98
0.15	2400	0.00714	0.00031	1665.32
0.2	1800	0.00952	0.00041	1272.32
0.3	1200	0.01428	0.00061	890.95
0.4	900	0.01904	0.00082	711.83
0.45	800	0.02142	0.00092	655.95
0.5	720	0.02380	0.00102	613.52
0.6	600	0.02856	0.00122	555.52
0.8	450	0.03808	0.00161	499.63
0.9	400	0.04284	0.00181	488.20
1	360	0.04760	0.00200	483.24
1.5	240	0.07141	0.00292	507.34
2	180	0.09521	0.00375	561.31
3	120	0.14281	0.00505	669.84
4	90	0.19042	0.00587	744.00
4.5	80	0.21422	0.00614	767.50
5	72	0.23802	0.00633	784.03
6	60	0.28562	0.00657	802.86
8	45	0.38083	0.00675	814.03
9	40	0.42843	0.00679	814.81
10	36	0.47604	0.00681	814.55
12	30	0.57125	0.00683	812.97
15	24	0.71406	0.00684	810.30
18	20	0.85687	0.00685	808.11
20	18	0.95208	0.00685	806.92
24	15	1.14249	0.00685	805.05
30	12	1.42812	0.00685	803.12
36	10	1.71374	0.00685	801.80

With 3 rings

a = 8.18E+04 N/m2
min ts = **0.00219** m

α	n	b (m)	min t (m)	est. mass (kg)
0.1	3600	0.00476	0.00018	2140.30
0.15	2400	0.00714	0.00027	1449.51
0.2	1800	0.00952	0.00035	1109.15
0.3	1200	0.01428	0.00053	778.85
0.4	900	0.01904	0.00071	623.67
0.45	800	0.02142	0.00079	575.23
0.5	720	0.02380	0.00088	538.44
0.6	600	0.02856	0.00105	488.07
0.8	450	0.03808	0.00139	439.24
0.9	400	0.04284	0.00156	429.02
1	360	0.04760	0.00172	424.33
1.5	240	0.07141	0.00249	441.91
2	180	0.09521	0.00315	482.76
3	120	0.14281	0.00412	558.00
4	90	0.19042	0.00464	600.78
4.5	80	0.21422	0.00479	612.06
5	72	0.23802	0.00489	619.02
6	60	0.28562	0.00501	625.34
8	45	0.38083	0.00510	626.32
9	40	0.42843	0.00511	625.21
10	36	0.47604	0.00512	623.93
12	30	0.57125	0.00513	621.48
15	24	0.71406	0.00514	618.56
18	20	0.85687	0.00514	616.44
20	18	0.95208	0.00514	615.34
24	15	1.14249	0.00514	613.65
30	12	1.42812	0.00514	611.94
36	10	1.71374	0.00514	610.78

With 4 rings

a = 65457.62 N/m2

min ts = 0.001957 m

α	n	b (m)	min t (m)	est. mass (kg)
0.1	3600	0.00476	0.00016	1921.93
0.15	2400	0.007141	0.00024	1304.06
0.2	1800	0.009521	0.00032	999.63
0.3	1200	0.014281	0.00047	704.17
0.4	900	0.019042	0.00063	565.33
0.45	800	0.021422	0.00071	521.97
0.5	720	0.023802	0.00079	489.01
0.6	600	0.028562	0.00094	443.84
0.8	450	0.038083	0.00124	399.78
0.9	400	0.042843	0.00138	390.36
1	360	0.047604	0.00153	385.82
1.5	240	0.071406	0.00219	398.67
2	180	0.095208	0.00274	430.25
3	120	0.142812	0.00348	483.23
4	90	0.190415	0.00383	507.87
4.5	80	0.214217	0.00392	513.06
5	72	0.238019	0.00398	515.64
6	60	0.285623	0.00404	516.79
8	45	0.380831	0.00409	514.14
9	40	0.428435	0.00410	512.48
10	36	0.476039	0.00410	510.93
12	30	0.571246	0.00411	508.34
15	24	0.714058	0.00411	505.51
18	20	0.856869	0.00411	503.53
20	18	0.952077	0.00411	502.52
24	15	1.142493	0.00411	500.98
30	12	1.428116	0.00411	499.44
36	10	1.713739	0.00411	498.40

With 5 rings

σ = **54548.01** N/m2

min ts

= **0.00179** m

α	n	b (m)	min t (m)	est. mass (kg)
0.1	3600	0.00476	0.00014	1762.24
0.15	2400	0.007141	0.00022	1198.20
0.2	1800	0.009521	0.00029	920.29
0.3	1200	0.014281	0.00043	650.55
0.4	900	0.019042	0.00057	523.76
0.45	800	0.021422	0.00065	484.15
0.5	720	0.023802	0.00072	454.02
0.6	600	0.028562	0.00085	412.68
0.8	450	0.038083	0.00113	372.10
0.9	400	0.042843	0.00126	363.25
1	360	0.047604	0.00138	358.79
1.5	240	0.071406	0.00197	367.97
2	180	0.095208	0.00243	392.56
3	120	0.142812	0.00301	429.85
4	90	0.190415	0.00325	443.51
4.5	80	0.214217	0.00331	445.45
5	72	0.238019	0.00335	445.86
6	60	0.285623	0.00339	444.64
8	45	0.380831	0.00341	440.56
9	40	0.428435	0.00342	438.73
10	36	0.476039	0.00342	437.14
12	30	0.571246	0.00342	434.59
15	24	0.714058	0.00343	431.91
18	20	0.856869	0.00343	430.06
20	18	0.952077	0.00343	429.13
24	15	1.142493	0.00343	427.72
30	12	1.428116	0.00343	426.30
36	10	1.713739	0.00343	425.35

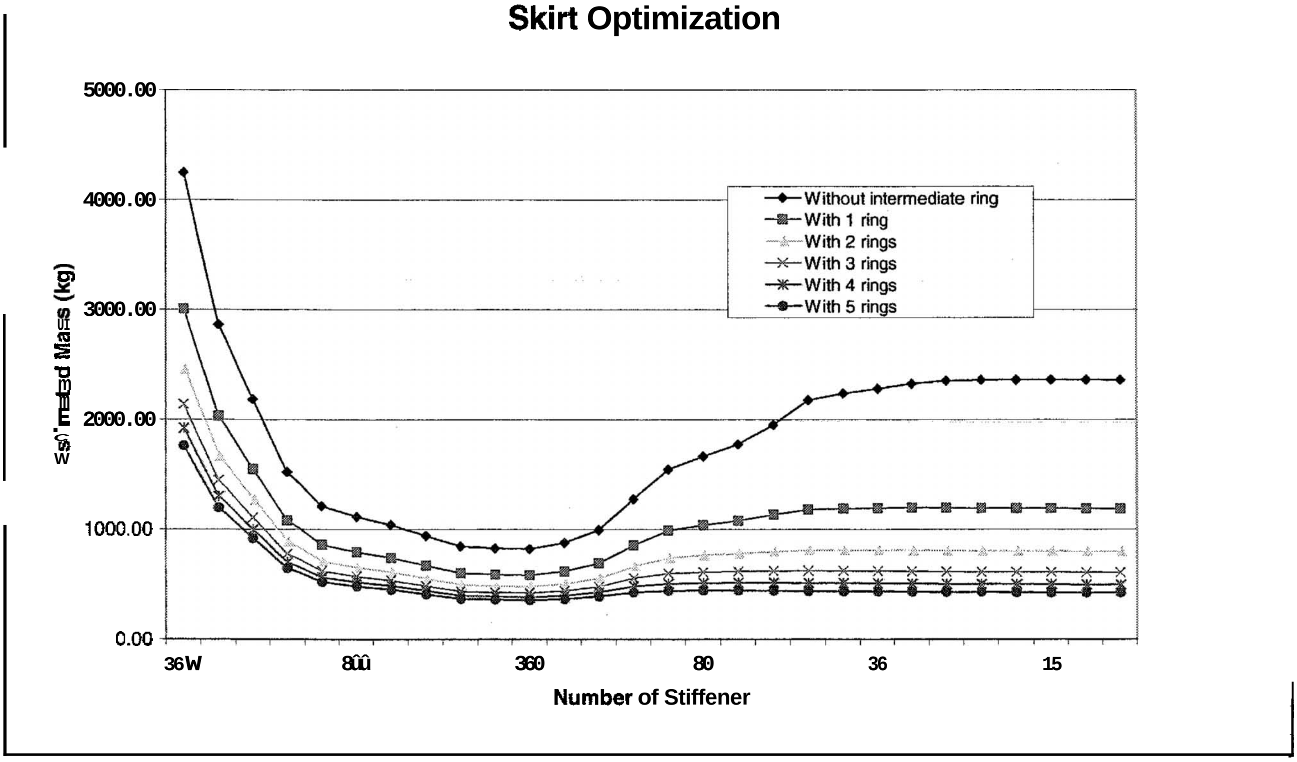

Beams Optimization

IPE	G (kg/m)	mass (kg)	Ix (cm4)	Ix (m4)	Pcr (N)	Py (N)	STATUS
80	6	87.828	80.1	8.01E-07	342.96	1924.567	NOT OK
100	8.1	118.5678	171	1.71E-06	732.16	2037.652	NOT OK
120	10.4	152.2352	318	3.18E-06	1361.56	2161.505	NOT OK
140	12.9	188.8302	541	5.41E-06	2316.37	2296.129	OK
160	15.8	231.2804	869	8.69E-06	3720.75	2452.293	OK
180	18.8	275.1944	1320	1.32E-05	5651.78	2613.842	OK
200	22.4	327.8912	1940	1.94E-05	8306.40	2807.7	OK
220	26.2	383.5156	2770	2.77E-05	11860.17	3012.328	OK
240	30.7	449.3866	3890	3.89E-05	16655.62	3254.651	OK
270	36.1	528.4318	5790	5.79E-05	24790.75	3545.439	OK
300	42.2	617.7236	8360	8.36E-05	35794.59	3873.921	OK
330	49.1	718.7258	11770	1.18E-04	50395.02	4245.483	OK
360	57.1	835.8298	16270	1.63E-04	69662.44	4676.279	OK
400	66.3	970.4994	23130	2.31E-04	99034.56	5171.695	OK
450	77.6	1135.9088	33740	3.37E-04	144462.87	5780.195	OK
500	90.7	1327.6666	48200	4.82E-04	206375.53	6485.624	OK
550	106	1551.628	67120	6.71E-04	287384.34	7309.522	OK
600	122	1785.836	92080	9.21E-04	394254.33	8171.114	OK